Title
Some applications of the higher-dimensional Heegaard Floer homology

Author
Yuan, Tianyu

Publication Date
2021

Peer reviewed|Thesis/dissertation

UNIVERSITY OF CALIFORNIA

Los Angeles

Some Applications of the Higher-Dimensional Heegaard Floer Homology

A dissertation submitted in partial satisfaction
of the requirements for the degree
Doctor of Philosophy in Mathematics

by

Tianyu Yuan

2021

ABSTRACT OF THE DISSERTATION

Some Applications of the Higher-Dimensional
Heegaard Floer Homology

by

Tianyu Yuan
Doctor of Philosophy in Mathematics
University of California, Los Angeles, 2021
Professor Ko Honda, Chair

Given a closed oriented Riemann surface Σ of genus greater than zero, we construct a map $\mathcal{F}$ from the higher-dimensional Heegaard Floer homology of cotangent fibers of $T^*\Sigma$ to the Hecke algebra associated to Σ. We show that $\mathcal{F}$ is an isomorphism of algebras. We also define a higher-dimensional analog of symplectic Khovanov homology. Consider the standard Lefschetz fibration $p : W \to D \subset \mathbb{C}$ of a $2n$-dimensional Milnor fiber of the $A_{2\kappa-1}$ singularity. We represent a link by a κ-strand braid, which in turn is represented as an element h of the symplectic mapping class group $\mathrm{Symp}(W, \partial W)$. We then apply the higher-dimensional Heegaard Floer homology machinery to the pair $(\boldsymbol{a}, h(\boldsymbol{a}))$, where $\boldsymbol{a}$ is a collection of κ unstable manifolds of W which are Lagrangian spheres. We prove its invariance under arc slides and Markov stabilizations, which shows that it is a link invariant.

The dissertation of Tianyu Yuan is approved.

Peter Petersen

Raphael Alexis Rouquier

Sucharit Sarkar

Ko Honda, Committee Chair

University of California, Los Angeles

2021

To my grandmother

TABLE OF CONTENTS

LIST OF FIGURES

ACKNOWLEDGMENTS

First I would like to express my deepest gratitude to my advisor, Ko Honda. His invaluable guidance on research directions has been extraordinary to me and helped me build my geometric intuitions. I could hardly do independent research without his advice on paper readings and explanation of my many questions. His constant encouragement and patience has always been a great support during the time of my academic research.

I would also like to thank my committee members, Peter Petersen, Sucharit Sarkar and Raphael Rouquier for their kindly help and insightful comments on my presentation.

Chapter 3 is based on the preprint [HTY], which is joint work with Ko Honda and Yin Tian. I express my great thanks to Yin Tian, who raised the topic of this paper, helped explain algebraic intuitions behind the question and contributed most to the main theorem. Chapter 4 is based on Chapter 9 of [CHT20]. I would like to express my gratitude to Eilon Tzur, for his careful proofreading and detailed comments. I thank Ko for his constructive ideas, endless patience and huge amount of comments on both chapters.

The communications with Yang Huang improved my understanding of contact topology. I give the deep thanks to him for the invaluable insights. His passion in mathematics also has great impact on me.

Many good friends composed the precious grad school life during my short stay in Los Angeles. I am grateful to everyone of you.

Thanks to Weiyu Gu, for her tolerance and company. We have a long way to go together with Zhuzi and Zaizi.

Finally I would like to thank my parents for their love and support. My father is the first teacher on my mathematical life and may be the origin why I can complete this dissertation today.

VITA

2015 Bachelor of Science in Mathematics,
Shanghai Jiaotong University, Shanghai, China.

2017 Master of Science in Electrical Engineering and Information Systems,
The University of Tokyo, Tokyo, Japan.

CHAPTER 1

Introduction

Aiming to study higher-dimensional contact topology, Colin, Honda and Tian [CHT20] developed the foundations of the higher-dimensional Heegaard Floer homology (HDHF). HDHF is supposed to model the Fukaya category of the Hilbert scheme of points on a Liouville domain and was used to analyze symplectic fillability questions in higher-dimensional contact topology. As an application, the HDHF of the 4-dimensional Milnor fibration of type A provided an invariant of links in S^3. This invariant is a close cousin of symplectic Khovanov homology [SS06; Man06] and especially its cylindrical reformulation [MS19]. As a categorified quantum invariant, Khovanov homology is directly related to the categorification of quantum groups and to various Hecke algebras, including affine Hecke algebras and quiver Hecke algebras (also called KLR algebras) [CR08; Rou08; KL09]. There are several approaches to these Hecke algebras from the point of view of geometric representation theory: The affine Hecke algebra can be realized as the equivariant K-theory of the ordinary Steinberg variety [KL87; CG10; Lus98]; the double affine Hecke algebra admits a similar realization in terms of the loop Steinberg variety [Vas05]. Moreover, the rational double affine Hecke algebra of type A is closely related to the Hilbert scheme of points on $\mathbb{C}^2$ [GS05; KR08]. It is therefore natural to ask:

Question: Is there a symplectic geometry interpretation of the various Hecke algebras?

We give a partial answer in Chapter 3. Specifically, let Σ denote a closed oriented Riemann surface of genus greater than zero, and $\mathring{\Sigma}$ denote a surface with punctures. The

goal of Chapter 3 is to use the HDHF of cotangent bundles of oriented surfaces to give an answer for the various Hecke algebras of type A, including the finite, affine, and double affine Hecke algebras (abbreviated DAHA and also called Cherednik algebras). We consider two cases:

1. a closed oriented surface Σ of genus $g > 0$;
2. a surface $\mathring{\Sigma}$ which is obtained from a closed oriented surface of genus $g \geq 0$ by removing a finite number (> 0) of punctures.

More precisely, we realize the various Hecke algebras as the HDHF of the disjoint cotangent fibers of $T^*\Sigma$ (or $T^*\mathring{\Sigma}$).

Type of Hecke algebra	*Surface*
finite Hecke algebra	open disk
affine Hecke algebra	cylinder
DAHA	torus

Remark 1.0.1. *Note that we exclude the case of a sphere which is more complicated since the homology of its loop space is not supported in degree zero. We hope to revisit this in a future paper.*

Remark 1.0.2. *Recently, Ben-Zvi, Chen, Helm and Nadler identified the affine Hecke algebra with the endomorphism algebra of the coherent Springer sheaf, for any reductive algebraic group [BZCHN20, Theorem 1.7]. It would be interesting to study the connection between the algebro-geometric realization of the affine Hecke algebra of type A and our symplectic geometry one.*

Remark 1.0.3. *In this thesis we consider $T^*\Sigma$ as a symplectic manifold, not as a holomorphic symplectic manifold corresponding to the Riemann surface Σ, which is more natural in many contexts (e.g., [Nak99, Chapter 7]).*

In addition to the definition of HDHF, this work crucially depends on three key ingredients:

1. the relationship between the wrapped Floer cochain complex of a cotangent fiber and chains on the loop space of the base due to Abbondandolo and Schwarz [AS10a] and Abouzaid [Abo12];

2. an interpretation of the HOMFLY skein relation in terms of holomorphic curve counting due to Ekholm and Shende [ES19];

3. a topological description of DAHA of $\mathfrak{gl}_\kappa$ as a *braid skein algebra* due to Morton and Samuelson [MS21].

Our first ingredient is the result of Abbondandalo-Schwarz [AS10a] which states that the wrapped Floer cochain complex $CW^*(T^*_q\Sigma)$ of a cotangent fiber and the chain complex $C_{-*}(\Omega_q\Sigma)$ of the loop space of the base Σ are isomorphic as graded algebras on the cohomology level. Abouzaid [Abo12] further improved this to an A_∞-equivalence on the chain level.

In Chapter 3 we investigate its generalization to HDHF. More precisely, we consider $CW(\sqcup_{i=1}^{\kappa} T^*_{q_i}\Sigma)$, the wrapped HDHF cochain complex of κ disjoint cotangent fibers of $T^*\Sigma$; it can be given the structure of an A_∞-algebra. The HDHF complex $CW(\sqcup_i T^*_{q_i}\Sigma)$ is defined over $\mathbb{Z}[[\hbar]]$, the ring of formal power series in $\hbar$, where $\hbar$ keeps track of the Euler characteristic of the holomorphic curves that are counted in the definition of the A_∞-operations. Since Σ is a surface, $CW(\sqcup_i T^*_{q_i}\Sigma)$ is supported in degree zero and hence is an ordinary algebra.

Our generalization of the loop space of the base will be the loop space of the unordered configuration space $\mathrm{UConf}_\kappa(\Sigma)$ of κ points on Σ. Generalizing Abouzaid's map $CW^*(T^*_q\Sigma) \to C_{-*}(\Omega_q\Sigma)$, we define an evaluation map

$$\mathcal{E}\colon CW(\sqcup_i T^*_{q_i}\Sigma) \to C_0(\Omega(\mathrm{UConf}_\kappa(\Sigma))) \otimes \mathbb{Z}[[\hbar]].$$

Here $C_0(\Omega(\mathrm{UConf}_\kappa(\Sigma)))$ is the 0th chain space of the loop space of $\mathrm{UConf}_\kappa(\Sigma)$ and all tensor products are over $\mathbb{Z}$, unless indicated otherwise. The map $\mathcal{E}$ is given by counting curves of

"Heegaard Floer type"; the precise definition will be given in Section 3.5.1. This map however fails to be a homomorphism of algebras due to an additional degeneration of curves: the nodal degeneration. This phenomenon was recently clarified by Ekholm and Shende [ES19]: It is the HOMFLY skein relation that controls the boundaries of 1-dimensional moduli spaces of varying Euler characteristics; see Figure 3.7.

Starting with the map $\mathcal{E}$, taking the homology of both sides and quotienting out by the HOMFLY skein relation, we obtain a map

$$\mathcal{F}\colon HW(\sqcup_i T^*_{q_i}\Sigma) \to H_0(\Omega(\mathrm{UConf}_\kappa(\Sigma))) \otimes \mathbb{Z}[[\hbar]]/\{\text{the skein relation}\}. \tag{1.0.1}$$

The map $\mathcal{F}$ is an algebra homomorphism; see Proposition 3.5.4.

At this point we observe that $H_0(\Omega(\mathrm{UConf}_\kappa(\Sigma)))$ is isomorphic to the group algebra of the surface braid group of Σ over $\mathbb{Z}$. In [MS21], Morton and Samuelson defined the *braid skein algebra* $\mathrm{BSk}_\kappa(\Sigma)$, which is a quotient of the group algebra of the surface braid group over $\mathbb{Z}[s^{\pm 1}, c^{\pm 1}]$ by the skein relation and the marked point relation; see Definition 3.3.1. Here s and c are parameters that appear in the skein and marked point relations, respectively. We define the *surface Hecke algebra* $\mathrm{H}_\kappa(\Sigma)$ by reformulating the marked point relation as a c-deformed homotopy relation, and making a change of variables $\hbar = s - s^{-1}$; see Definition 3.3.4. We show that $\mathrm{H}_\kappa(\Sigma)$ and $\mathrm{BSk}_\kappa(\Sigma)$ are isomorphic, up to a change of variables.

Motivated by the c-deformed homotopy relation, we consider $CW(\sqcup_i T^*_{q_i}\Sigma)_c$, the wrapped HDHF with a parameter c. Adding the parameter c to the map in (1.0.1), we obtain

$$\mathcal{F}\colon HW(\sqcup_i T^*_{q_i}\Sigma)_c \to \mathrm{H}_\kappa(\Sigma) \otimes_{\mathbb{Z}[\hbar]} \mathbb{Z}[[\hbar]], \tag{1.0.2}$$

which is still denoted $\mathcal{F}$ by abuse of notation.

We then apply the Abbondandolo-Schwarz result [AS06] to show that the restriction of $\mathcal{F}$ to $\hbar = 0$ is an isomorphism. The following is the main result of Chapter 3 and directly follows from the isomorphism of $\mathcal{F}|_{\hbar=0}$:

Theorem 1.0.4. *The map $\mathcal{F}$ in (1.0.2) is an isomorphism of algebras.*

The main result from Morton-Samuelson [MS21] is that the double affine Hecke algebra $\ddot{\mathrm{H}}_\kappa$ of $\mathfrak{gl}_\kappa$ is naturally isomorphic to $\mathrm{BSk}_\kappa(T^2)$. Hence we have:

Corollary 1.0.5. *The algebra $HW(\sqcup_i T^*_{q_i} T^2)_c$ is isomorphic to $\ddot{\mathrm{H}}_\kappa|_{\hbar=s-s^{-1}} \otimes_{\mathbb{Z}[\hbar]} \mathbb{Z}[[\hbar]]$.*

When the base $\mathring{\Sigma}$ has punctures, one can similarly define the A_∞ algebra $CW(\sqcup_i T^*_{q_i}\mathring{\Sigma})$. It is possible to formally include a c-parameter, but we expect that it does not yield any extra information. The isomorphism (1.0.2) still holds and the corresponding surface Hecke algebra $\mathrm{H}_\kappa(\mathring{\Sigma})$ is isomorphic to the finite Hecke algebra H_κ and the affine Hecke algebra $\dot{\mathrm{H}}_\kappa$ of $\mathfrak{gl}_\kappa$ when $\mathring{\Sigma}$ is an open disk and a cylinder, respectively.

Corollary 1.0.6. *The algebra $HW(\sqcup_i T^*_{q_i}\mathring{\Sigma})$ is isomorphic to $\mathrm{H}_\kappa|_{\hbar=s-s^{-1}} \otimes_{\mathbb{Z}[\hbar]} \mathbb{Z}[[\hbar]]$ (resp. $\dot{\mathrm{H}}_\kappa|_{\hbar=s-s^{-1}} \otimes_{\mathbb{Z}[\hbar]} \mathbb{Z}[[\hbar]]$), when $\mathring{\Sigma}$ is an open disk (resp. a cylinder).*

Returning to the discussion of categorification, the affine Hecke algebra is related to categorified quantum groups of type A [CR08]. This can be explained symplectically by noting that $T^*\mathring{\Sigma}$ for a cylinder $\mathring{\Sigma}$ is symplectomorphic to $\mathbb{R}^2 \times T^*S^1$. The latter naturally appears in the 4-dimensional Milnor fibration and the HDHF approach to symplectic Khovanov homology [CHT].

The isomorphism (1.0.2) holds only after tensoring with $\mathbb{Z}[[\hbar]]$. Nevertheless, we believe that the coefficient ring could be taken to be $\mathbb{Z}[\hbar]$.

Conjecture 1.0.7. *The algbera $HW(\sqcup_i T^*_{q_i}\Sigma)_c$ is well-defined over $\mathbb{Z}[\hbar]$ and Theorem 1.0.4 still holds over $\mathbb{Z}[\hbar]$.*

There is some evidence for this conjecture: In particular, direct computations of the third author [Yua] (in preparation) show the well-definedness over $\mathbb{Z}[\hbar]$ when $\Sigma = \mathbb{R}^2$ and the surface Hecke algebra is the finite Hecke algebra.

Question 1.0.8. *What is the geometric meaning of the change of variables $\hbar = s - s^{-1}$?*

Question 1.0.8 is important from the perspective of representation theory. For instance, the affine Hecke algebra with parameter s has interesting modules, but the situation is not

clear for the affine Hecke algebra with parameter $\hbar$. A possible explanation of $\hbar = s - s^{-1}$ may require additional data of flat bundles which is well-studied in mirror symmetry and Fukaya categories.

On the HDHF side, other κ-tuples of Lagrangians in $T^*\Sigma$ give rise to modules over $HW(\sqcup_i T^*_{q_i}\Sigma)_c$. It is interesting to look at the category of such modules and try to relate it to the Fukaya category of the Hilbert scheme $\mathrm{Hilb}^\kappa(T^*\Sigma)$.

The other topic we are interested in is the symplectic Khovanov homology by Seidel and Smith [SS06].

Over the last twenty years many powerful Floer-theoretic invariants of knots and links have appeared, e.g. Heegaard Floer homology [OS04] and knot Floer homology in dimension 1; symplectic Khovanov homology [SS06] and knot contact homology [EENS13] in dimension 2. Here when we say "dimension n", we are taking the ambient symplectic manifold to be $2n$-dimensional and the Lagrangian submanifolds (if we are talking about Lagrangian intersection Floer thoeries) to be n-dimensional. In [Man07] Manolescu also used quiver varieties to define a higher-dimensional analog of $\mathfrak{sl}(n)$-homologies.

Along similar lines, in Chapter 4, we use HDHF to define a link invariant which is a variant of the symplectic Khovanov homology, following Chapter 9 of [CHT20]. This is a higher-dimensional analog of the usual Heegaard Floer homology by [OS04].

Specifically, in dimension 1, Lipschitz [Lip06] proved the equivalence between Ozsváth and Szabó's Heegaard Floer homology [OS04] and its cylindrical analog. In dimension 2, Mak and Smith [MS19] proved the equivalence of symplectic Khovanov homology and its cylindrical interpretation. Colin, Honda and Tian [CHT20] then defined a higher-dimensional analog of cylindrical Heegaard Floer homology, which helps place the cylindrical symplectic Khovanov homology in a more general framework. In Chapter 4, the ambient manifold is a $2n$-dimensional Milnor fiber of the $A_{2\kappa-1}$-singularity $p : W \to D \subset \mathbb{C}$, extending the case of

$n = 1$ considered in [CHT20]. Given a link, we consider its κ-strand braid representation σ, which is in fact an element h of the symplectic mapping class group $\mathrm{Symp}(W, \partial W)$. There is a natural collection of κ Lagrangian spheres $\boldsymbol{a}$ by the matching cycle construction between pairs of critical points of p. We then apply the higher-dimensional Heegaard Floer homology machinery to the pair $(\boldsymbol{a}, h(\boldsymbol{a}))$ to define the link invariant and denote the homology group by $Kh^\sharp(\widehat{\sigma})$.

Though cylindrical versions of Heegaard Floer theories are more convenient for visualizing pseudoholomorphic curves, the original theories defined in the symmetric products $\mathrm{Sym}^\kappa(X)$ have their advantages: In dimension 1, Perutz [Per08] proved that Lagrangians in $\mathrm{Sym}^\kappa(\Sigma)$ related by a handle slide are in fact Hamiltonian isotopic for some specific symplectic form, which directly implies the handle slide invariance property without pseudoholomorphic curve counting techniques in [OS04]. In dimension 2, Seidel and Smith [SS06] considered nilpotent slices instead of $\mathrm{Sym}^\kappa(X)$, which was shown to be a subset of $\mathrm{Hilb}^\kappa(X)$ by Manolescu [Man06]. Inside the nilpotent slice, matching cycles as Lagrangians related by arc slides are also Hamiltonian isotopic, which is not obvious in the cylindrical formulation. Mak and Smith [MS19] then showed that the cylindrical version is equivalent to the original symplectic Khovanov homology in nilpotent slices.

However, in higher dimensions, the cylindrical symplectic Khovanov homology with vanishing cycles κ-tuples of S^n does not have its "original" version; at this moment we do not know how to put the theory inside a nilpotent slice setting. Another problem is that Hilbert schemes of points in higher dimensions are not smooth, so we need new ways to resolve the singularities along the diagonal of $\mathrm{Sym}^\kappa(X)$. One possible solution is to restrict to some smooth stratum of $\mathrm{Hilb}^\kappa(X)$. For example, the subset of subschemes where each support point is of length at most 3 (at most triple point) is smooth. However we will not continue the discussion in this dissertation further. It would be interesting to study this problem in future.

Therefore, we will follow the curve counting strategy as in [OS04] and [CHT20] to prove the invariance under arc slides and Markov stabilizations.

Organization:

Chapter 2:

We review the symplectic backgrounds and the basic settings of HDHF.

Chapter 3:

In Section 3.1, we consider HDHF of cotangent bundles and define $CW(\sqcup_i T^*_{q_i}\Sigma)$.

In Section 3.2, we review the chain complex of the loop space and the results of [AS06; Abo12].

In Section 3.3, we discuss the homology of the based loop space of $\mathrm{UConf}_\kappa(\Sigma)$, which degenerates to surface braid groups. We then define the Hecke algebra $\mathrm{H}_\kappa(\Sigma)$, a variant of $\mathrm{BSk}_\kappa(\Sigma)$ by [MS21].

In Section 3.4, we include the parameter c originated from $\mathrm{BSk}_\kappa(\Sigma)$ to the HDHF and define $CW(\sqcup_i T^*_{q_i}\Sigma)_c$.

In Section 3.5, we construct the map $\mathcal{F}$ and prove that $\mathcal{F}$ is an isomorphism of algebras.

In Section 3.6, we show that our results can be extended to surfaces with punctures.

Chapter 4:

In Section 4.1, we begin with a brief review of Section 9 of [CHT20], describe the notations, definitions and prerequisite theorems. Then we state the main result. We use a subsection to explain the Morse gradient tree theory and its relation to pseudoholomorphic curves originated from [FO97], which is crucial in our proof.

In Section 4.2, we show the arc slide invariance by counting pseudoholomorphic curves with certain boundary Lagrangians. The idea is to stretch the curve into several parts so that each one is easy to count by elementary model calculation.

In Section 4.4, we translate the Markov stabilization into the gluing of some pseudoholomorphic curves, which we count by Morse gradient tree arguments instead.

In Section 4.5, we compute $Kh^\sharp(\widehat{\sigma})$ for unknots, Hopf links and trefoils, which is mainly

based on the count of simple pseudoholomorphic quadrilaterals.

CHAPTER 2

Review of the higher-dimensional Heegaard Floer homology

We review the general facts of HDHF. The main reference for the basic settings of HDHF is [CHT20].

Definition 2.0.1. *A symplectic manifold is a pair (X^{2n}, ω) consisting of a smooth $2n$-dimensional manifold X and a closed nondegenerate 2-form ω on X. We call (X, ω) exact if there exists a 1-form θ so that $\omega = d\theta$.*

Definition 2.0.2. *A Lagrangian submanifold L is a n-dimensional submanifold of (X^{2n}, ω) so that $\omega|_L = 0$. We call L exact if $\omega = d\theta$ and $\theta|_L = df$ for some function $f \in C^\infty(L, \mathbb{R})$.*

Definition 2.0.3. *Let (X^{2n}, ω) be an exact symplectic manifold of dimension $2n$. The objects of the A_∞-category $\mathcal{F}_\kappa(X)$ are κ-tuples of disjoint exact Lagrangians. Given two objects $L_i = L_{i1} \sqcup \cdots \sqcup L_{i\kappa}$, $i = 0, 1$, whose components are mutually transverse, $\mathrm{Hom}_{\mathcal{F}_\kappa(X)}(L_0, L_1) = CF(L_0, L_1)$ is the free abelian group generated by all $\mathbf{y} = \{y_1, \ldots, y_\kappa\}$ where $y_j \in L_{0j} \cap L_{1\sigma(j)}$ and σ is some permutation of $\{1, \ldots, \kappa\}$. The coefficient ring is set to be $\mathbb{Z}[[\hbar]]$. The A_∞-operations μ^m, $m = 1, 2, \ldots,$ will be defined by (2.0.2).*

To define the A_∞ operation μ^m, for $i = 1, \ldots, m$, let $L_i = \sqcup_{j=1}^{\kappa} L_{ij}$ so that L_{i-1} and L_i are transverse. Let $\mathbf{y}_i = \{y_{i1}, \ldots, y_{i\kappa}\}$ be a κ-tuple of points so that $y_{ij} \in L_{(i-1)j} \cap L_{i\sigma_i(j)}$ where σ_i is some permutation of $\{1, \ldots, \kappa\}$.

As in the cylindrical reformulation of Heegaard Floer homology by Lipschitz [Lip06], we also need an extra "cylindrical" direction to keep track of points in "$\mathrm{Sym}^\kappa(X)$". Specifically,

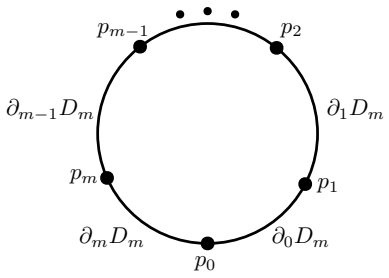

Figure 2.1

as shown in Figure 2.1, let D be the unit disk in $\mathbb{C}$ and $D_m = D - \{p_0, \ldots, p_m\}$, where $p_i \in \partial D_m$ are boundary punctures arranged counterclockwise. Let $\partial_i D_m$ be the boundary arc from p_i to p_{i+1}. Let $\mathcal{A}_m$ be the moduli space of D_m modulo automorphisms; we choose representatives D_m of equivalence classes of $\mathcal{A}_m$ in a smooth manner (e.g., by setting $p_0 = -i$ and $p_1 = i$) and abuse notation by writing $D_m \in \mathcal{A}_m$. We call D_m the "A_∞ base direction".

The full ambient symplectic manifold is then $(D_m \times X, \Omega_m = \omega_m + \omega)$, where ω_m is an area form on D_m which restricts to $ds_i \wedge dt_i$ on each strip-like end e_i around p_i. As we approach the puncture p_i, $s_i \to -\infty$ for $i = 0$ and $s_i \to +\infty$ for $i = 1, \ldots, m$. Then we extend the Lagrangians to the A_∞ base direction: for $i = 0, \ldots, m$, let $\tilde{L}_i = \partial_i D_m \times L_i$ and $\tilde{L}_{ij} = \partial_i D_m \times L_{ij}$. Let $\pi_X : D_m \times X \to X$ be the projection to X and π_{D_m} be the symplectic fibration

$$\pi_{D_m} \colon (D_m \times X, \Omega_m) \to (D_m, \omega_m).$$

There is a smooth assignment $D_m \mapsto J_{D_m}$, where $D_m \in \mathcal{A}_m$, such that:

1. J_{D_m} is close to a split almost complex structure $j_m \times J_X$, where J_X is a compatible almost complex structure on (X, ω);

2. J_{D_m} projects holomorphically onto D_m;

3. when $m = 1$, J_{D_1} is invariant under $\mathbb{R}$-translation of the base.

One can construct such an assignment for all $m \geq 1$ in a manner which is (A) consistent with the boundary strata and (B) for which all the moduli spaces $\mathcal{M}(\mathbf{y}_1, \ldots, \mathbf{y}_m, \mathbf{y}_0)$, defined

below, are transversely cut out. A collection $\{J_{D_m} \mid D_m \in \mathcal{A}_m,\ m \in \mathbb{Z}_{>0}\}$ satisfying (A) will be called a *consistent collection* of almost complex structures; if it satisfies (B) in addition, it is a *sufficiently generic* consistent collection.

Remark 2.0.4. *To avoid cumbersome terminology, in what follows, when we say* sufficiently generic*, we mean that all the moduli spaces under consideration are transversely cut out.*

Let $\mathcal{M}(\mathbf{y}_1, \dots, \mathbf{y}_m, \mathbf{y}_0)$ be the moduli space of maps

$$u\colon (\dot{F}, j) \to (D_m \times X, J_{D_m}),$$

where (F, j) is a compact Riemann surface with boundary, $\mathbf{p}_0, \dots, \mathbf{p}_m$ are disjoint κ-tuples of boundary punctures of F, $\dot{F} = F \setminus \cup_i \mathbf{p}_i$, and $D_m \in \mathcal{A}_m$, so that u satisfies

$$\begin{cases} du \circ j = J_{D_m} \circ du; \\ \text{each component of } \partial \dot{F} \text{ is mapped to a unique } \tilde{L}_{ij}; \\ \pi_X \circ u \text{ tends to } \mathbf{y}_i \text{ as } s_i \to +\infty \text{ for } i = 1, \dots, m; \\ \pi_X \circ u \text{ tends to } \mathbf{y}_0 \text{ as } s_0 \to -\infty; \\ \pi_{D_m} \circ u \text{ is a } \kappa\text{-fold branched cover of } D_m, \end{cases} \tag{2.0.1}$$

where the 3rd condition means that $\pi_X \circ u$ maps the neighborhoods of the punctures of $\mathbf{p}_i$ asymptotically to the Reeb chords of $\mathbf{y}_i$ for $i = 1, \dots, m$ at the positive ends. The 4th condition is similar.

The μ^m-composition map of $\mathcal{F}_\kappa(X)$ is then defined as

$$\mu^m(\mathbf{y}_1, \dots, \mathbf{y}_m) = \sum_{\mathbf{y}_0, \chi \le \kappa} \#\mathcal{M}^{\mathrm{ind}=0,\chi}(\mathbf{y}_1, \dots, \mathbf{y}_m, \mathbf{y}_0) \cdot \hbar^{\kappa - \chi} \cdot \mathbf{y}_0, \tag{2.0.2}$$

where the superscript χ denotes that the Euler characteristic $\chi(u) = \chi$.

Theorem 2.0.5. *The Fredholm index of $\mathcal{M}^\chi(\mathbf{y}_1, \dots, \mathbf{y}_m, \mathbf{y}_0)$ is*

$$\mathrm{ind}(u) = (n-2)\chi + \mu + 2\kappa - m\kappa n + m - 2, \tag{2.0.3}$$

where μ is the Maslov index of u, defined as in [CHT20, Section 4].

If $2c_1(TX) = 0$ and the Maslov classes of all involved Lagrangians vanish, then there exists a well-defined $\mathbb{Z}$-grading. In this case, the dimension of $\mathcal{M}^\chi(\mathbf{y}_1, \ldots, \mathbf{y}_m, \mathbf{y}_0)$ can be rewritten as

$$\mathrm{ind}(u) = (n-2)(\chi - \kappa) + |\mathbf{y}_0| - |\mathbf{y}_1| - \cdots - |\mathbf{y}_m| + m - 2, \tag{2.0.4}$$

where $|\mathbf{y}_i| = |y_{i1}| + \cdots + |y_{i\kappa}|$. Note also that

$$|\hbar| = 2 - n. \tag{2.0.5}$$

We omit the details about the orientation of $\mathcal{M}(\mathbf{y}_1, \ldots, \mathbf{y}_m, \mathbf{y}_0)$ and the A_∞-relation, and refer the reader to [CHT20, Section 4].

CHAPTER 3

HDHF of cotangent bundles and the Hecke algebra

3.1 Wrapped HDHF of disjoint cotangent fibers

Recall the notations of Chapter 2. From now on, we restrict to the case $X = T^*M$, where M is a compact oriented manifold of dimension n. Let $\pi_M : T^*M \to M$ be the standard projection; by abuse of notation we also denote the projection map $\pi_M \circ \pi_{T^*M}$ simply by π_M.

The wrapped HDHF category is denoted by $\mathcal{F}_\kappa(T^*M)$. Let $q_1, \ldots, q_\kappa$ be κ distinct points in a small disk $U \subset M$. We discuss the wrapped Heegaard Floer homology of the object $\sqcup_i T^*_{q_i} M$, where we assume i to range from 1 to κ in what follows.

Let g be a Riemannian metric on M and $|\cdot|$ be the induced norm on T^*M. Choose a time-dependent Hamiltonian $H_V : [0,1] \times T^*M \to \mathbb{R}$:

$$H_V(t,q,p) = \frac{1}{2}|p|^2 + V(t,q), \tag{3.1.1}$$

where $t \in [0,1]$, $q \in M$, $p \in T^*_q M$, and V is some perturbation term with small $W^{1,2}$-norm. The Hamiltonian vector field X_{H_V} with respect to the canonical symplectic form $\omega = dq \wedge dp$ is then given by $i_{X_{H_V}}\omega = dH_V$. Let $\phi^t_{H_V}$ be the time-t flow of X_{H_V}.

By choosing g and V generically, we can guarantee that all Hamiltonian chords of $\phi^t_{H_V}$ between the cotangent fibers $\{T^*_{q_1} M, \ldots, T^*_{q_\kappa} M\}$ are nondegenerate.

Definition 3.1.1. *The* wrapped Heegaard Floer chain complex *of* $CW(\sqcup_i T^*_{q_i} M)$ *is defined to be* $CF(\phi^1_{H_V}(\sqcup_i T^*_{q_i} M), \sqcup_i T^*_{q_i} M)$.

There is a subtlety when defining A_∞-operations for wrapped HDHF and we briefly review the rescaling argument of [Abo10, Section 3].

Choose a consistent collection $\{J_{D_m} \mid D_m \in \mathcal{A}_m,\ m \in \mathbb{Z}_{>0}\}$. We would like to impose Lagrangian boundary conditions $\phi_{H_V}^{m-j}(\sqcup_i T^*_{q_i} M)$ over the arc $\partial_j D_m$, but there is some subtlety near the end e_0 since $CF(\phi_{H_V}^m(\sqcup_i T^*_{q_i} M), \sqcup_i T^*_{q_i} M)$ is not naturally isomorphic to $CF(\phi_{H_V}^1(\sqcup_i T^*_{q_i} M), \sqcup_i T^*_{q_i} M)$. We will explain how to modify the Lagrangian boundary condition and the family J_{D_m} for $D_m \in \mathcal{M}_m - N(\partial \mathcal{M}_m)$, where $N(\partial \mathcal{M}_m)$ is a small neighborhood of $\partial \mathcal{M}_m$ in $\overline{\mathcal{M}}_m$. It is not hard to extend these modifications to all of $\mathcal{M}_m$ which is consistent with boundary strata. Let ψ^ρ be the time-$\log \rho$ flow of the Liouville vector field $p\partial_p$ of (T^*M, pdq). There is an isomorphism

$$\begin{aligned} &CF(\psi^\rho(\phi_{H_V}^1(\sqcup_i T^*_{q_i} M)), \psi^\rho(\sqcup_i T^*_{q_i} M); \psi^\rho_* J_{D_m}) \\ \cong\ &CF(\phi_{H_V}^1(\sqcup_i T^*_{q_i} M), \sqcup_i T^*_{q_i} M; J_{D_m}) \cong CW(\sqcup_i T^*_{q_i} M). \end{aligned}$$

Taking $\rho = 1/m$, $\psi^{1/m}(\phi_{H_V}^1(\sqcup_i T^*_{q_i} M))$ limits to $\phi_{H_V}^m(\sqcup_i T^*_{q_i} M)$ as $|p| \to \infty$ and $\psi^{1/m}(\sqcup_i T^*_{q_i} M)$ remains the same as $\sqcup_i T^*_{q_i} M$. We then take the Lagrangian boundary condition over $\partial_0 D_m$ to be the trace of the Lagrangian isotopy from $\phi_{H_V}^m(\sqcup_i T^*_{q_i} M)$ to $\psi^{1/m}(\phi_{H_V}^1(\sqcup_i T^*_{q_i} M))$ as $s_0 \to -\infty$ and take the boundary condition over $\partial_m D_m$ to be the trace from $\sqcup_i T^*_{q_i} M$ to $\psi^{1/m}(\sqcup_i T^*_{q_i} M)$ as $s_0 \to -\infty$ which we can take to be $\sqcup_i T^*_{q_i} M$. The boundary condition over $\partial_j D_m$ for $j \neq 0, m$ is the usual one $\phi_{H_V}^{m-j}(\sqcup_i T^*_{q_i} M)$.

We modify J_{D_m} to a compatible almost complex structure $\tilde{J}_{D_m}$ so that on the output end e_0 of D_m, $\tilde{J}_{D_m} \to \psi_*^{1/m} J_{D_m}$ as $s_0 \to -\infty$; also, in the context of wrapped HDHF a consistent collection of almost complex structures is a collection of $\tilde{J}_{D_m}$. By abuse of notation, we write J_{D_m} instead of $\tilde{J}_{D_m}$ from now on.

Lemma 3.1.2. *Let $d = 0$ or 1. Given $\mathbf{y}_1, \ldots, \mathbf{y}_m \in CW(\sqcup_i T^*_{q_i} M)$, $\mathcal{M}^{\mathrm{ind}=d,\chi}(\mathbf{y}_1, \ldots, \mathbf{y}_m, \mathbf{y}_0)$ is empty for all but finitely many $\mathbf{y}_0$. If it is nonempty, $\mathcal{M}^{\mathrm{ind}=d,\chi}(\mathbf{y}_1, \ldots, \mathbf{y}_m, \mathbf{y}_0)$ (and $\mathcal{M}^{\mathrm{ind}=d,\chi}(\mathbf{y}_1, \mathbf{y}_0)/\mathbb{R}$ if $m = 1$) admits a compactification for each χ.*

Proof. This is similar to [Abo10, Appendix B] or [AS10b, Section 7]. □

Therefore, the A_∞-operation

$$\mu^m \colon CW(\sqcup_i T^*_{q_i} M) \otimes \cdots \otimes CW(\sqcup_i T^*_{q_i} M) \to CW(\sqcup_i T^*_{q_i} M),$$

can be defined using a sufficiently generic consistent collection, making the chain complex $CW(\sqcup_i T^*_{q_i} M)$ into an A_∞-algebra.

Remark 3.1.3. *The same prescription gives us the wrapped HDHF category $\mathcal{F}_\kappa(X)$ of a Liouville domain, which generalizes the wrapped Fukaya category $\mathcal{F}_1(X)$ of X.*

We now discuss the grading on $CW(\sqcup_i T^*_{q_i} M)$. Since $c_1(T(T^*M)) = 0$ and the Maslov class of the Lagrangian vanishes, there is a well-defined $\mathbb{Z}$-grading. Following [Aur14, Section 1.3], we choose a nonzero section μ of the trivial complex line bundle $\Lambda^2_{\mathbb{C}} T^*(T^*M)$: Let $\{U_\alpha\}$ be a cover of M. On any local chart U_α with coordinates $(x^1_\alpha, \ldots, x^n_\alpha)$, we define

$$\mu_\alpha = (dx^1_\alpha - i \circ dx^1_\alpha \circ J) \wedge \cdots \wedge (dx^n_\alpha - i \circ dx^n_\alpha \circ J); \tag{3.1.2}$$

here J can be viewed as a bundle map which takes $v \in TM$ to its dual $v^* \in T^*M$ via g. Let $\mu = \sum_\alpha \varphi_\alpha \mu_\alpha$ where $\{\varphi_\alpha\}$ is some partition of unity with respect to $\{U_\alpha\}$. Then we consider the phase function

$$\begin{aligned} \varphi_\mu \colon LGr(T(T^*M)) &\to S^1 \\ A &\mapsto \frac{\mu(v_1 \wedge \cdots \wedge v_n)^2}{||\mu(v_1 \wedge \cdots \wedge v_n)||^2} \end{aligned} \tag{3.1.3}$$

where $LGr(T(T^*M))$ is the Grassmannian of Lagrangian planes in $T(T^*M)$, $\{v_1, \ldots, v_n\}$ are tangent vectors that span A. Note that φ_μ is independent of the choice of $\{v_1, \ldots, v_n\}$. For any loop l in $LGr(T(T^*M))$, the Maslov index of l is then defined as the degree of φ_μ on l. Moreover, if the Maslov class of some Lagrangian L vanishes, we can lift φ_μ on L to a grading function $\tilde{\varphi}_\mu \colon L \to \mathbb{R}$.

Given any $q \in M$, denote the tangent space of the zero section of T^*M at q by $T_q M$. One can check that $\varphi_\mu(T_q M) = 1 \in S^1$ for any choice of μ. Hence we can define a grading function on the zero section M which is identically 0. Similarly, given any $x \in T^*M$, denote

the vertical space at x by V_x. We check that $\varphi_\mu(V_x) = (-1)^n \in S^1$ for any choice of μ. Therefore we can define a grading function on any (unwrapped) cotangent fiber T_q^*M which is identically 0.

Now let $M = \Sigma$, a closed oriented surface of genus greater than 0. In this case $|\hbar| = 2 - n = 0$ from (2.0.5). Let g be a Riemannian metric on Σ which is a small perturbation of the flat metric when Σ is a torus and of the hyperbolic metric when Σ has genus greater than 1. In this case:

Lemma 3.1.4. *Fix μ by any choice satisfying (3.1.2). Then the grading $|\mathbf{y}| = 0$ for every $\mathbf{y} \in CF(\phi^1_{H_V}(\sqcup_i T^*_{q_i}\Sigma), \sqcup_i T^*_{q_i}\Sigma)$.*

Proof. Given $\mathbf{y} = \{y_1, \ldots, y_\kappa\} \in CF(\phi^1_{H_V}(\sqcup_i T^*_{q_i}\Sigma), \sqcup_i T^*_{q_i}\Sigma)$, each $y_i \in \phi^1_{H_V}(L_i) \cap L_{i'}$ corresponds to a time-1 Hamiltonian chord from L_i to $L_{i'}$, parametrized by $(q(t), p(t))$, $t \in [0, 1]$. Its Legendre transform (see Definition 3.2.2) gives a perturbed geodesic γ on Σ. By classical results of Duistermaat [Dui76, Theorem 4.3] and [AS06, Section 1.2], the Conley-Zehnder index of y_i with respect to μ is equal to the Morse index of γ with respect to its Lagrangian action. Lemma 3.2.6 then implies that $|y_i| = 0$. Hence $|\mathbf{y}| = \sum_{i=1}^{\kappa} |y_i| = 0$. □

Proposition 3.1.5. *The A_∞-algebra $CW(\sqcup_i T^*_{q_i}\Sigma)$ is supported in degree zero, and hence is an ordinary algebra.*

Proof. The complex $CW(\sqcup_i T^*_{q_i}\Sigma)$ is supported in degree zero by Lemma 3.1.4 and $|\hbar| = 0$. The A_∞-operation $\mu^m = 0$ for all $m \neq 2$ since the degree of μ^m is $2 - m$. Hence μ^2 is the only nontrivial A_∞-operation and $CW(\sqcup_i T^*_{q_i}\Sigma)$ is an ordinary algebra. □

3.2 Review of works on the loop space and the wrapped Floer homology of a cotangent fiber

Let M be a compact oriented manifold of dimension n. We review some basic properties of loop spaces on M and in particular the relationship to the wrapped Floer homology of a single cotangent fiber of T^*M, i.e., the case when $\kappa = 1$. We refer the reader to [AS06; Abo12] for more details.

Let g be a generic Riemannian metric on M and let ∇ be its associated Levi-Civita connection.

Consider the path space

$$\Omega(M, q_0, q_1) = \{\gamma \in C^0([0,1], M) \mid \gamma(0) = q_0, \gamma(1) = q_1\}.$$

There is a composition map which is simply the concatenation of paths:

$$\Omega(M, q_0, q_1) \times \Omega(M, q_1, q_2) \to \Omega(M, q_0, q_2),$$
$$\gamma_1\gamma_2(t) = \begin{cases} \gamma_1(2t), & 0 \le t \le 1/2, \\ \gamma_2(2t-1), & 1/2 \le t \le 1. \end{cases}$$

In order to do Morse theory on the path space, we use $\Omega^{1,2}(M, q_0, q_1)$, the subset of $\Omega(M, q_0, q_1)$ consisting of paths in the class $W^{1,2}$.

There is a natural action functional on $\Omega^{1,2}(M, q_0, q_1)$. Recall the Hamiltonian H_V, the Hamiltonian vector field X_{H_V}, and the time-t Hamiltonian flow $\phi^t_{H_V}$ from Section 3.1. Consider the function $L_V \colon [0,1] \times TM \to \mathbb{R}$ given by:

$$L_V(t, q, v) = \frac{1}{2}|v|^2 - V(t, q), \tag{3.2.1}$$

where $t \in [0,1]$, $q \in M$, and $v \in T_qM$. For each $\gamma \in \Omega^{1,2}(M, q_0, q_1)$, let

$$\mathcal{A}_V(\gamma) = \int_0^1 L_V(t, \gamma, \dot{\gamma})\, dt. \tag{3.2.2}$$

It is well-known that $\mathcal{A}_V$ is a Morse function on $\Omega^{1,2}(M, q_0, q_1)$. Therefore we can define $CM_*(\Omega^{1,2}(M, q_0, q_1))$ as the Morse complex generated by the critical points of $\mathcal{A}_V$ and with

differential induced by $\mathcal{A}_V$ and the metric g. We omit the details which can be found in [AS06, Section 2] and simply denote the Morse homology group of $CM_*(\Omega^{1,2}(M, q_0, q_1))$ by $HM_*(\Omega^{1,2}(M, q_0, q_1))$.

Definition 3.2.1. *A* V-perturbed geodesic γ *is a map* $[0,1] \to M$ *such that*

$$\nabla_{\dot\gamma}\dot\gamma = -\nabla V, \tag{3.2.3}$$

where ∇V *denotes the gradient of* V *with respect to* g.

By a standard calculus of variations computation, the critical points of $\mathcal{A}_V$ on $\Omega^{1,2}(M, q_0, q_1)$ are exactly V-perturbed geodesics.

We now recall some standard facts following [AS06, Section 2.1]. Let $\mathcal{C}_{H_V}$ be the set of time-1 integral curves of X_{H_V} on T^*M and let $\mathcal{C}_{L_V}$ be the set of time-1 V-perturbed geodesics on M, i.e.,

$$\mathcal{C}_{H_V} \coloneqq \{\zeta : [0,1] \to T^*M \mid \zeta(t) = \phi^t_{H_V} \circ \zeta(0)\},$$
$$\mathcal{C}_{L_V} \coloneqq \{\gamma : [0,1] \to M \mid \nabla_{\dot\gamma}\dot\gamma = -\nabla V\}.$$

We define a map $\mathcal{L}\colon \mathcal{C}_{H_V} \to \mathcal{C}_{L_V}$ as follows: Given $\zeta \in \mathcal{C}_{H_V}$, let $\mathcal{L}(\zeta)$ be the path $[0,1] \to M$ given by

$$\mathcal{L}(\zeta)(t) \coloneqq \pi_M \circ \zeta(t).$$

One can verify that $\mathcal{L}(\zeta)$ satisfies (3.2.3) and hence belongs to $\mathcal{C}_{L_V}$.

We define the inverse map $\mathcal{L}^{-1}\colon \mathcal{C}_{L_V} \to \mathcal{C}_{H_V}$ as follows: Given $\gamma \in \mathcal{C}_{L_V}$, we define $\mathcal{L}^{-1}(\gamma)\colon [0,1] \to T^*M$ as

$$\mathcal{L}^{-1}(\gamma) \coloneqq (\gamma(t), dL(t, \gamma(t), \dot\gamma(t))|_{T^v_{(\gamma(t),\dot\gamma(t))}TM}), \tag{3.2.4}$$

where $T^v_{(\gamma(t),\dot\gamma(t))}TM$ is the vertical fiber $\ker D\pi_M \cong T_{\gamma(t)}M$ at $(\gamma(t), \dot\gamma(t)) \in TM$ and $\pi_M\colon TM \to M$ is the projection.

Definition 3.2.2. *We call* $\mathcal{L}$ *the* Legendre transform *and call* $\mathcal{L}^{-1}$ *the* inverse Legendre transform.

Remark 3.2.3. *Each generator* $y \in CF(\phi^1_{H_V}(T^*_{q_0}M), T^*_{q_1}M)$ *corresponds to a time-1 integral curve of* X_{H_V} *from* $T^*_{q_0}M$ *to* $T^*_{q_1}M$*:*

$$l_y \colon [0,1] \to T^*M, \quad l_y(t) = \phi^{t-1}_{H_V}(y). \tag{3.2.5}$$

We define $\mathcal{L}(y)$ *to be* $\mathcal{L}(l_y)$*. Conversely,* $\mathcal{L}^{-1}$ *maps each time-1 integral curve of* X_{H_V} *from* $T^*_{q_0}M$ *to* $T^*_{q_1}M$ *to a generator of* $CF(\phi^1_{H_V}(T^*_{q_0}M), T^*_{q_1}M)$*.*

Since the inclusion

$$\Omega^{1,2}(M, q_0, q_1) \hookrightarrow \Omega(M, q_0, q_1) \tag{3.2.6}$$

is a homotopy equivalence, we deduce that $HM_*(\Omega^{1,2}(M, q_0, q_1))$ is isomorphic to the singular homology group $H_*(\Omega(M, q_0, q_1))$.

When $q_0 = q_1 = q$, we get the based loop space

$$\Omega(M, q) = \{\gamma \in C^0([0,1], M) \mid \gamma(0) = \gamma(1) = q\}.$$

Theorem 3.2.4 (Theorem B of [AS10a])**.** *There is an isomorphism of graded algebras:*

$$H_{-*}(\Omega(M, q)) \to HW^*(T^*_q M). \tag{3.2.7}$$

In the opposite direction, Abouzaid constructed a chain level evaluation map

$$CW^*(T^*_q M) \to C_{-*}(\Omega(M, q)).$$

It induces an isomorphism on the level of homology:

$$\tilde{\mathcal{F}} \colon HW^*(T^*_q M) \to H_{-*}(\Omega(M, q)). \tag{3.2.8}$$

Remark 3.2.5. *Theorem 3.2.4 also holds for path spaces by [AS06], i.e., there is an isomorphism*

$$H_{-*}(\Omega(M, q_0, q_1)) \to HW^*(T^*_{q_0}M, T^*_{q_1}M) \tag{3.2.9}$$

where the right-hand side is the wrapped Floer homology group whose generators are time-1 Hamiltonian flows of $\phi^t_{H_V}$ *from* $T^*_{q_0}M$ *to* $T^*_{q_1}M$*.*

Let us now specialize to $M = \Sigma$, a closed oriented surface of genus greater than 0. In this case we further see:

Lemma 3.2.6. *$H_*(\Omega(\Sigma, q_0, q_1))$ is supported in degree 0.*

Proof. Recall that V is small in the $W^{1,2}$-norm. If Σ is a torus, then we can assume that g is the flat metric, where all V-perturbed geodesics with V sufficiently small are minimal and isolated. If the genus of Σ is greater than 1, then we can assume that g is the hyperbolic metric with constant curvature -1. It is well known that on a hyperbolic surface, there is a unique V-perturbed geodesic in each homotopy class of paths with fixed endpoints for V sufficiently small. For details the reader is referred to Milnor [Mil63, Lemma 19.1]. Hence the Morse indices of all critical points of $\Omega^{1,2}(\Sigma, q_0, q_1)$ are 0. □

Note that when $M = \Sigma$, all terms of (3.2.7) vanish except for $* = 0$ by Lemma 3.2.6. We write $HW(T^*_q\Sigma)$ for $HW^0(T^*_q\Sigma)$. Moreover, $H_0(\Omega(\Sigma, q))$ is isomorphic to the group algebra $\mathbb{Z}[\pi_1(\Sigma, q)]$ of the fundamental group $\pi_1(\Sigma, q)$.

3.3 The Hecke algebra

Theorem (3.2.4) and the isomorphism (3.2.8) relate $H_0(\Omega(\Sigma, q))$ to the wrapped Floer homology $HW(T^*_q\Sigma)$ of a single cotangent fiber, and represent the special case of $\kappa = 1$ in HDHF. In this section, we discuss the generalization of $H_0(\Omega(\Sigma, q))$ to $\kappa \geq 1$, which we show to be equivalent to $HW(\sqcup_i T^*_{q_i}\Sigma)$ in later sections.

Summary. Consider the loop space of the unordered configuration space of κ points on Σ. Its 0th homology is isomorphic to the group algebra of the braid group of Σ. The *braid skein algebra* $\mathrm{BSk}_\kappa(\Sigma, \mathbf{q})$, due to Morton and Samuelson [MS21, Definition 3.1], is a quotient of the group algebra of the braid group by the HOMFLY skein relation and the marked point relation. Here $\mathbf{q}$ is a κ-tuple of distinct points on Σ. By reformulating the marked point relation, we obtain the *surface Hecke algebra* $\mathrm{H}_\kappa(\Sigma, \mathbf{q})$ in Definition 3.3.4. This surface Hecke

algebra serves as an intermediary between the wrapped Floer homology and the braid skein algebra. On one hand, we show that $\mathrm{H}_\kappa(\Sigma, \mathbf{q})$ and $\mathrm{BSk}_\kappa(\Sigma)$ are isomorphic up to a change of variables in Proposition 3.3.5. On the other hand, we will construct an evaluation map from the wrapped Floer homology to $\mathrm{H}_\kappa(\Sigma, \mathbf{q})$ in Section 3.5.1.

Note that the braid skein algebra for $\Sigma = T^2$ is isomorphic to the double affine Hecke algebra (DAHA) of $\mathfrak{gl}_\kappa$ [MS21, Theorem 3.7]. Hence $\mathrm{H}_\kappa(T^2, \mathbf{q})$ is also isomorphic to the DAHA.

Let $\mathrm{UConf}_\kappa(\Sigma) = \{\{q_1, \ldots, q_\kappa\} \mid q_i \in \Sigma,\ q_i \neq q_j \text{ for } i \neq j\}$ be the configuration space of κ unordered points on Σ. Fix a basepoint $\mathbf{q} \in \mathrm{UConf}_\kappa(\Sigma)$. The based loop space $\Omega(\mathrm{UConf}_\kappa(\Sigma), \mathbf{q})$ consists of κ-strand braids in Σ. Note that $H_0(\Omega(\mathrm{UConf}_\kappa(\Sigma), \mathbf{q}))$ is isomorphic to the group algebra $\mathbb{Z}[\mathrm{Br}_\kappa(\Sigma, \mathbf{q})]$, where $\mathrm{Br}_\kappa(\Sigma, \mathbf{q})$ denotes the braid group of Σ.

Fix a marked point $\star \in \Sigma$ which is disjoint from $\mathbf{q}$. Let $\mathrm{Br}_{\kappa,1}(\Sigma, \mathbf{q}, \star)$ be the subgroup of $\mathrm{Br}_{\kappa+1}(\Sigma, \mathbf{q} \sqcup \{\star\})$ consisting of braids whose last strand connects $\star$ to itself by a straight line in $[0, 1] \times \Sigma$.

Definition 3.3.1 (Morton-Samuelson)**.** *The braid skein algebra* $\mathrm{BSk}_\kappa(\Sigma, \mathbf{q})$ *is the quotient of the group algebra* $\mathbb{Z}[s^{\pm 1}, c^{\pm 1}][\mathrm{Br}_{\kappa,1}(\Sigma, \mathbf{q}, \star)]$ *by two local relations:*

1. *the HOMFLY skein relation*

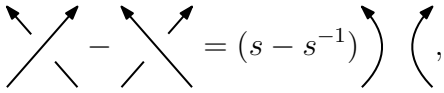

(3.3.1)

2. *the marked point relation* $P = c^2$

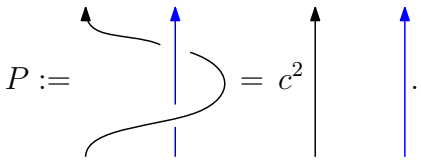

(3.3.2)

Here the black lines are strands between basepoints in $\mathbf{q}$ *and the straight blue line connects the marked point* $\star$ *to itself.*

The product is given by the concatenation of braids.

For the purposes of relating $\mathrm{BSk}_\kappa(\Sigma, \mathbf{q})$ to the wrapped Floer homology, it is more convenient to give another description of the marked point relation (3.3.2). Let

$$\begin{aligned} &\Omega(\mathrm{UConf}_\kappa(\Sigma \setminus \{\star\}), \mathbf{q}) \\ &\quad = \{\gamma \in C^0([0,1], \mathrm{UConf}_\kappa(\Sigma \setminus \{\star\})) \mid \gamma(0) = \gamma(1) = \mathbf{q}\}. \end{aligned} \tag{3.3.3}$$

Given $\gamma_1, \gamma_2 \in \Omega(\mathrm{UConf}_\kappa(\Sigma \setminus \{\star\}), \mathbf{q})$ viewed as based loops on $\mathrm{UConf}_\kappa(\Sigma)$, let $H\colon [0,1]^2 \to \mathrm{UConf}_\kappa(\Sigma)$ be a homotopy between γ_1 and γ_2 relative to the boundary, i.e.,

$$H(t,0) = \gamma_1(t), \quad H(t,1) = \gamma_2(t), \quad H(0,s) = H(1,s) = \mathbf{q}.$$

Note that the homotopy H may intersect the marked point $\star$. Let

$$Y = \{\{p_1, \ldots, p_\kappa\} \in \mathrm{UConf}_\kappa(\Sigma) \mid p_i = \star \text{ for some } i\};$$

it is a codimension two submanifold of $\mathrm{UConf}_\kappa(\Sigma)$. Define $\langle H, \star\rangle \coloneqq \langle H, Y\rangle$, the algebraic intersection number of H and Y. This is well-defined since $H(\partial([0,1]^2)) \cap Y = \varnothing$.

We identify $H_0(\Omega(\mathrm{UConf}_\kappa(\Sigma \setminus \{\star\}), \mathbf{q}))$ with the group algebra $\mathbb{Z}[\mathrm{Br}_\kappa(\Sigma \setminus \{\star\}, \mathbf{q})]$ of the braid group $\mathrm{Br}_\kappa(\Sigma \setminus \{\star\}, \mathbf{q})$.

Definition 3.3.2. *The c-deformed braid group $\mathrm{Br}_\kappa(\Sigma, \mathbf{q})_c$ of Σ is generated by $\mathrm{Br}_\kappa(\Sigma \setminus \{\star\}, \mathbf{q})$ and a central element c, subject to the following c-deformed homotopy relation:*

$$[\gamma_2] = c^{2\langle H, \star\rangle}[\gamma_1], \tag{3.3.4}$$

where $\gamma_i \in \Omega(\mathrm{UConf}_\kappa(\Sigma \setminus \{\star\}), \mathbf{q})$, H is the homotopy between them as above, and $[\gamma_i] \in H_0(\Omega(\mathrm{UConf}_\kappa(\Sigma \setminus \{\star\}), \mathbf{q})) \cong \mathbb{Z}[\mathrm{Br}_\kappa(\Sigma \setminus \{\star\}, \mathbf{q})]$.

Remark 3.3.3. *The group algebra $\mathbb{Z}[\mathrm{Br}_\kappa(\Sigma, \mathbf{q})_c]$ is naturally isomorphic to the quotient of $C_0(\Omega(\mathrm{UConf}_\kappa(\Sigma \setminus \{\star\}), \mathbf{q})) \otimes \mathbb{Z}[c^{\pm 1}]$ by the c-deformed homotopy relation (3.3.4).*

See Figure 3.1 for an example when $\kappa = 1$ and $\langle H, Y\rangle = 1$.

Specializing to $c = 1$, $\mathrm{Br}_\kappa(\Sigma, \mathbf{q})_c$ recovers $\mathrm{Br}_\kappa(\Sigma, \mathbf{q})$. Hence there is a central extension of groups:

$$0 \to \langle c\rangle \to \mathrm{Br}_\kappa(\Sigma, \mathbf{q})_c \to \mathrm{Br}_\kappa(\Sigma, \mathbf{q}) \to 0, \tag{3.3.5}$$

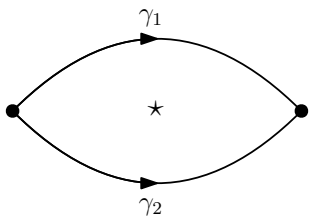

Figure 3.1: The deformed homotopy relation $[\gamma_2] = c^2[\gamma_1]$. Both dotted points are $q \in \Sigma$.

where $\langle c \rangle$ is the free abelian group generated by c.

Let $\langle \mathrm{Br}_{\kappa,1}(\Sigma, \mathbf{q}, \star), c \rangle$ denote the group generated by $\mathrm{Br}_{\kappa,1}(\Sigma, \mathbf{q}, \star)$ and a central element c. Define the group $\mathrm{Br}_\kappa(\Sigma, \mathbf{q})'_c$ as the quotient of $\langle \mathrm{Br}_{\kappa,1}(\Sigma, \mathbf{q}, \star), c \rangle$ by the marked point relation $P = c^2$ (3.3.2). There are two natural projections from $\langle \mathrm{Br}_{\kappa,1}(\Sigma, \mathbf{q}, \star), c \rangle$ to $\mathrm{Br}_\kappa(\Sigma, \mathbf{q})'_c$ and $\mathrm{Br}_\kappa(\Sigma, \mathbf{q})_c$, respectively:

$$\begin{array}{ccc} & \langle \mathrm{Br}_{\kappa,1}(\Sigma, \mathbf{q}, \star), c \rangle & \\ {\scriptstyle P=c^2}\swarrow & & \searrow \\ \mathrm{Br}_\kappa(\Sigma, \mathbf{q})'_c & \xrightarrow{\quad\phi\quad} & \mathrm{Br}_\kappa(\Sigma, \mathbf{q})_c \end{array}$$

The relation $P = c^2$ also holds in $\mathrm{Br}_\kappa(\Sigma, \mathbf{q})_c$. Therefore, there is a natural induced map $\phi \colon \mathrm{Br}_\kappa(\Sigma, \mathbf{q})'_c \to \mathrm{Br}_\kappa(\Sigma, \mathbf{q})_c$.

The algebra $\mathrm{Br}_\kappa(\Sigma, \mathbf{q})'_c$ also fits into a central extension similar to (3.3.5):

$$0 \to \langle c \rangle \to \mathrm{Br}_\kappa(\Sigma, \mathbf{q})'_c \to \mathrm{Br}_\kappa(\Sigma, \mathbf{q}) \to 0.$$

Moreover, the following diagram commutes:

$$\begin{array}{ccccccccc} 0 & \longrightarrow & \langle c \rangle & \longrightarrow & \mathrm{Br}_\kappa(\Sigma, \mathbf{q})_c & \longrightarrow & \mathrm{Br}_\kappa(\Sigma, \mathbf{q}) & \longrightarrow & 0 \\ & & \| & & \uparrow{\scriptstyle \phi} & & \| & & \\ 0 & \longrightarrow & \langle c \rangle & \longrightarrow & \mathrm{Br}_\kappa(\Sigma, \mathbf{q})'_c & \longrightarrow & \mathrm{Br}_\kappa(\Sigma, \mathbf{q}) & \longrightarrow & 0. \end{array}$$

By the Five Lemma, ϕ is an isomorphism.

Recall from Definition 3.3.1 that the braid skein algebra $\mathrm{BSk}_\kappa(\Sigma, \mathbf{q})$ is the quotient of $\mathbb{Z}[s^{\pm 1}][\mathrm{Br}_\kappa(\Sigma, \mathbf{q})'_c]$ by the skein relation (3.3.1). We introduce the variable $\hbar = s - s^{-1}$ and add the corresponding skein relation to $\mathrm{Br}_\kappa(\Sigma, \mathbf{q})_c$.

Definition 3.3.4. *The Hecke algebra* $\mathrm{H}_\kappa(\Sigma, \mathbf{q})$ *of* Σ *is the quotient of the group algebra* $\mathbb{Z}[\hbar][\mathrm{Br}_\kappa(\Sigma, \mathbf{q})_c]$ *by the local skein relation:*

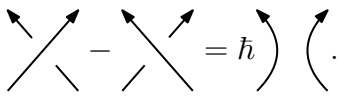

(3.3.6)

Proposition 3.3.5. *The algebra* $\mathrm{H}_\kappa(\Sigma, \mathbf{q})$ *is naturally isomorphic to* $\mathrm{BSk}_\kappa(\Sigma, \mathbf{q})$*, up to a change of variables* $\hbar = s - s^{-1}$*.*

Finally, we consider the degeneration $\hbar = 0$ for later use. The skein relation (3.3.6) then reduces to the symmetric group relation. Further setting $c = 1$, we have $\mathrm{H}_\kappa(\Sigma, \mathbf{q})|_{\hbar=0,c=1} \cong \mathbb{Z}[(\prod_i \pi_1(\Sigma, q_i)) \rtimes S_\kappa]$, where the symmetric group S_κ acts on $\prod_i \pi_1(\Sigma, q_i)$ by permuting the factors. Adding the parameter c, let $\pi_1(\Sigma, q)_c$ denote $\mathrm{Br}_1(\Sigma, q)_c$, the 1-strand c-deformed braid group. Its group algebra $\mathbb{Z}[\pi_1(\Sigma, q)_c]$ is a $\mathbb{Z}[c^{\pm 1}]$-algebra. The following is straightforward.

Lemma 3.3.6. *There is an isomorphism of* $\mathbb{Z}[c^{\pm 1}]$*-algebras:*

$$\mathrm{H}_\kappa(\Sigma, \mathbf{q})|_{\hbar=0} \cong (\otimes_i \mathbb{Z}[\pi_1(\Sigma, q_i)_c]) \rtimes S_\kappa, \tag{3.3.7}$$

where the tensor product is over $\mathbb{Z}[c^{\pm 1}]$*.*

3.4 The parameter c in HDHF

Motivated by the c-deformed homotopy relation (3.3.4), in this section we define $CW(\sqcup_i T^*_{q_i}\Sigma)_c$, the wrapped HDHF homology of disjoint cotangent fibers with an additional parameter c. We inherit the notation from Section 3.1.

Let $CF(\phi^1_{H_V}(\sqcup_i T^*_{q_i}\Sigma), \sqcup_i T^*_{q_i}\Sigma)_c \coloneqq CF(\phi^1_{H_V}(\sqcup_i T^*_{q_i}\Sigma), \sqcup_i T^*_{q_i}\Sigma) \otimes \mathbb{Z}[c^{\pm 1}]$.

Given $u \in \mathcal{M}(\mathbf{y}_1, \ldots, \mathbf{y}_m, \mathbf{y}_0)$ of index 0 or 1, consider its projection to Σ and denote the image by $\pi_\Sigma(u)$. We enhance the A_∞-operations from Section 3.1 to include c-coefficients by keeping track of modified intersections of $\pi_\Sigma \circ u$ and a fixed marked point $\star \in \Sigma$. Note that we cannot directly take the intersection number of $\pi_\Sigma(u)$ and $\star$ since the boundary of $\pi_\Sigma(u)$ could cross $\star$ in a generic 1-parameter family and the A_∞-relation would not be satisfied.

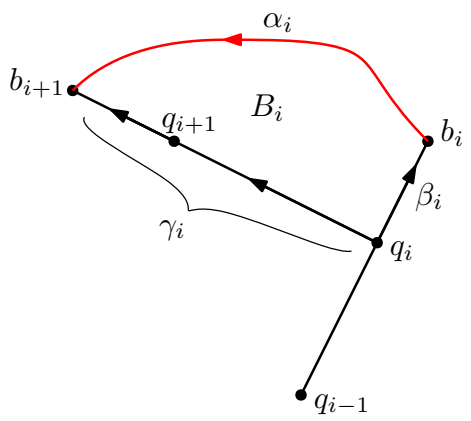

Figure 3.2: The projection of some curve u to Σ. The path α_i is the projection of some component $\partial_i \dot{F} \subset \partial \dot{F}$. We choose any homotopy from α_i to $-\beta_i + \gamma_i$, where the relative homology class B_i that is swept out does not depend on the choice of homotopy. Note that q_i, q_{i+1} and b_{i+1} lie on the same V-perturbed geodesic.

To remedy this issue, we carefully choose the marked point $\star \in \Sigma$ and modify $\pi_\Sigma(u)$. Consider the set of V-perturbed geodesics (see Definition 3.2.1) with endpoints in $\{q_1, \ldots, q_\kappa\}$. Since there are only countably many such V-perturbed geodesics, we can choose a generic marked point $\star \in \Sigma$ in the complement of the images of these perturbed geodesics.

We then homotop the boundary of $\pi_\Sigma(u)$ on Σ to piecewise V-perturbed geodesics, which can be guaranteed to be disjoint from $\star$. Specifically, suppose the domain of u is $\dot{F}$ and $\{p_{i-1}, p_i, p_{i+1}\}$ are three consecutive boundary punctures on ∂F, ordered according to the boundary orientation of ∂F. Write $\pi_{T^*\Sigma} \circ u(p_i)$ etc. for the values of the continuous extensions of $\pi_{T^*\Sigma} \circ u$ to the puncture p_i etc. Denote the boundary arc from p_i to p_{i+1} by $\partial_i \dot{F}$. Suppose the cotangent fibers $T^*_{q_{i-1}}\Sigma$, $T^*_{q_i}\Sigma$ and $T^*_{q_{i+1}}\Sigma$ are wrapped using the wrapping functions ψ_{i-1}, ψ_i and ψ_{i+1}, respectively. For $r = 0, 1$, suppose $\pi_{T^*\Sigma} \circ u(p_{i+r}) \in \psi_{i+r-1}(T^*_{q_{i+r-1}}\Sigma) \cap \psi_{i+r}(T^*_{q_{i+r}}\Sigma)$, which corresponds to the intersection of two Hamiltonian chords that start from $T^*_{q_{i+r-1}}\Sigma$ and $T^*_{q_{i+r}}\Sigma$. The Legendre transforms of these Hamiltonian chords (see Definition 3.2.2) correspond to certain V-perturbed geodesics on Σ: Let β_{i+r-1} be that from q_{i+r-1} to b_{i+r-1}, and γ_{i+r-1} be that from q_{i+r-1} to b_{i+r}, where $b_i = \pi_\Sigma \circ u(p_i)$. Observe that q_i, q_{i+1} and b_{i+1} lie on the same V-perturbed geodesic. Let α_i be the path $\pi_\Sigma \circ u(\partial_i \dot{F})$. See Figure

3.2.

Fix parametrizations of α_i, β_i and γ_i by the interval $[0,1]$. Note that α_i and $\beta_i^{-1}\cdot\gamma_i$ are homotopic as paths from b_i to b_{i+1}; this is due to the facts that α_i, β_i and γ_i are all projections of paths in $\psi_i(T^*_{q_i}\Sigma)$ and that $T^*_{q_i}\Sigma$ is contractible. Let B_i be a homotopy between α_i and $\beta_i^{-1}\cdot\gamma_i$ relative to boundary. We extend the image $\pi_\Sigma(u)$ on Σ by the homotopy B_i for all $\partial_i\dot{F}\subset\partial\dot{F}$ so that its new boundary lies in $C\coloneqq\bigcup_i(\beta_i\cup\gamma_i)$; this defines a relative homology class $[\pi_\Sigma(u)]'\in H_2(\Sigma,C)$.

Given two homotopies B_i and B_i' from α_i to $\beta_i^{-1}\cdot\gamma_i$, their difference determines a map $S^2\to\Sigma$, which induces the zero map on $H_2(S^2)\to H_2(\Sigma,C)$. Hence $[\pi_\Sigma(u)]'$ does not depend on the choice of $\{B_i\}$ and the algebraic intersection number $\langle u,\star\rangle\coloneqq\langle[\pi_\Sigma(u)]',\star\rangle$ is well-defined.

We modify the μ^m-composition map so that

$$\mu^m(\mathbf{y}_1,\dots,\mathbf{y}_m)=\sum_{u\in\mathcal{M}^{\mathrm{ind}=0}(\mathbf{y}_1,\dots,\mathbf{y}_m,\mathbf{y}_0)} c^{2\langle u,\star\rangle}\cdot\hbar^{\kappa-\chi(u)}\cdot\mathbf{y}_0, \tag{3.4.1}$$

where u ranges over curves of index 0.

Since C is disjoint from $\star$, $\langle u,\star\rangle$ is constant for any 1-parameter family of u. Therefore, by analyzing the degeneration of index-1 moduli spaces, we see that $CW(\sqcup_i T^*_{q_i}\Sigma)_c$ is an A_∞-algebra. Proposition 3.1.5 can then be improved to:

Proposition 3.4.1. *The A_∞-algebra $CW(\sqcup_i T^*_{q_i}\Sigma)_c$ is supported in degree zero, and hence is an ordinary algebra.*

3.5 The evaluation map

Following Abouzaid [Abo12], we construct the evaluation map

$$\mathcal{F}\colon CW(\sqcup_i T^*_{q_i}\Sigma)_c\to \mathrm{H}_\kappa(\Sigma)\otimes_{\mathbb{Z}[\hbar]}\mathbb{Z}[[\hbar]]$$

in Section 3.5.1. It is given by counting holomorphic curves between cotangent fibers and the zero section of $T^*\Sigma$ in the framework of HDHF. We then show that $\mathcal{F}$ is a homomorphism

of algebras in Section 3.5.2. The key ingredient is the holomorphic curve interpretation of the HOMFLY skein relation due to Ekholm-Shende [ES19]. We finally prove Theorem 1.0.4 which states that the map $\mathcal{F}$ is an isomorphism.

3.5.1 The definition

At this point we rename D_m as T_{m-1}, where $\partial_i T_{m-1} = \partial_i D_m$ for $i = 0, \dots, m$. The disk T_{m-1} will be the A_∞ base direction, where $p_1, \dots, p_{m-1} \in \partial D_m = \partial T_{m-1}$ correspond to inputs (κ-tuples of intersection points) and $\partial_m D_m = \partial_m T_{m-1}$ corresponds to the output (κ-tuples of arcs on Σ). Let $\mathcal{T}_{m-1}$ be the moduli space of T_{m-1} modulo automorphisms; again we choose representatives T_{m-1} of equivalence classes of $\mathcal{T}_{m-1}$ in a smooth manner.

Let $\pi_{T^*\Sigma}$ be the projection $T_{m-1} \times T^*\Sigma \to T^*\Sigma$. Choose a sufficiently generic consistent collection $T_{m-1} \mapsto J_{T_{m-1}}$ of compatible almost complex structures on $T_{m-1} \times T^*\Sigma$ for all $T_{m-1} \in \mathcal{T}_{m-1}$ and all $m \geq 2$ such that $J_{T_{m-1}}$ is close to a split almost complex structure on $T_{m-1} \times T^*\Sigma$ and which projects holomorphically to T_{m-1}.

Recall that $\phi^t_{H_V}$ is the time-t Hamiltonian flow of (3.1.1). We will refer to Σ as the zero section of $T^*\Sigma$ when it is clear from the context. Let $\mathbf{q}$ (resp. $\mathbf{q}'$) be the set of intersection points between $\phi^1_{H_V}(\sqcup_i T^*_{q_i}\Sigma)$ (resp. $\sqcup_i T^*_{q_i}\Sigma$) and Σ and let $\mathbf{y} \in CF(\phi^1_{H_V}(\sqcup_i T^*_{q_i}\Sigma), \sqcup_i T^*_{q_i}\Sigma)$.

We define $\mathcal{H}(\mathbf{q}, \mathbf{y}, \mathbf{q}')$ as the moduli space of maps

$$u \colon (\dot{F}, j) \to (T_1 \times T^*\Sigma, J_{T_1}),$$

where (F, j) is a compact Riemann surface with boundary, $\mathbf{p}_0, \mathbf{p}_1, \mathbf{p}_2$ are disjoint tuples of

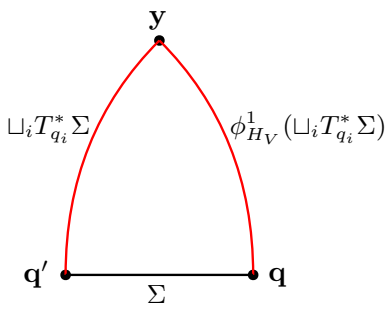

Figure 3.3: The A_∞ base direction T_1 for $\mathcal{H}(\mathbf{q}, \mathbf{y}, \mathbf{q}')$. The notation denotes the corresponding preimages of π_{T_1} in $T^*\Sigma$, e.g., p_0 is denoted by $\mathbf{q}$ since $\pi_{T^*\Sigma} \circ u$ tends to $\mathbf{q}$ as $\pi_{T_1} \circ u \to p_0$.

boundary punctures of F and $\dot{F} = F \setminus \cup_i \mathbf{p}_i$ so that u satisfies

$$\begin{cases} du \circ j = J_{T_1} \circ du; \\ \pi_{T^*\Sigma} \circ u(z) \in \phi^1_{H_V}(\sqcup_i T^*_{q_i}\Sigma) \text{ if } \pi_{T_1} \circ u(z) \subset \partial_0 T_1; \\ \text{each component of } \partial\dot{F} \text{ that projects to } \partial_0 T_1 \text{ maps to a distinct } \phi^1_{H_V}(T^*_{q_i}\Sigma); \\ \pi_{T^*\Sigma} \circ u(z) \in \sqcup_i T^*_{q_i}\Sigma \text{ if } \pi_{T_1} \circ u(z) \subset \partial_1 T_1; \\ \text{each component of } \partial\dot{F} \text{ that projects to } \partial_1 T_1 \text{ maps to a distinct } T^*_{q_i}\Sigma; \\ \pi_{T^*\Sigma} \circ u(z) \in \Sigma \text{ if } \pi_{T_1} \circ u(z) \subset \partial_2 T_1; \\ \pi_{T^*\Sigma} \circ u \text{ tends to } \mathbf{q} \text{ as } s_0 \to -\infty; \\ \pi_{T^*\Sigma} \circ u \text{ tends to } \mathbf{y} \text{ as } s_1 \to +\infty; \\ \pi_{T^*\Sigma} \circ u \text{ tends to } \mathbf{q}' \text{ as } s_2 \to +\infty; \\ \pi_{T_1} \circ u \text{ is a } \kappa\text{-fold branched cover of a fixed } T_1 \in \mathcal{T}_1, \end{cases}$$

where we follow conventions of (2.0.1). See Figure 3.3.

Lemma 3.5.1. *Fixing generic J_{T_1}, $\mathcal{H}(\mathbf{q}, \mathbf{y}, \mathbf{q}')$ is of dimension 0 and consists of discrete regular curves for all $\mathbf{q}$, $\mathbf{y}$ and $\mathbf{q}'$.*

Proof. By the discussion before Lemma 3.1.4, $|q_1| = \cdots = |q_\kappa| = |q'_1| = \cdots = |q'_\kappa|$=0. Hence $|\mathbf{q}| = |\mathbf{q}'| = 0$. By Lemma 3.1.4, $|\mathbf{y}| = 0$. We then see that the virtual dimension of $\mathcal{H}(\mathbf{q}, \mathbf{y}, \mathbf{q}')$ is 0 by the index formula (2.0.4); note that the same index formula holds even when we do not assume that the copies of the zero section Σ are disjoint. The lemma then follows from standard transversality arguments. □

Let $\mathcal{H}^\chi(\mathbf{q}, \mathbf{y}, \mathbf{q}')$ be the subset of $\mathcal{H}(\mathbf{q}, \mathbf{y}, \mathbf{q}')$ such that $\chi(\dot{F}) = \chi$.

Lemma 3.5.2. *Given* $\mathbf{q}$, $\mathbf{y}$ *and* $\mathbf{q}'$, *the moduli space* $\mathcal{H}^\chi(\mathbf{q}, \mathbf{y}, \mathbf{q}')$ *consists of finitely many curves for each Euler characteristic* χ.

Proof. Each $\mathbf{y}$ determines a unique $\mathbf{q}$ and $\mathbf{q}'$. Since there is an energy bound for curves in $\mathcal{H}(\mathbf{q}, \mathbf{y}, \mathbf{q}')$, by Gromov compactness, $\mathcal{H}(\mathbf{q}, \mathbf{y}, \mathbf{q}')$ contains a finite number of curves for each χ. □

Fix a parametrization of the arc $\partial_2 T_1$ from p_0 to p_2 by $\tau\colon [0,1] \to \partial_2 T_1$. There exists a sufficiently generic consistent collection $\{T_m \mapsto J_{T_m}\}$ such that for all $u \in \mathcal{H}(\mathbf{q}, \mathbf{y}, \mathbf{q}')$, $(\pi_{T^*\Sigma} \circ u) \circ (\pi_{T_1} \circ u)^{-1} \circ \tau(t)$ consists of κ distinct points on $\Sigma \setminus \{\star\}$ for each $t \in [0,1]$ and hence gives a path in $\mathrm{UConf}_\kappa(\Sigma \setminus \{\star\})$:

$$\gamma(u)\colon [0,1] \to \mathrm{UConf}_\kappa(\Sigma \setminus \{\star\}), \quad t \mapsto (\pi_{T^*\Sigma} \circ u) \circ (\pi_{T_1} \circ u)^{-1} \circ \tau(t).$$

Define

$$\Omega(\mathrm{UConf}_\kappa(\Sigma \setminus \{\star\}), \mathbf{q}, \mathbf{q}') = \{\gamma\colon [0,1] \to \mathrm{UConf}_\kappa(\Sigma \setminus \{\star\}) \mid \gamma(0) = \mathbf{q}, \gamma(1) = \mathbf{q}'\}.$$

Then $\gamma(u) \in \Omega(\mathrm{UConf}_\kappa(\Sigma \setminus \{\star\}), \mathbf{q}, \mathbf{q}')$.

For $u \in \mathcal{H}(\mathbf{q}, \mathbf{y}, \mathbf{q}')$, we can define $[\pi_\Sigma(u)]'$ as in Section 3.4: We extend the image $\pi_\Sigma(u)$ by the homotopies B_i from Section 3.4, where $\partial_i \dot{F}$ ranges over all boundary arcs of $\partial \dot{F}$ which are not of "output type". Here $\partial_i \dot{F}$ is of "output type" if $\pi_{T_1} \circ u(\partial_i \dot{F}) \subset \partial_2 T_1$. We then define the algebraic intersection number

$$\langle u, \star \rangle \coloneqq \langle [\pi_\Sigma(u)]', \star \rangle.$$

We now define the evaluation map

$$\begin{aligned} \mathcal{E}\colon CW(\sqcup_i T^*_{q_i}\Sigma)_c \to C_0(\Omega(\mathrm{UConf}_\kappa(\Sigma \setminus \{\star\}), \mathbf{q}, \mathbf{q}')) \otimes \mathbb{Z}[c^{\pm 1}] \otimes \mathbb{Z}[[\hbar]], \qquad (3.5.1) \\ \mathbf{y} \mapsto \sum_{u \in \mathcal{H}(\mathbf{q}, \mathbf{y}, \mathbf{q}')} c^{2\langle u, \star \rangle} \cdot \hbar^{\kappa - \chi(u)} \cdot \gamma(u). \end{aligned}$$

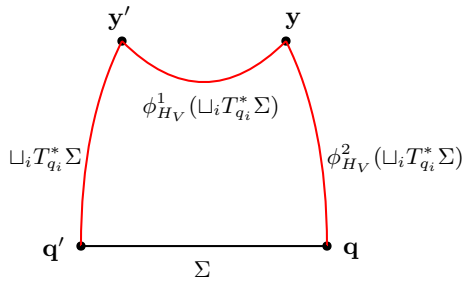

Figure 3.4: The A_∞ base direction T_2 for $\mathcal{H}(\mathbf{q}, \mathbf{y}, \mathbf{y}', \mathbf{q}')$.

The Hamiltonian flow $\phi^t_{H_V}$ of (3.1.1) fixes the zero section Σ and hence $\mathbf{q}' = \mathbf{q}$. Note that $\Omega(\mathrm{UConf}_\kappa(\Sigma \setminus \{\star\}), \mathbf{q}, \mathbf{q}) = \Omega(\mathrm{UConf}_\kappa(\Sigma \setminus \{\star\}), \mathbf{q})$ as in (3.3.3). By Definitions 3.3.2 and 3.3.4 there is a natural projection map

$$\mathcal{P}\colon C_0(\Omega(\mathrm{UConf}_\kappa(\Sigma \setminus \{\star\}), \mathbf{q})) \otimes \mathbb{Z}[c^{\pm 1}] \otimes \mathbb{Z}[[\hbar]] \to \mathrm{H}_\kappa(\Sigma, \mathbf{q}) \otimes_{\mathbb{Z}[\hbar]} \mathbb{Z}[[\hbar]], \tag{3.5.2}$$

by first taking the c-deformed homotopy class and then quotienting by the skein relation. We finally define the evaluation map

$$\mathcal{F} = \mathcal{P} \circ \mathcal{E}\colon CW(\sqcup_i T^*_{q_i}\Sigma)_c \to \mathrm{H}_\kappa(\Sigma, \mathbf{q}) \otimes_{\mathbb{Z}[\hbar]} \mathbb{Z}[[\hbar]]. \tag{3.5.3}$$

Note that $\mathcal{E}$ depends on the choice of the parametrization τ but $\mathcal{F}$ does not.

3.5.2 The isomorphism

Both the domain and target of the map $\mathcal{F}$ in (3.5.3) are ordinary algebras. We will show that $\mathcal{F}$ is an isomorphism of algebras in this subsection.

We consider a moduli space of curves whose A_∞ base direction is $T_2 \in \mathcal{T}_2$. See Figure 3.4. In this case, a 1-parameter family of $T_2 \in \mathcal{T}_2$ may degenerate into broken curves in $\partial\mathcal{T}_2$ as shown in Figure 3.5. As in Section 3.1, we need to modify the consistent collection near the point T_2' of $\partial\mathcal{T}_2$ corresponding to the left-hand side of Figure 3.5.

Let $U \subset V$ be ends of $\mathcal{T}_2$ that limit to T_2' such that each $T_2 \in V$ is close to breaking into $D_2 \cup T_1$ and $U \cup \{T_2'\}$ is a relatively compact subset of $V \cup \{T_2'\}$ in $\overline{\mathcal{T}}_2$. For each $T_2 \in V$ we choose the neck region $N(T_2)$ (chosen to be smoothly dependent on T_2) such that

$T_2 \setminus N(T_2)$ is independent of T_2 and write T_2^+ and T_2^- for the two components of $T_2 \setminus N(T_2)$ corresponding to D_2 and T_1, respectively.

We then modify $T_2 \mapsto J_{T_2}$ to $T_2 \mapsto J_{T_2}^\Diamond$ such that:

$$J_{T_2}^\Diamond = \begin{cases} J_{T_2} \text{ for } T_2 \in \mathcal{T}_2 \setminus V; \\ J_{T_2} = J_{D_2} \text{ on } T_2^+ \text{ for } T_2 \in V; \\ J_{D_2} \text{ on } T_2^+ \cup N(T_2) \text{ for } T_2 \in U; \\ \psi_*^{1/2} J_{T_1} \text{ on } N(T_2) \cup T_2^- \text{ for } T_2 \in U, \end{cases}$$

where ψ^ρ is the time-log ρ Liouville flow defined in Section 3.1. Note that the definition of $J_{T_2}^\Diamond$ above can be taken to agree on the overlap. Given $\mathbf{y} \in CF(\phi^2_{H_V}(\sqcup_i T^*_{q_i}\Sigma), \phi^1_{H_V}(\sqcup_i T^*_{q_i}\Sigma))_c$ and $\mathbf{y}' \in CF(\phi^1_{H_V}(\sqcup_i T^*_{q_i}\Sigma), \sqcup_i T^*_{q_i}\Sigma)_c$, let $\mathcal{H}(\mathbf{q}, \mathbf{y}, \mathbf{y}', \mathbf{q}')$ be the moduli space of of maps $u\colon (\dot{F}, j) \to (T_2 \times T^*\Sigma, J_{T_2}^\Diamond)$, where (F, j) is a compact Riemann surface with boundary, $T_2 \in \mathcal{T}_2$, $\mathbf{p}_0, \ldots, \mathbf{p}_3$ are disjoint tuples of boundary punctures of F and $\dot{F} = F \setminus \cup_i \mathbf{p}_i$ so that u satisfies:

$$\begin{cases} du \circ j = J_{T_2}^\Diamond \circ du; \\ \pi_{T^*\Sigma} \circ u(z) \in \Psi(\pi_{T_2} \circ u(z))(\sqcup_i T^*_{q_i}\Sigma) \text{ if } \pi_{T_2} \circ u(z) \subset \partial_0 T_2; \\ \text{each component of } \partial\dot{F} \text{ that projects to } \partial_0 T_2 \text{ maps to a distinct} \\ \Psi(\pi_{T_2} \circ u(z))(T^*_{q_i}\Sigma); \\ \pi_{T^*\Sigma} \circ u(z) \in \phi^1_{H_V}(\sqcup_i T^*_{q_i}\Sigma) \text{ if } \pi_{T_2} \circ u(z) \subset \partial_1 T_2; \\ \text{each component of } \partial\dot{F} \text{ that projects to } \partial_1 T_2 \text{ maps to a distinct } \phi^1_{H_V}(T^*_{q_i}\Sigma); \\ \pi_{T^*\Sigma} \circ u(z) \in \sqcup_i T^*_{q_i}\Sigma \text{ if } \pi_{T_2} \circ u(z) \subset \partial_2 T_2; \\ \text{each component of } \partial\dot{F} \text{ that projects to } \partial_2 T_2 \text{ maps to a distinct } T^*_{q_i}\Sigma; \\ \pi_{T^*\Sigma} \circ u(z) \in \Sigma \text{ if } \pi_{T_2} \circ u(z) \subset \partial_3 T_2; \\ \pi_{T^*\Sigma} \circ u \text{ tends to } \mathbf{q} \text{ as } s_0 \to -\infty; \\ \pi_{T^*\Sigma} \circ u \text{ tends to } \mathbf{y} \text{ as } s_1 \to +\infty; \\ \pi_{T^*\Sigma} \circ u \text{ tends to } \mathbf{y}' \text{ as } s_2 \to +\infty; \\ \pi_{T^*\Sigma} \circ u \text{ tends to } \mathbf{q}' \text{ as } s_3 \to +\infty; \\ \pi_{T_2} \circ u \text{ is a } \kappa\text{-fold branched cover of some } T_2 \in \mathcal{T}_2, \end{cases}$$

where we follow conventions of (2.0.1) and $\Psi\colon \partial_0 T_2 \to \mathrm{Symp}(T^*\Sigma, \omega)$ depends smoothly on $T_2 \in \mathcal{T}_2$ such that

$$\Psi = \begin{cases} \phi^2_{H_V} \text{ for } T_2 \in \mathcal{T}_2 \setminus V; \\ \phi^2_{H_V} \text{ on } \partial_0 T_2 \setminus N(T_2) \text{ for } T_2 \in V; \\ \psi^{1/2} \circ \phi^1_{H_V} \text{ on } \partial_0 T_2 \cap (N_-(T_2) \cup T_2^-) \text{ for } T_2 \in U, \end{cases}$$

where $N_-(T_2)$ is the bottom half of $N(T_2)$ (the part adjacent to T_2^-).

Lemma 3.5.3. *There exists a sufficiently generic consistent collection of almost complex structures such that $\mathcal{H}(\mathbf{q}, \mathbf{y}, \mathbf{y}', \mathbf{q}')$ is of dimension 1 and is transversely cut out for all $\mathbf{q}$, $\mathbf{y}$, $\mathbf{y}'$ and $\mathbf{q}'$. Moreover, $\mathcal{H}(\mathbf{q}, \mathbf{y}, \mathbf{y}', \mathbf{q}')$ admits a compactification $\overline{\mathcal{H}}(\mathbf{q}, \mathbf{y}, \mathbf{y}', \mathbf{q}')$ such that its boundary $\partial\overline{\mathcal{H}}(\mathbf{q}, \mathbf{y}, \mathbf{y}', \mathbf{q}')$ is of dimension 0 and contains discrete broken or nodal curves.*

Proof. Similar to Lemma 3.5.1, since $|\mathbf{y}| = |\mathbf{y}'| = 0$ and $|\mathbf{q}| = |\mathbf{q}'|$, $\mathcal{H}(\mathbf{q}, \mathbf{y}, \mathbf{y}', \mathbf{q}')$ has virtual dimension 0 by (2.0.4). By standard transversality arguments and Gromov compactness, a 1-parameter family of curves in $\mathcal{H}(\mathbf{q}, \mathbf{y}, \mathbf{y}', \mathbf{q}')$ may limit to broken curves by pinching boundaries of T_2 or to nodal curves by letting branch points approach ∂T_2. □

Similar to the definitions of $\mathcal{E}$ in (3.5.1) and $\mathcal{F}$ in (3.5.3), we define a partially-defined evaluation map

$$\mathcal{G}\colon \mathcal{H}(\mathbf{q}, \mathbf{y}, \mathbf{y}', \mathbf{q}') \dashrightarrow \mathrm{H}_\kappa(\Sigma, \mathbf{q}) \otimes_{\mathbb{Z}[\hbar]} \mathbb{Z}[[\hbar]], \quad u \mapsto c^{2\langle u, \star\rangle} \cdot \hbar^{\kappa - \chi(u)} \cdot [\gamma(u)],$$

where

$$\gamma(u)(t) = (\pi_{T^*\Sigma} \circ u) \circ (\pi_{T_2} \circ u)^{-1} \circ \tau(t) \tag{3.5.4}$$

and $[\gamma] = \mathcal{P}(\gamma)$ defined by (3.5.2); the domain of the definition of $\mathcal{G}$ is the set of u for which $\gamma(u)$ is an element of $\mathrm{UConf}_\kappa(\Sigma \setminus \{\star\})$. Here $\tau\colon [0,1] \to \partial_3 T_2$ parametrizes the boundary arc $\partial_3 T_2$ from p_0 to p_3. The definition of $[\pi_\Sigma(u)]'$ is similar to that in Section 3.5.1. For a generic $u \in \mathcal{H}(\mathbf{q}, \mathbf{y}, \mathbf{y}', \mathbf{q}')$, the boundary of $[\pi_\Sigma(u)]'$ is disjoint from $\star$. Therefore, the algebraic intersection number $\langle u, \star\rangle := \langle [\pi_\Sigma(u)]', \star\rangle$ is well-defined.

Proposition 3.5.4. *The map $\mathcal{F}$ in (3.5.3) is a homomorphism of algebras.*

Proof. It suffices to show that

$$\mathcal{F}(\mu^2(\mathbf{y},\mathbf{y}')) = \mathcal{F}(\mathbf{y})\mathcal{F}(\mathbf{y}')$$

for any $\mathbf{y},\mathbf{y}' \in CW(\sqcup_i T^*_{q_i}\Sigma)_c$. We analyze the boundary of the index 1 moduli space $\overline{\mathcal{H}}^{\chi}(\mathbf{q},\mathbf{y},\mathbf{y}',\mathbf{q}')$.

For each $u \in \mathcal{H}^{\chi}(\mathbf{q},\mathbf{y},\mathbf{y}',\mathbf{q}')$, consider the path $\gamma(u)$ defined by (3.5.4) as a κ-tuple of paths in Σ. For a generic point $u \in \mathcal{H}^{\chi}(\mathbf{q},\mathbf{y},\mathbf{y}',\mathbf{q}')$, $\gamma(u)$ does not pass through $\star$ and $\mathcal{G}(u)$ is defined but for a generic 1-parameter family $u_t \in \mathcal{H}^{\chi}(\mathbf{q},\mathbf{y},\mathbf{y}',\mathbf{q}')$, $t \in [0,1]$, $\gamma(u_t)$ may intersect $\star$ at some t. At any rate $\mathcal{G}(u_0) = \mathcal{G}(u_1)$, so we may ignore the intersections with $\star$ in this proof.

Note that codimension-1 degenerations only occur in the A_∞ base direction, i.e., the projection of curves to the A_∞ base direction leads to codimension-1 degenerations of D_m. The schematic picture is shown in Figures 3.5 and 3.6.

There are three types of boundary degenerations:

(1) $\coprod_{\mathbf{y}'',\chi'+\chi''-\kappa=\chi} \mathcal{M}^{\mathrm{ind}=0,\chi'}(\mathbf{y},\mathbf{y}',\mathbf{y}'') \times \mathcal{H}^{\mathrm{ind}=0,\chi''}(\mathbf{q},\mathbf{y}'',\mathbf{q}')$;

(2) $\coprod_{\mathbf{q}'',\chi'+\chi''-\kappa=\chi} \mathcal{H}^{\mathrm{ind}=0,\chi'}(\mathbf{q},\mathbf{y},\mathbf{q}'') \times \mathcal{H}^{\mathrm{ind}=0,\chi''}(\mathbf{q}'',\mathbf{y}',\mathbf{q}')$;

(3) the set $\partial_n \mathcal{H}^{\mathrm{ind}=1,\chi}(\mathbf{q},\mathbf{y},\mathbf{y}',\mathbf{q}')$ with a nodal degeneration along Σ.

(1) is given on the left-hand side of Figure 3.5 and contributes $\mathcal{F}(\mu^2(y,y'))$. (2) is given on the right-hand side of Figure 3.5 and contributes $\mathcal{F}(y)\mathcal{F}(y'')$. A standard gluing argument shows that all contributions to $\mathcal{F}(\mu^2(\mathbf{y},\mathbf{y}'))$ and $\mathcal{F}(\mathbf{y})\mathcal{F}(\mathbf{y}')$ come from such broken degenerations.

We now discuss (3), which is given in Figure 3.6. Let u_t, $t \in [0,1)$, be a generic 1-parameter family such that $\pi_{T_2} \circ u_t$ has a branch point (generically a double branch point) that limits to ∂T_2 as $t \to 1$. Moreover, the only component of ∂T_2 that a branch point can approach is $\partial_3 T_2$ (corresponding to the zero section Σ) since all other boundary arcs correspond to disjoint sets of Lagrangians where nodal degenerations cannot occur. By Gromov compactness, $\partial_n \mathcal{H}^{\mathrm{ind}=1,\chi}(\mathbf{q},\mathbf{y},\mathbf{y}',\mathbf{q}')$ is finite. If we continue this family past the

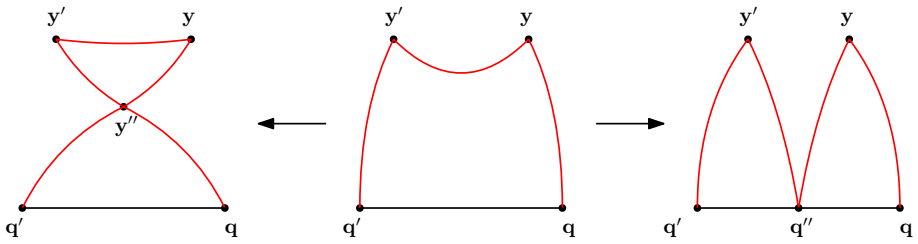

Figure 3.5: Degeneration of $\mathcal{H}^{\mathrm{ind}=1,\chi}(\mathbf{q},\mathbf{y},\mathbf{y}',\mathbf{q}')$ in the T_2 direction: concatenation of curves in $\mathcal{M}^{\mathrm{ind}=0,\chi'}(\mathbf{y},\mathbf{y}',\mathbf{y}'')$ and $\mathcal{H}^{\mathrm{ind}=0,\chi''}(\mathbf{q},\mathbf{y}'',\mathbf{q}')$ (left); concatenation of curves in $\mathcal{H}^{\mathrm{ind}=0,\chi'}(\mathbf{q},\mathbf{y},\mathbf{q}'')$ and $\mathcal{H}^{\mathrm{ind}=0,\chi''}(\mathbf{q}'',\mathbf{y}',\mathbf{q}')$ (right).

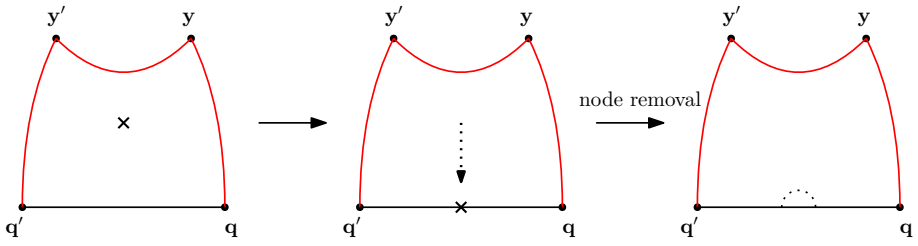

Figure 3.6: Nodal degeneration of $\mathcal{H}^{\mathrm{ind}=1,\chi}(\mathbf{q},\mathbf{y},\mathbf{y}',\mathbf{q}')$ in the T_2 direction: a nodal point on Σ (middle); removal of the nodal point (right).

nodal curve, then the nodal point is removed and χ increases by 1 as seen on the right-hand side of Figure 3.6. Interpreted in another way, given $u_n \in \partial_n \mathcal{H}^{\mathrm{ind}=1,\chi}(\mathbf{q},\mathbf{y},\mathbf{y}',\mathbf{q}')$, there exists a 1-parameter family of curves u_t, $t \in (-\delta,\delta)$, in $\mathcal{H}^{\mathrm{ind}=1,\chi+1}(\mathbf{q},\mathbf{y},\mathbf{y}',\mathbf{q}')$ such that $u_0 = u_n$ and the family $\gamma(u_t)$ corresponds to a crossing of two paths in $[0,1]\times\Sigma$. This is illustrated in Figure 3.7 as a skein relation on $[0,1]\times\Sigma$.

On the other hand, suppose there is a 1-parameter family u_t, $t \in (-\delta,\delta)$, of curves in $\mathcal{H}^{\mathrm{ind}=1,\chi+1}(\mathbf{q},\mathbf{y},\mathbf{y}',\mathbf{q}')$ such that $\gamma(u_t)$ exhibits a single crossing of two strands (see the bottom blue line of Figure 3.7), let $u_n = u_0$ be the nodal curve as in the middle of Figure 3.6. Suppose the nodal point on the domain of u_n is $p_n \in \dot{F}$. Since a neighborhood of $u_n(p_n)$ in the ambient symplectic manifold $T_2 \times T^*\Sigma$ is diffeomorphic to $T^*\mathbb{R}\times T^*\mathbb{R}^2 \approx \mathbb{R}^6$, we can construct a preglued curve $\tilde{u}_n^\epsilon$ using a cut-off version of the standard hyperbolic node model of [ES19, Section 4.1.1], where $\epsilon \in [0,\epsilon_0)$ is the pregluing parameter for some small $\epsilon_0 > 0$ so that $u_n = \tilde{u}_n^0$. By a standard Newton iteration technique, there exists a unique 1-parameter family of holomorphic curves $u_n^\epsilon \in \overline{\mathcal{H}}^{\mathrm{ind}=1,\chi}(\mathbf{q},\mathbf{y},\mathbf{y}',\mathbf{q}')$ for each $\epsilon \in [0,\epsilon_0)$, where $u_n = u_n^0$; see [ES19, Lemma 4.16] for details. Therefore, a small neighborhood of u_n in $\overline{\mathcal{H}}^{\mathrm{ind}=1,\chi}(\mathbf{q},\mathbf{y},\mathbf{y}',\mathbf{q}')$ is homeomorphic to $[0,\epsilon_0)$, which corresponds to the upper arc of Figure 3.7.

Summarizing the above discussion, $\sqcup_\chi \overline{\mathcal{H}}^{\mathrm{ind}=1,\chi}(\mathbf{q},\mathbf{y},\mathbf{y}',\mathbf{q}')$ is a uni-trivalent graph with trivalent vertices such that for each $u \in \partial_n \mathcal{H}^{\mathrm{ind}=1,\chi}(\mathbf{q},\mathbf{y},\mathbf{y}',\mathbf{q}')$, we can pick three nearby curves u_+, u_- and u_n that locally correspond to  ,  and  in Figure 3.7, respectively. Ranging over all $u \in \partial_n \mathcal{H}^{\mathrm{ind}=1,\chi}(\mathbf{q},\mathbf{y},\mathbf{y}',\mathbf{q}')$ and comparing the count of boundary curves

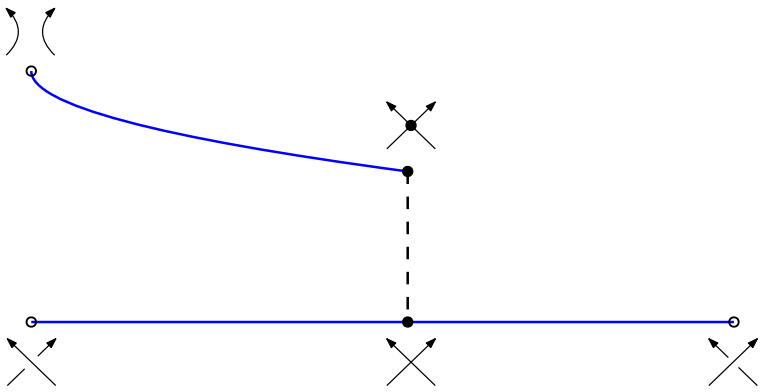

Figure 3.7: Representing a curve u by its image $\gamma(u)$ on $[0,1] \times \Sigma$. The upper arc denotes the moduli space with a nodal degeneration. The lower arc denotes the companion moduli space with χ increased by 1, whose evaluation by $\mathcal{G}$ on $[0,1] \times \Sigma$ exhibits a crossing of two braid strands.

with different Euler characteristics, we have

$$\begin{aligned}
&\mathcal{F}(\mathbf{y})\mathcal{F}(\mathbf{y}') - \mathcal{F}(\mu^2(\mathbf{y},\mathbf{y}')) \qquad (3.5.5)\\
&= 1 \cdot [\sum_{\chi(u_+)=\kappa} \mathcal{G}(u_+) - \sum_{\chi(u_-)=\kappa} \mathcal{G}(u_-)]\\
&+ \hbar \cdot [\sum_{\chi(u_+)=\kappa-1} \mathcal{G}(u_+) - \sum_{\chi(u_-)=\kappa-1} \mathcal{G}(u_-) - \sum_{\chi(u_n)=\kappa-1} \mathcal{G}(u_n)]\\
&+ \hbar^2 \cdot [\sum_{\chi(u_+)=\kappa-2} \mathcal{G}(u_+) - \sum_{\chi(u_-)=\kappa-2} \mathcal{G}(u_-) - \sum_{\chi(u_n)=\kappa-2} \mathcal{G}(u_n)]\\
&+ \cdots
\end{aligned}$$

The skein relation in Definition 3.3.4 implies that

$$\mathcal{G}(u_+) - \mathcal{G}(u_-) = \hbar \cdot \mathcal{G}(u_n) \in \mathrm{H}_\kappa(\Sigma, \mathbf{q}) \otimes_{\mathbb{Z}[\hbar]} \mathbb{Z}[[\hbar]].$$

So the right-hand side of (3.5.5) is zero. This completes the proof. □

To show $\mathcal{F}$ is an isomorphism, it suffices to show that $\mathcal{F}$ is a bijection. We use a perturbation argument and start with the case where $\hbar = 0$:

Lemma 3.5.5. *The restriction of $\mathcal{F}$ to $\hbar = 0$ is an isomorphism:*

$$\mathcal{F}|_{\hbar=0} \colon HW(\sqcup_i T^*_{q_i}\Sigma)_c|_{\hbar=0} \to \mathrm{H}_\kappa(\Sigma, \mathbf{q})|_{\hbar=0}.$$

Proof. For simplicity, we write $\mathcal{F}_0 = \mathcal{F}|_{\hbar=0}$ throughout this proof.

We first prove the lemma for $\kappa = 1$. In this case $\mathrm{H}_1(\Sigma, \mathbf{q})|_{\hbar=0} \cong \mathbb{Z}[\pi_1(\Sigma, q)_c]$. Setting $c = 1$, $\pi_1(\Sigma, q)_c$ is isomorphic to $\pi_1(\Sigma, q)$. In each homotopy class of $\pi_1(\Sigma, q)$, there is a unique generator $y \in HW(T^*_q\Sigma)$ whose Legendre transform $\mathcal{L}(y)$ represents this class. By [Abo12, Lemma 5.1], $\mathcal{F}_0|_{c=1}(y) = [\mathcal{L}(y)]$. Hence, $\mathcal{F}_0|_{c=1}$ is an isomorphism. Add the parameter c and view $y \in HW(T^*_q\Sigma)_c$. We have $\mathcal{F}_0(y) = c^d[\mathcal{L}(y)]_c$ for some integer d, where $[\mathcal{L}(y)]_c \in \pi_1(\Sigma, q)_c$ is a lift of $[\mathcal{L}(y)] \in \pi_1(\Sigma, q)$. Hence $\mathcal{F}_0$ is an isomorphism. For later use, we denote the map $\mathcal{F}_0$ for $\kappa = 1$ as

$$\tilde{\mathcal{F}}_c \colon HW(T^*_q\Sigma)_c \to \mathbb{Z}[\pi_1(\Sigma, q)_c], \tag{3.5.6}$$

which is the version of (3.2.8) with the c-parameter.

We now prove the lemma for $\kappa \geq 1$. The μ^2-operation of $HW(\sqcup_i T^*_{q_i}\Sigma)_c|_{\hbar=0}$ only counts curves with $\chi = \kappa$, i.e., where there are κ trivial pseudoholomorphic disks. In this case one can easily compute that $HW(\sqcup_i T^*_{q_i}\Sigma)_c|_{\hbar=0}$ is isomorphic to $\left(\otimes_i HW(T^*_{q_i}\Sigma)_c\right) \rtimes S_\kappa$. On the other hand, $\mathrm{H}_\kappa(\Sigma, \mathbf{q})_c|_{\hbar=0}$ degenerates to $(\otimes_i \mathbb{Z}[\pi_1(\Sigma, q_i)_c]) \rtimes S_\kappa$ by Lemma 3.3.6. Here, both tensor products are over $\mathbb{Z}[c^{\pm 1}]$.

Since $HW(\sqcup_i T^*_{q_i}\Sigma)_c|_{\hbar=0}$ is generated by $\otimes_i HW(T^*_{q_i}\Sigma)_c$ and S_κ as an algebra, it suffices to show that

1. $\mathcal{F}_0|_{\otimes_i HW(T^*_{q_i}\Sigma)_c} = \tilde{\mathcal{F}}_c^{\otimes\kappa} \colon \otimes_i HW(T^*_{q_i}\Sigma)_c \to \otimes_i \mathbb{Z}[\pi_1(\Sigma, q_i)_c]$, where the map $\tilde{\mathcal{F}}_c$ is in (3.5.6);
2. $\mathcal{F}_0|_{S_\kappa} = \mathrm{id} \colon S_\kappa \to S_\kappa$.

By Theorem 3.2.4, Remark 3.2.5 and [Abo12, Lemma 5.1], $\tilde{\mathcal{F}}_c$ maps the time-1 Hamiltonian flow to the homotopy class of its Legendre transform. The first equation follows since $\mathcal{F}_0|_{\otimes_i HW(T^*_{q_i}\Sigma)_c}$ maps κ time-1 Hamiltonian flows to their Legendre transforms.

The symmetric group S_κ is generated by transpositions $\sigma_i = (i, i+1)$. Let $\mathbf{y}_i = \{y_{i1}, \dots, y_{i\kappa}\} \in HW(\sqcup_i T^*_{q_i}\Sigma)_c|_{\hbar=0}$ be the corresponding generator in the Floer homology, where $y_{ij} \in CF(\phi^1_{H_V}(T^*_{q_j}\Sigma), T^*_{q_{\sigma_i(j)}}\Sigma)$. Since $\hbar = 0$, the map $\mathcal{F}_0(\mathbf{y}_i)$ counts curves with $\chi = \kappa$. There is a unique such curve consisting of κ trivial pseudoholomorphic disks. The image of the boundary of the curve in the zero section of $T^*\Sigma$ gives a loop in $\mathrm{UConf}_\kappa(\Sigma, \mathbf{q})$. The loop consists of two short paths from q_i to q_{i+1} and from q_{i+1} to q_i, and trivial paths from q_j to q_j for $j \neq i, i+1$. This loop gives a class in $\mathrm{H}_\kappa(\Sigma, \mathbf{q})_c|_{\hbar=0} \cong (\otimes_i \mathbb{Z}[\pi_1(\Sigma, q_i)_c]) \rtimes S_\kappa$ corresponding to $\sigma_i \in S_\kappa$. Hence, the second equation follows. □

Proof of Theorem 1.0.4.

Injectivity of $\mathcal{F}$. Suppose that there exists $\mathbf{a} \neq 0$ such that $\mathcal{F}(\mathbf{a}) = 0$. Let $\mathbf{a} = \sum_{i\geq 0} \hbar^i \mathbf{a}_i$, where $\mathbf{a}_i \in CW(\sqcup_i T^*_{q_i}\Sigma)_c|_{\hbar=0}$. Without loss of generality we may assume that $\mathbf{a}_0 \neq 0$. Setting $\hbar = 0$, we have $\mathcal{F}(\mathbf{a}_0) = \mathcal{F}(\mathbf{a}) = 0$. Hence $\mathcal{F}|_{\hbar=0}(\mathbf{a}_0) = 0$, which means $\mathbf{a}_0 = 0$ since $\mathcal{F}|_{\hbar=0}$ is an isomorphism. This leads to contradiction. Thus $\mathcal{F}$ is injective.

Surjectivity of $\mathcal{F}$. It suffices to show that any $\mathbf{b} \in \mathrm{H}_\kappa(\Sigma, \mathbf{q})$ is in $\operatorname{Im}\mathcal{F}$. Since $\mathcal{F}|_{\hbar=0}$ is an isomorphism, there exists $\mathbf{a}_0 \in CW(\sqcup_i T^*_{q_i}\Sigma)_c|_{\hbar=0}$ such that $\mathcal{F}(\mathbf{a}_0) \equiv \mathbf{b} \pmod{\hbar}$. Let

$$\mathbf{b}_1 = \left.\frac{(\mathbf{b} - \mathcal{F}(\mathbf{a}_0))}{\hbar}\right|_{\hbar=0}.$$

Then there exists $\mathbf{a}_1 \in CW(\sqcup_i T^*_{q_i}\Sigma)_c|_{\hbar=0}$ such that $\mathcal{F}(\mathbf{a}_1) \equiv \mathbf{b}_1 \pmod{\hbar}$. Repeating this procedure, we get $\mathcal{F}(\sum_{i\geq 0} \mathbf{a}_i \hbar^i) = \mathbf{b}$. Hence $\mathcal{F}$ is surjective. □

3.6 Surfaces with punctures

In this section we show that Theorem 1.0.4 still holds for $\mathring{\Sigma}$, which is obtained from a closed oriented surface of genus $g \geq 0$ by removing a finite number (> 0) of punctures. For simplicity we assume that $c = 1$.

In this case, the wrapped Floer homology of the cotangent fibers and the $\mathcal{F}$ map of (3.5.3) can be defined similarly but need modifications near the punctures. The main issue is the

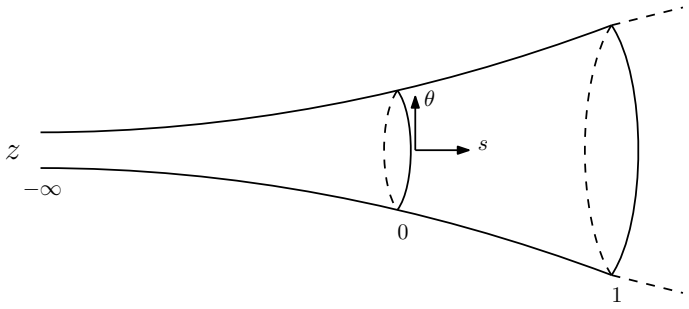

Figure 3.8

noncompactness of the moduli space of holomorphic curves: if the wrapped Lagrangians on $T^*\mathring{\Sigma}$ approach the punctures when projected to $\mathring{\Sigma}$, then a sequence of curves bounded by those wrapped Lagrangians projected to $\mathring{\Sigma}$ may also approach the punctures.

To remedy this, we confine the wrapped Lagrangians and all involved holomorphic curves to stay over a compact subset of $\mathring{\Sigma}$. Our approach is a simple application of the partially wrapped Fukaya category by Sylvan [Syl19] and its further development by Ganatra, Pardon and Shende [GPS18; GPS20]. A similar approach in the context of sutured contact manifolds is due to Colin, Ghiggini, Honda and Hutchings [CGHH11].

Let g be the standard flat metric on $\mathring{\Sigma}$ if $\mathring{\Sigma}$ is homeomorphic to $\mathbb{R}^2$ or $\mathbb{R}\times S^1$. Otherwise let g be a complete finite-volume hyperbolic metric on $\mathring{\Sigma}$, i.e., all the punctures of $\mathring{\Sigma}$ correspond to cusps.

Suppose Σ is a closed oriented surface and $z \in \Sigma$. We consider the once punctured surface $\mathring{\Sigma} = \Sigma \setminus \{z\}$ (the case of more than one puncture is similar).

Let $\mathbf{q} = \{q_1, \dots, q_\kappa\} \subset \mathring{\Sigma}$ be a κ-tuple of points. Pick an end $\mathcal{N} \approx (-\infty, 1)_s \times S^1_\theta$ near the puncture of $\mathring{\Sigma}$ so that $\{q_1, \dots, q_\kappa\} \subset \mathring{\Sigma} \setminus \mathcal{N}$. We have a trivialization of $T\mathcal{N}$ by $\{\frac{\partial}{\partial s}, \frac{\partial}{\partial \theta}\}$. See Figure 3.8. Let (p_s, p_θ) be the dual coordinates to (s, θ) so that we have a trivialization of $T^*\mathcal{N}$ by $\{\frac{\partial}{\partial p_s}, \frac{\partial}{\partial p_\theta}\}$. The canonical symplectic form ω on $\mathring{\Sigma}$ restricts to $\omega = ds \wedge dp_s + d\theta \wedge dp_\theta$ on $T^*\mathcal{N}$. We fix the trivial almost complex structure $J_\mathcal{N}$ on $T^*\mathcal{N}$ so that $J_\mathcal{N}(\frac{\partial}{\partial s}) = \frac{\partial}{\partial p_s}$ and $J_\mathcal{N}(\frac{\partial}{\partial \theta}) = \frac{\partial}{\partial p_\theta}$. Then there is a $(J_\mathcal{N}, j)$-holomorphic map

$$\pi_s \colon T^*\mathcal{N} \to \mathbb{C}_{\mathrm{Re}<1}, \quad (s, \theta, p_s, p_\theta) \mapsto s + jp_s,$$

where j is the standard complex structure on $\mathbb{C}_{\mathrm{Re}<1}$.

Fix a diffeomorphism $f\colon (0,1)_s \to (-\infty,1)_s$ such that $f'>0$, $f''\le 0$, and $f(s)=s$ for $s\ge 1/2$. It induces the diffeomorphism $\mathcal{N}\cap\{s>0\}\xrightarrow{\sim}\mathcal{N}$, $(s,\theta)\mapsto(f(s),\theta)$. Extending by the identity, we obtain a diffeomorphism

$$\tilde{f}\colon \mathring{\Sigma}_0 \coloneqq \mathring{\Sigma}\setminus\{s\le 0\}\to\mathring{\Sigma}.$$

The pullback metric $\tilde{f}^*g$ on $\mathring{\Sigma}_0$ induces a norm $|\cdot|_f$ on $T^*\mathring{\Sigma}_0$. Choose a time-dependent Hamiltonian $H_{V,f}\colon [0,1]\times T^*\mathring{\Sigma}_0\to\mathbb{R}$ with $|p|_f$ instead of $|p|$ in Equation (3.1.1), where V has compact support in $\mathring{\Sigma}\setminus\mathcal{N}$ and has small $W^{1,2}$-norm; $X_{H_{V,f}}$ and $\phi^t_{H_{V,f}}$ are as before with respect to $H_{V,f}$. Note that the wrapped Lagrangians $\phi^t_{H_V}(\sqcup_i T^*_{q_i}\mathring{\Sigma})\subset\mathring{\Sigma}_0\subset\mathring{\Sigma}$ for all $t\ge 0$, and hence cannot cross $\{s=0\}$.

We follow the notation of Section 3.1. Similar to Definition 3.1.1, we define

Definition 3.6.1. *The wrapped Heegaard Floer cochain complex of $CW(\sqcup_i T^*_{q_i}\mathring{\Sigma})$ is defined to be $CF(\phi^1_{H_V}(\sqcup_i T^*_{q_i}\mathring{\Sigma}),\sqcup_i T^*_{q_i}\mathring{\Sigma})$.*

Choose a ω-compatible almost complex structure $J_{T^*\Sigma}$ on $T^*\Sigma$ so that it coincides with $J_{\mathcal{N}}$ on $T^*\mathcal{N}$. Let j_m be the standard complex structure on D_m. Choose a generic almost complex structure $J^0_{D_m}$ on $D_m\times T^*\Sigma$ which is close to $j_m\times J_{T^*\Sigma}$. We then apply the rescaling argument of Section 3.1 on $J^0_{D_m}$ to get J_{D_m}.

Given $\mathbf{y}_1,\dots,\mathbf{y}_m\in CW(\sqcup_i T^*_{q_i}\mathring{\Sigma})$, let $\mathcal{M}(\mathbf{y}_1,\dots,\mathbf{y}_m,\mathbf{y}_0)$ be the moduli space of maps

$$u\colon (\dot{F},j)\to(D_m\times T^*\mathring{\Sigma},J_{D_m}),$$

where (F,j) is a compact Riemann surface with boundary and u satisfies the conditions similar to (2.0.1).

It is easy to check that all conclusions in Section 3.1 still hold except for Lemma 3.1.2 and the A_∞-relation. However, we claim that the standard proof of A_∞-relation (see [CHT20, Proposition 4.0.3]) works by showing that

Lemma 3.6.2. *Let $d = 0$ or 1. Given $\mathbf{y}_1, \dots, \mathbf{y}_m \in CW(\sqcup_i T^*_{q_i}\mathring{\Sigma})$, $\mathcal{M}^{\mathrm{ind}=d,\chi}(\mathbf{y}_1, \dots, \mathbf{y}_m, \mathbf{y}_0)$ is empty for all but finitely many $\mathbf{y}_0$. When it is nonempty, $\mathcal{M}^{\mathrm{ind}=d,\chi}(\mathbf{y}_1, \dots, \mathbf{y}_m, \mathbf{y}_0)$ (and $\mathcal{M}^{\mathrm{ind}=d,\chi}(\mathbf{y}_1, \mathbf{y}_0)/\mathbb{R}$ if $m = 1$) admits a compactification for each Euler characteristic χ.*

Proof. We follow [GPS20, Lemma 2.41]. Let $\pi\colon T^*\mathring{\Sigma} \to \mathring{\Sigma}$ be the projection. For each $u \in \mathcal{M}(\mathbf{y}_1, \dots, \mathbf{y}_m, \mathbf{y}_0)$, we show that $\pi \circ u(\dot{F}) \cap \{s < 0\} = \emptyset$.

Consider the holomorphic map

$$\pi_s \circ u\colon u^{-1}(\pi_s^{-1}(\mathbb{C}_{\mathrm{Re}<0})) \to \mathbb{C}_{\mathrm{Re}<0}.$$

By definition, $\pi \circ u(\partial\dot{F}) \cap \{s \le 0\} = \emptyset$, hence $u^{-1}(\pi_s^{-1}(\mathbb{C}_{\mathrm{Re}<0})) \subset F \setminus \partial F$ is an open subset of the interior of F. Therefore, $K \coloneqq (\pi_s \circ u)(u^{-1}(\pi_s^{-1}(\mathbb{C}_{\mathrm{Re}<0})))$ is an open subset of $\mathbb{C}_{\mathrm{Re}<0}$ by the open mapping theorem.

On the other hand, $u^{-1}(\pi_s^{-1}(\mathbb{C}_{\mathrm{Re}\le 0})) \subset F \setminus \partial F$ is a compact subset of the interior of F. Therefore, the function

$$\mathrm{Re} \circ \pi_s \circ u\colon u^{-1}(\pi_s^{-1}(\mathbb{C}_{\mathrm{Re}\le 0})) \to \mathbb{R}$$

attains its minimum on $u^{-1}(\pi_s^{-1}(\mathbb{C}_{\mathrm{Re}\le 0}))$. Since K is open, this is only possible if $K = \emptyset$. Hence $u^{-1}(\pi_s^{-1}(\mathbb{C}_{\mathrm{Re}<0})) = \emptyset$ and then $\pi \circ u(\dot{F}) \cap \{s < 0\} = \emptyset$.

We have shown how to prevent curves from crossing the vertical boundary of $T^*\mathring{\Sigma}_0$. The remaining proof is the same as that of Lemma 3.1.2. □

Therefore $CW(\sqcup_i T^*_{q_i}\mathring{\Sigma})$ is a well-defined ordinary algebra supported in degree 0.

To modify Section 3.2, we consider paths in $\mathring{\Sigma}_0$ instead of Σ. We now use the metric $\tilde{f}^*g$. The Legendre transform $L_{f,v}$ is with $|v|_f$ instead of $|v|$ in (3.2.1), where $|\cdot|_f$ is the norm on $T\mathring{\Sigma}_0$ induced by $\tilde{f}^*g$. Given $q_0, q_1 \in \mathring{\Sigma}_0 \setminus \mathcal{N}$, the Lagrangian action functional $\mathcal{A}_{V,f}$ is defined as in (3.2.2) with L_V replaced by $L_{V,f}$. By the choice of the metric $\tilde{f}^*g$ it is easy to see that

1. no V-perturbed geodesics can exit $\mathring{\Sigma}_0$;

2. the induced negative gradient flow of $\mathcal{A}_V$ always stays inside a compact region of $\mathring{\Sigma}_0$.

Since $\tilde{f}\colon (\mathring{\Sigma}_0, \tilde{f}^*g) \to (\mathring{\Sigma}, g)$ is an isometry, we have:

Lemma 3.6.3. *The Morse homology $HM_*(\Omega^{1,2}(\mathring{\Sigma}_0, q_0, q_1))$ induced by the metric $\tilde{f}^*g$ is well-defined and is isomorphic to $HM_*(\Omega^{1,2}(\mathring{\Sigma}, q_0, q_1))$ induced by the metric g.*

It is easy to verify that all the definitions and conclusions in Section 3.3 hold for $\mathring{\Sigma}_0$. Hence the Hecke algebra $\mathrm{H}_\kappa(\mathring{\Sigma}_0, \mathbf{q})$ is well-defined.

Next we consider the modification of the map $\mathcal{F}$ defined by (3.5.3). We use the notation from Section 3.5 with the following modifications:

1. H_V is replaced by $H_{V,f}$;
2. choose a sufficiently generic consistent collection $T_{m-1} \mapsto J_{T_{m-1}}$ of compatible almost complex structures on $T_{m-1} \times T^*\mathring{\Sigma}$ for $T_{m-1} \in \mathcal{T}_{m-1}$ and all $m \geq 2$, where $J_{T^*\mathring{\Sigma}}$ coincides with $j_m \times J_{\mathcal{N}}$ on $T_{m-1} \times T^*\mathcal{N}$.

All of Section 3.5.1 carries over with the exception of Lemma 3.5.2. Recall that we denote the set of intersection points between $\phi^1_{H_V}(\sqcup_i T^*_{q_i}\mathring{\Sigma})$ (resp. $\sqcup_i T^*_{q_i}\mathring{\Sigma}$) and $\mathring{\Sigma}$ by $\mathbf{q}$ (resp. $\mathbf{q}'$). Let $\mathbf{y} \in CF(\phi^1_{H_V}(\sqcup_i T^*_{q_i}\mathring{\Sigma}), \sqcup_i T^*_{q_i}\mathring{\Sigma})$. We show that

Lemma 3.6.4. *The moduli space $\mathcal{H}^\chi(\mathbf{q}, \mathbf{y}, \mathbf{q}')$ admits a compactification for each Euler characteristic χ.*

Proof. This is similar to the proof of Lemma 3.6.2. Let $\pi : T^*\mathring{\Sigma} \to \mathring{\Sigma}$ be the projection. For each $u \in \mathcal{H}^\chi(\mathbf{q}, \mathbf{y}, \mathbf{q}')$, consider the holomorphic map

$$\pi_s \circ u\colon u^{-1}(\pi_s^{-1}(\mathbb{C}_{\mathrm{Re}<0})) \to \mathbb{C}_{\mathrm{Re}<0}.$$

By definition, $u(\partial\dot{F}) \cap T^*\mathcal{N}|_{s<0}$ is a subset of the zero section $\mathcal{N}|_{s<0}$. Since $u^{-1}(\pi_s^{-1}(\mathbb{C}_{\mathrm{Re}\leq 0})) \subset F \setminus \partial F$ is an compact closed subset of F, its image $P \coloneqq (\pi_s \circ u)(u^{-1}(\pi_s^{-1}(\mathbb{C}_{\mathrm{Re}\leq 0}))) \subset \mathbb{C}$ is also compact.

Note that $(\pi_s \circ u)(u^{-1}(\pi_s^{-1}(\mathbb{C}_{\mathrm{Re}<0,\,\mathrm{Im}\neq 0}))) \subset \mathbb{C}$ is open by the open mapping theorem. As a result, $\partial P \cap \mathbb{C}_{\mathrm{Re}<0,\,\mathrm{Im}\neq 0} = \emptyset$, hence $P \subset \mathbb{C}_{\mathrm{Re}=0} \cup \mathbb{C}_{\mathrm{Im}=0}$. This implies $u^{-1}(\pi_s^{-1}(\mathbb{C}_{\mathrm{Re}\leq 0})) \subset \partial F$, which is only possible if $P \subset \mathbb{C}_{\mathrm{Re}=0}$. Therefore we conclude that $\pi \circ u(\dot{F}) \cap \{s < 0\} = \emptyset$.

We have shown that curves in $\mathcal{H}^\chi(\mathbf{q}, \mathbf{y}, \mathbf{q}')$ cannot cross the vertical boundary of $T^*\mathring{\Sigma}_0$. The remaining proof is the same as that of Lemma 3.5.2. □

The parallel modification of Lemma 3.5.3 and its proof are similar. Also note that Proposition 3.5.4 still holds. Therefore

$$\mathcal{F}\colon CW(\sqcup_i T^*_{q_i}\mathring{\Sigma}) \to \mathrm{H}_\kappa(\mathring{\Sigma}_0, \mathbf{q})|_{c=1} \otimes_{\mathbb{Z}[\hbar]} \mathbb{Z}[[\hbar]] \cong \mathrm{H}_\kappa(\mathring{\Sigma}, \mathbf{q})|_{c=1} \otimes_{\mathbb{Z}[\hbar]} \mathbb{Z}[[\hbar]]$$

is well-defined.

To modify the proof of Theorem 1.0.4, it suffices to modify the proof of Lemma 3.5.5 when $\kappa = 1$. Note that $\hbar = 0$ is automatically satisfied in this case.

Lemma 3.6.5. *When $\kappa = 1$, the map $\mathcal{F}$ is an isomorphism:*

$$\mathcal{F}\colon HW(T^*_q\mathring{\Sigma}) \to \mathrm{H}_1(\mathring{\Sigma}_0, q)|_{c=1} \cong \mathrm{H}_1(\mathring{\Sigma}, q)|_{c=1}.$$

Proof. This is essentially Lemma 5.1 of [Abo12], replacing Σ by $\mathring{\Sigma}$.

Recall that Abbondandolo and Schwarz [AS06, Theorem 3.1] constructed a chain isomorphism

$$\Theta\colon CM_*(\Omega^{1,2}(\Sigma, q)) \to CW(T^*_q\Sigma)$$

by a specific moduli space $\mathcal{M}^+_\Omega$ of holomorphic curves of index 0 (see [AS06, p.35]). Abouzaid then showed that $\mathcal{F}$ is a homotopy inverse of Θ by constructing another moduli space $\mathcal{C}$ of curves of index 1 (see [Abo12, p.33]).

In the case of $\mathring{\Sigma}$, we define the moduli spaces $\mathcal{M}^+_\Omega$ and $\mathcal{C}$ in a similar manner. Again it suffices to show that no curves in $\mathcal{M}^+_\Omega$ or $\mathcal{C}$ can cross the vertical boundary of $T^*\mathring{\Sigma}_0$. We omit the details which are similar to the proofs of Lemma 3.6.2 and Lemma 3.6.4. □

CHAPTER 4

A variant of symplectic Khovanov homology

4.1 Definitions and main results

4.1.1 Higher-dimensional analog of Sympletic Khovanov Homology

Let $\widetilde{D} = \{-2 \leq \operatorname{Re} z, \operatorname{Im} z \leq 2\} \subset \mathbb{C}_z$. We consider the standard $2n$-dimensional Lefschetz fibration

$$\widetilde{p} : \widetilde{W} \to \widetilde{D} \subset \mathbb{C}_z$$

for a Milnor fiber of the A_{2k-1} singularity, where the regular fiber is T^*S^{n-1}. There are 2κ critical values $\widetilde{\boldsymbol{z}} = \{z_1, \ldots, z_{2\kappa}\}$, where $\operatorname{Re} z_i = \operatorname{Re} z_{i+\kappa}$, $\operatorname{Im} z_i = -1$ and $\operatorname{Im} z_{i+\kappa} = 1$, $i = 1, \ldots, \kappa$. Let

$$p : W := \widetilde{p}^{-1}(D) \to D$$

be the restriction of $\widetilde{p}$ to $D = \widetilde{D} \cap \{\operatorname{Im} z \leq 0\}$. For $i = 1, \ldots, \kappa$, connect z_i and $z_{i+\kappa}$ by straight arcs $\widetilde{\gamma}_i$. Then the matching cycles $\widetilde{a} = \{\widetilde{a}_1, \ldots, \widetilde{a}_\kappa\}$ over $\{\widetilde{\gamma}_1, \ldots, \widetilde{\gamma}_\kappa\}$ are Lagrangian spheres. Let $\boldsymbol{z}$, a_i and γ_i be "half" of $\widetilde{\boldsymbol{z}}$, $\widetilde{a}_i$ and $\widetilde{\gamma}_i$, that is, their restrictions to W.

Given a κ-strand braid $\sigma \in \operatorname{Diff}^+(D, \partial D, \boldsymbol{z})$, let $h_\sigma \in \operatorname{Symp}(W, \partial W)$ be the monodromy on W which descends to σ and let $\widetilde{h}_\sigma$ be the extension of h_σ to $\widetilde{W}$ by the identity.

In this chapter we always do cohomology. Recall the settings of Chapter 2. The variant $CKh^\sharp(\widehat{\sigma})$ of the symplectic Khovanov cochain complex is defined as the higher-dimensional Heegaard Floer cochain complex, in the sense of [Lip06] and [CHT20], denoted by $\widehat{CF}(\widetilde{W}, \widetilde{h}_\sigma(\widetilde{\boldsymbol{a}}), \widetilde{\boldsymbol{a}})$. Specifically, a κ-tuple of intersection points of $\widetilde{h}_\sigma(\widetilde{\boldsymbol{a}})$ and $\widetilde{\boldsymbol{a}}$ is a κ-tuple $\boldsymbol{y} = \{y_1, \ldots, y_\kappa\}$ where $y_i \in \widetilde{\alpha}_i \cap \widetilde{h}_\sigma(\widetilde{a}_{\beta(i)})$ and β is some permutation of $\{1, \ldots, \kappa\}$. Then

$\widehat{CF}(\widetilde{W},\widetilde{h}_\sigma(\widetilde{\boldsymbol{a}}),\widetilde{\boldsymbol{a}})$ is the free $\mathbb{F}[\mathcal{A}][\![\hbar,\hbar^{-1}]$-module generated by all such κ-tuples $\boldsymbol{y}$, where the coefficient ring is discussed below.

To define the differential, let F be a surface with boundary of Euler characteristic χ and $\dot{F}$ be the surface with boundary punctures. We start with the split almost complex structure $J_{\mathbb{R}\times[0,1]}\times J_{\widetilde{W}}$ on $\mathbb{R}\times[0,1]\times\widetilde{W}$, and apply a perturbation to achieve transversality, denoted by $J^\Diamond$.

For $\boldsymbol{y},\boldsymbol{y}'\in\widehat{CF}(\widetilde{W},\widetilde{h}_\sigma(\widetilde{\boldsymbol{a}}),\widetilde{\boldsymbol{a}})$, let $\mathcal{M}_{J^\Diamond}^{\mathrm{ind}=1,A,\chi}(\boldsymbol{y},\boldsymbol{y}')$ be the moduli space of $u:\dot{F}\to\mathbb{R}\times[0,1]\times\widetilde{W}$ satisfying

1. $du\circ J^\Diamond = J^\Diamond\circ du$,
2. $u(\partial\dot{F})\subset\mathbb{R}\times((\{1\}\times\widetilde{\boldsymbol{a}})\cup(\{0\}\times\widetilde{h}_\sigma(\widetilde{\boldsymbol{a}})))$,
3. As $\pi_{\mathbb{R}}\circ u$ tends to $+\infty$ (resp. $-\infty$), $\pi_{\widetilde{W}}$ tends to $\boldsymbol{y}$ (resp. $\boldsymbol{y}'$), where $\pi_{\mathbb{R}},\pi_{\widetilde{W}}$ are the projections of u to $\mathbb{R}$ and $\widetilde{W}$.

The differential is then defined as

$$d\boldsymbol{y}=\sum_{\boldsymbol{y}',\chi\le\kappa,A\in\mathcal{A}}\#\mathcal{M}_{J^\Diamond}^{\mathrm{ind}=1,A,\chi}(\boldsymbol{y},\boldsymbol{y}')/\mathbb{R}\cdot\hbar^{\kappa-\chi}e^A\cdot\boldsymbol{y}'. \tag{4.1.1}$$

We write $Kh^\sharp(\widehat{\sigma})$ for the cohomology group $\widehat{HF}(\widetilde{W},\widetilde{h}_\sigma(\widetilde{\boldsymbol{a}}),\widetilde{\boldsymbol{a}})$.

The coefficient ring $\mathbb{F}[\mathcal{A}][\![\hbar,\hbar^{-1}]$ (power series in $\hbar$ and polynomial in $\hbar^{-1}$) keeps track of the relative homology class and Euler characteristic of the domain, where

$$\mathcal{A}=H_2([0,1]\times\widetilde{W},(\{1\}\times\widetilde{\boldsymbol{a}})\cup(\{0\}\times\widetilde{h}_\sigma(\widetilde{\boldsymbol{a}}));\mathbb{Z}). \tag{4.1.2}$$

The following lemmas justify the use of coefficient $\mathbb{F}[\mathcal{A}][\![\hbar,\hbar^{-1}]$ for $n=2$ and $\mathbb{F}[\![\hbar,\hbar^{-1}]$ for $n>3$:

Lemma 4.1.1. *For fixed $\boldsymbol{y}$,$\boldsymbol{y}'$ and χ, $\#\mathcal{M}_{J^\Diamond}^{ind=1,\chi}(\boldsymbol{y},\boldsymbol{y}')/\mathbb{R}$ is finite.*

Lemma 4.1.2. *Suppose $\widetilde{W}$ is of dimension $2n$. For $n=2$, $\mathcal{A}\simeq\mathbb{Z}^{r-1}$, where r is the number of connected components of $\widehat{\sigma}$; for $n>2$, $\mathcal{A}\simeq\{0\}$.*

Proof. Denote $X = [0,1] \times \widetilde{W}$, $Y = (\{1\} \times \widetilde{\boldsymbol{a}}) \cup (\{0\} \times \widetilde{h}_\sigma(\widetilde{\boldsymbol{a}}))$ and $i : Y \to X$ for the inclusion.

If $n = 2$, $H_3(X, Y)$ and $H_1(Y)$ are trivial. By the long exact sequence for relative singular homology, $H_2(X, Y) \simeq H_2(X)/i_* H_2(Y)$. Since there are 2κ critical points of $\widetilde{p} : \widetilde{W} \to \widetilde{D}$, $H_2(X)$ is generated by $2\kappa - 1$ matching cycles over arcs connecting pairs of critical values in $\widetilde{D}$. $H_2(Y)$ is simply generated by collections $\widetilde{\boldsymbol{a}}$ and $\widetilde{h}_\sigma(\widetilde{\boldsymbol{a}})$. Therefore, $H_2(X, Y)$ generated by $2\kappa - 1$ arcs quotient by collapsing arcs corresponding to $\widetilde{\boldsymbol{a}}$ and $\widetilde{h}_\sigma(\widetilde{\boldsymbol{a}})$. The number of remaining nontrivial arcs is $r - 1$, where r is the number of connected components of the braid $\widehat{\sigma}$.

If $n > 2$, $H_2(X)$ and $H_1(Y)$ are trivial, so $H_2(X, Y) \simeq \{0\}$ by the relative homology sequence. □

The following lemma computes the Fredholm index, which is a generalization from [CGH12] and the proof is omitted:

Lemma 4.1.3. *The Fredholm index of u is*

$$\mathrm{ind}(u) = (n-2)(\chi - \kappa) + \mu(u), \tag{4.1.3}$$

where $\mu(u)$ is the Maslov index.

The Floer homology group $Kh^\sharp(\widehat{\sigma})$ is well-defined and now we state our main result, which is a higher-dimensional version of Theorem 1.2.1 of [CHT20]:

Theorem 4.1.4. *For $n = 2$ or $n > 3$, $Kh^\sharp(\widehat{\sigma})$ is a link invariant, that is, it is independent of the choice of arcs $\{\widetilde{\gamma}_1, \ldots, \widetilde{\gamma}_\kappa\}$ and Lagrangian thimbles $\{\widetilde{a}_1, \ldots, \widetilde{a}_\kappa\}$, and is invariant under Markov stabilizations.*

Remark 4.1.5. *$Kh^\sharp(\widehat{\sigma})$ is a relative graded module over $\mathbb{F}[\mathcal{A}][\![\hbar, \hbar^{-1}]$. From (4.1.1) and Lemma 4.1.3, $\hbar$ is of degree $2 - n$.*

Remark 4.1.6. *Note that in Theorem 4.1.4, the case of $n = 3$ is excluded. The reason is explained by the remark after Lemma 4.2.2 in Section 4.2.*

The computation of $Kh^\sharp(\widehat{\sigma})$ for simple links in Section 4.5 gives results highly similar to Khovanov homology [Kho00][Wil08]. We will not discuss their relation further in this dissertation. Instead, we leave it as a conjecture:

Conjecture 4.1.7.

$$Kh^{\sharp,k}(\widehat{\sigma}) \simeq \bigoplus_{i-j=k \bmod n-2} Kh^{i,j}(\sigma). \tag{4.1.4}$$

Note that Conjecture 4.1.7 implies that we have found nothing new other than the symplectic Khovanov homology [SS06].

4.1.2 Moduli space of gradient trees

If two closed Lagrangian submanifolds L_0, L_1 of a symplectic manifold (M, ω) are C^1-close to each other, and moreover they are exact Lagrangian isotopic, then by the Lagrangian neighbourhood theorem, one can view L_1 as the graph $\Gamma_{df} \subset T^*L_0$, where $f : L_0 \to \mathbb{R}$. In this case, the count of pseudoholomorphic disks bounding L_0, L_1 can be reduced to the count of Morse gradient trajectories on L_0, which is much more convenient to compute. More generally, if we have exact Lagrangian isotopic $L_0, \ldots, L_{k-1}$, where $L_i = \Gamma_{df_i} \subset T^*L_0$ for $f_i : L_0 \to \mathbb{R}$, $i = 0, \ldots, k-1$, then we count gradient trees, to be explained below. This alternative method of counting appears several times in Section 4.2 and 4.4, so we make the statement precise here. The main reference is [FO97], which generalizes Floer's correspondence between gradient trajectories and pseudoholomorphic strips [Flo88]. There is also a simpler proof of [FO97] by Iacovino [Iac08], which considers the perturbation of Floer equations.

Definition 4.1.8. *A ribbon tree is a directed tree T which satisfies:*

1. *T has no degree 2 vertex.*
2. *For each internal vertex $v \in T$, there is a cyclic order of the edges attached to v, i.e. we have a labeling bijection $\ell_v : E_v \to \{0, 1, \ldots, k_v - 1\}$, where E_v is the set of edges*

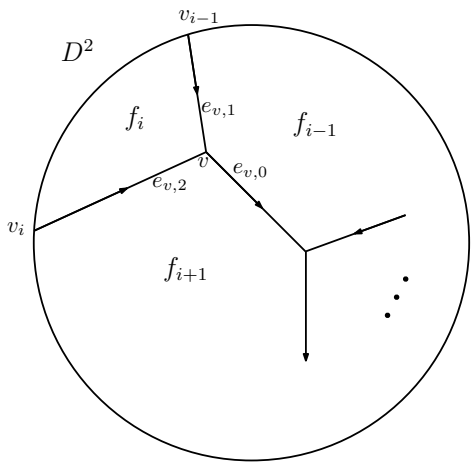

Figure 4.1: An embedding of T into D^2.

attached to v and k_v is the degree of v so that there is a unique outgoing edge and it is labeled 0. Therefore, there are two labels for each internal edge coming from the two labeling functions corresponding to the endpoints of the edge and one label for each external edge.

3. *There is a cyclic order of external vertices of T so that the root has label 0, i.e. we have a bijection $\ell : V_{ext} \to \{0, \dots, k-1\}$ where V_{ext} is the set of external vertices and the one adjacent to the unique outgoing edge is labeled by 0.*

4. *We can define an embedding $\phi : T \to D^2$ so that the above cyclic orders agree with counterclockwise orders, i.e. at each internal vertex v, $\phi(\ell_v^{-1}(0)), \dots, \phi(\ell_v^{-1}(k_v - 1))$ are in counterclockwise order around $\phi(v)$. Also, $\phi(V_{ext}) \subset \partial D^2$ and $\phi(\ell^{-1}(0)), \dots, \phi(\ell^{-1}(0))$ are in counterclockwise order on ∂D^2. Note that the way we embed T is not important.*

In the definition univalent vertices are called external and the others are internal; edges adjacent to external vertices are called external and the others are internal.

The edges of T will represent gradient flows. Specifically, let (M, g) be a Riemannian manifold and $f_0, \dots, f_{k-1}$ be C^∞-functions on M so that $f_i - f_{i+1}$ is Morse for each i (where $f_k = f_0$). We define the moduli space of gradient trees $\mathcal{M}_g(M; \boldsymbol{f}, \boldsymbol{p})$ to consist of pairs (T, I) where T is a ribbon tree and $I : T \backslash V_{ext} \to M$ is a continuous function satisfying:

1. $\lim_{x \to v_i} I(x) = p_i$, where p_i is a critical point of Morse function $f_i - f_{i+1}$.

2. External edges are identified with $(-\infty, 0]$ except the outgoing one which is identified with $[0, \infty)$; each internal edge e is identified with $[0, t(e)]$ where $t : E_{int} \to [0, \infty)$ is a length function defined on internal edges. Now I takes the above intervals to M. For each edge e of T, $I|_e$ is a reparametrization of the gradient flow of $-\nabla_g(f_{l(e)} - f_{r(e)})$, where $l(e)$ and $r(e)$ are defined with respect to the direction of e, i.e. if one looks in the positive direction of e on D^2, then $l(e)$ (resp. $r(e)$) is the component of $D^2 \backslash T$ on the left (resp. right) side of e.

Figure 4.1 shows an element T, together with an embedding of T in D^2. Note that we assign each function f_i to a corresponding region of $D^2 \backslash T$.

Lemma 4.1.9 ([FO97])**.** *$\mathcal{M}_g(M, \boldsymbol{f}, \boldsymbol{p})$ is of dimension*

$$\sum_v \text{ind}(v) - (k-1)n + (k-3), \tag{4.1.5}$$

where k is the number of boundary vertices and n is the dimension of the manifold.

Next we define the moduli space of pseudoholomorphic disks bounding exact Lagrangian submanifolds in T^*M. Let (M, g) be a Riemannian manifold. Let $\boldsymbol{f} = (f_0, \ldots, f_{k-1})$ be a generic collection of functions on M, and let $\boldsymbol{\Gamma} = (\Gamma_{df_0}, \ldots, \Gamma_{df_{k-1}})$ be the graphs of their differentials. We associate each critical point p_i of $f_i - f_{i+1}$ with $x_i = (p_i, \epsilon df_i(p_i)) \in \epsilon\Gamma_{df_{i+1}} \cap \epsilon\Gamma_{df_i}$ where $\epsilon > 0$ is small.

We then fix a canonical almost complex structure J_g on T^*M associated to the metric g on M so that

1. J_g is compatible with the canonical symplectic form ω on T^*M.

2. J_g maps vertical tangent vectors to horizontal tangent vectors of T^*M with respect to g.

3. On the zero section of T^*M, for $v \in T_qM \subset T_{(q,0)}(T^*M)$, let $J_g(v) = g(v, \cdot) \in T_q^*M \subset T_{(q,0)}(T^*M)$.

Definition 4.1.10. *Let $\mathcal{M}_{J_g}(T^*M; \epsilon\mathbf{\Gamma}, \boldsymbol{x})$ consist of pairs $(u, D^2_{\boldsymbol{z}})$ where $D^2_{\boldsymbol{z}}$ is the domain D^2 with marked points $\boldsymbol{z} = (z_0, \ldots, z_{k-1})$ arranged in counterclockwise order on ∂D^2 and $u : D^2 \backslash \{z_0, \ldots, z_{k-1}\} \to T^*M$ satisfies*

1. *$u(z_i) = p_i$,*
2. *$u(\partial_i D^2) \subset \epsilon\Gamma_{df_i}$,*
3. *$J_g \circ du = du \circ J_g$,*

where $\partial_i D^2$ is the shortest counterclockwise arc between z_i and z_{i+1} on ∂D^2. Here we are identifying pairs $(u, D^2_{\boldsymbol{z}})$ and $(v, D^2_{\boldsymbol{z}'})$ which are related by an isomorphism of the domain.

The following theorem relates Morse gradient trees on M to pseudoholomorphic disks on T^*M:

Theorem 4.1.11 ([FO97])**.** *For $\epsilon > 0$ sufficiently small, there is an oriented diffeomorphism $\mathcal{M}_g(M; \boldsymbol{f}, \boldsymbol{p}) \cong \mathcal{M}_{J_g}(T^*M; \epsilon\mathbf{\Gamma}, \boldsymbol{x})$.*

Roughly speaking, for each gradient tree $((T, i), I)$, we can construct a pseudoholomorphic curve near $I(T)$ inside T^*M by some gluing techniques. We should note that the theorem depends on a specific choice of almost complex structure J_g.

The following example counts pseudoholomorphic triangles with 3 Lagrangian boundaries, which we will meet again in Section 4.2.

Example 4.1.12. *We give an example of a gradient tree with 3 vertices here. Consider functions f_0, f_1, f_2 on S^n so that the domain D^2 looks like the left side of Figure 4.2. We can perturb f_0, f_1, f_2 generically so that v_1 is a source (top generator) of $\nabla(f_2 - f_1)$, v_2 is a sink (bottom generator) of $\nabla(f_0 - f_2)$ and v_0 is a sink (bottom generator) of $\nabla(f_0 - f_1)$. The middle of Figure 4.2 shows a possible perturbation when $n = 1$ for illustration. Sources*

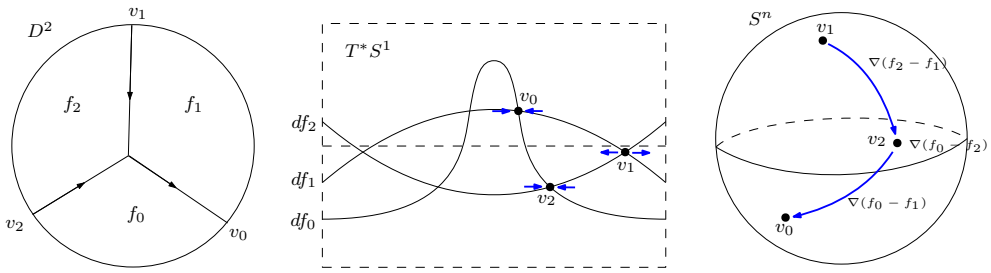

Figure 4.2: The gradient tree T viewed inside D^2 (left), the perturbation of Lagrangians in the special case of T^*S^1 (middle) and the image of T on S^n (right). We abuse notation and label both the domain and image of a vertex by v_i since there is no ambiguity.

and sinks are denoted by blue arrows. The right side of Figure 4.2 shows what happens on S^n: v_1 is the unique top generator of $f_2 - f_1$ on S^n, so the flows from v_1 form a S^{n-1}-family and pass through all the points of S^n except two critical points. v_2 is the bottom generator of $f_0 - f_2$, so the flow from v_2 of $\nabla(f_0 - f_2)$ is of length 0. Therefore the flow from v_1 should pass v_2 and there is a unique such flow line. Similarly, there is a unique flow line from v_2 to v_0 of $\nabla(f_0 - f_1)$. To conclude, there is a unique gradient tree. Thus there is a unique pseudoholomorphic disk bounded by the Lagrangians $\epsilon\Gamma_{df_0}, \epsilon\Gamma_{df_1}, \epsilon\Gamma_{df_2}$ for small ϵ by Theorem 4.1.11.

4.2 Invariance under arc slides

Given $\{\widetilde{\gamma}_1, \dots, \widetilde{\gamma}_\kappa\}$ from Section 4.1.1, consider the arc slide of $\widetilde{\gamma}_1$ over $\widetilde{\gamma}_2$: Let $\{\widetilde{\gamma}'_1, \dots, \widetilde{\gamma}'_\kappa\}$ be the new set of arcs as in Figure 4.3. Let $\widetilde{\boldsymbol{a}}' = \{\widetilde{a}'_1, \dots, \widetilde{a}'_\kappa\}$ be the new tuple of Lagrangians over $\{\widetilde{\gamma}'_1, \dots, \widetilde{\gamma}'_\kappa\}$. For $i = 1, \dots, \kappa$, let Θ_i (resp. Ξ_i) be the intersection point of $\widetilde{a}_i$ and $\widetilde{a}'_i$ that lies over z_i (resp. $z_{i+\kappa}$). Denote $\boldsymbol{\Theta} = \{\Theta_1, \dots, \Theta_\kappa\}$ and $\boldsymbol{\Xi} = \{\Xi_1, \dots, \Xi_\kappa\}$.

The purpose of this section is to prove:

Theorem 4.2.1. *$\widehat{CF}(\widetilde{W}, \widetilde{h}_\sigma(\widetilde{\boldsymbol{a}}), \widetilde{\boldsymbol{a}})$ and $\widehat{CF}(\widetilde{W}, \widetilde{h}_\sigma(\widetilde{\boldsymbol{a}}'), \widetilde{\boldsymbol{a}}')$ are quasi-isomorphic.*

Proof. It suffices to prove that $\widehat{CF}(\widetilde{W}, \widetilde{h}_\sigma(\widetilde{\boldsymbol{a}}), \widetilde{\boldsymbol{a}})$ and $\widehat{CF}(\widetilde{W}, \widetilde{h}_\sigma(\widetilde{\boldsymbol{a}}), \widetilde{\boldsymbol{a}}')$ are quasi-isomorphic. The quasi-isomorphism between $\widehat{CF}(\widetilde{W}, \widetilde{h}_\sigma(\widetilde{\boldsymbol{a}}), \widetilde{\boldsymbol{a}}')$ and $\widehat{CF}(\widetilde{W}, \widetilde{h}_\sigma(\widetilde{\boldsymbol{a}}'), \widetilde{\boldsymbol{a}}')$ is similar.

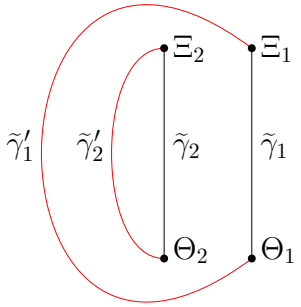

Figure 4.3: Arc sliding of $\widetilde{\gamma}_1$ over $\widetilde{\gamma}_2$.

We define the cochain map by the μ_2 composition map of the A_∞-relation:

$$\Phi : \widehat{CF}(\widetilde{W}, \widetilde{h}_\sigma(\widetilde{\boldsymbol{a}}), \widetilde{\boldsymbol{a}}) \to \widehat{CF}(\widetilde{W}, \widetilde{h}_\sigma(\widetilde{\boldsymbol{a}}), \widetilde{\boldsymbol{a}}'), \tag{4.2.1}$$

$$\boldsymbol{y} \mapsto \mu_2(\boldsymbol{\Xi} \otimes \boldsymbol{y}),$$

where μ_2 is the product map

$$\mu_2 : \widehat{CF}(\widetilde{W}, \widetilde{\boldsymbol{a}}, \widetilde{\boldsymbol{a}}') \otimes \widehat{CF}(\widetilde{W}, \widetilde{h}_\sigma(\widetilde{\boldsymbol{a}}), \widetilde{\boldsymbol{a}}) \to \widehat{CF}(\widetilde{W}, \widetilde{h}_\sigma(\widetilde{\boldsymbol{a}}), \widetilde{\boldsymbol{a}}').$$

Similarly we define the cochain map going back by

$$\Psi : \widehat{CF}(\widetilde{W}, \widetilde{h}_\sigma(\widetilde{\boldsymbol{a}}), \widetilde{\boldsymbol{a}}') \to \widehat{CF}(\widetilde{W}, \widetilde{h}_\sigma(\widetilde{\boldsymbol{a}}), \widetilde{\boldsymbol{a}}), \tag{4.2.2}$$

$$\boldsymbol{y} \mapsto \mu_2'(\boldsymbol{\Theta} \otimes \boldsymbol{y}).$$

The following lemma justifies that Φ, Ψ are well-defined:

Lemma 4.2.2. *For $n = 2$ or $n > 3$, $\boldsymbol{\Xi}$ is a cocycle in $\widehat{CF}(\widetilde{W}, \widetilde{\boldsymbol{a}}, \widetilde{\boldsymbol{a}}')$ and $\boldsymbol{\Theta}$ is a cocycle in $\widehat{CF}(\widetilde{W}, \widetilde{\boldsymbol{a}}', \widetilde{\boldsymbol{a}})$.*

Proof of Lemma 4.2.2: For simplicity assume $\kappa = 2$. By Lemma 4.1.3 and a Maslov index calculation,

$$\mathrm{ind}(u; \boldsymbol{\Theta}, \boldsymbol{\Xi}) = (n-2)(\chi - 2) + 4n - 4, \tag{4.2.3}$$

$$\mathrm{ind}(u; \boldsymbol{\Theta}, \{\Xi_2, \Theta_1\}) = (n-2)(\chi - 2) + n, \tag{4.2.4}$$

$$\mathrm{ind}(u; \boldsymbol{\Theta}, \{\Xi_1, \Theta_2\}) = (n-2)(\chi - 2) + 3n - 4, \tag{4.2.5}$$

where for example, $\mathrm{ind}(u;\boldsymbol{\Theta},\boldsymbol{\Xi})$ denotes the Fredholm index of curves $u:\dot{F}\to\mathbb{R}\times[0,1]\times\widetilde{W}$ so that

1. $du\circ J^{\Diamond}=J^{\Diamond}\circ du$,
2. $u(\partial\dot{F})\subset\mathbb{R}\times((\{1\}\times\widetilde{\boldsymbol{a}})\cup(\{0\}\times\widetilde{\boldsymbol{a}}'))$,
3. As $\pi_{\mathbb{R}}\circ u$ tends to $+\infty$ (resp. $-\infty$), $\pi_{\widetilde{W}}$ tends to $\boldsymbol{\Theta}$ (resp. $\boldsymbol{\Xi}$), where $\pi_{\mathbb{R}}$ and $\pi_{\widetilde{W}}$ are the projections of u to $\mathbb{R}$ and $\widetilde{W}$.

We explain (4.2.3)-(4.2.5) now. First, the Maslov index of a closed path over $\widetilde{\gamma}_2'$ and $\widetilde{\gamma}_2$ is n by definition, which implies (4.2.4). To get (4.2.5), observe that the projection to $\widetilde{D}$ of the curve from Θ_1 to Ξ_1 is over the region surrounded by $\widetilde{\gamma}_1'$ and $\widetilde{\gamma}_1$, which contains two critical values of the Lefschetz fibration. The region surrounded by $\widetilde{\gamma}_1'$ and $\widetilde{\gamma}_1$ can be viewed as the outcome after applying Lagrangian surgery twice on a trivial strip to incorporate the two critical values. By Theorem 55.5 of [FOOO09], each Lagrangian surgery increases the Fredholm index by $n-2$. Therefore, $\mathrm{ind}(u;\boldsymbol{\Theta},\{\Xi_1,\Theta_2\})=(n-2)(\chi-2)+3n-4$ by comparing with (4.2.4). Finally, (4.2.3) follows by adding the Maslov index terms of (4.2.4) and (4.2.5).

For $n=2$, the Fredholm index does not depend on χ:

$$\mathrm{ind}(u;\boldsymbol{\Theta},\boldsymbol{\Xi})=4,\quad \mathrm{ind}(u;\boldsymbol{\Theta},\{\Xi_2,\Theta_1\})=\mathrm{ind}(u;\boldsymbol{\Theta},\{\Xi_1,\Theta_2\})=2.$$

For $n>3$, observe that in all 3 cases the domain F has 2 punctures and thus χ is even. In particular, $\mathrm{ind}(u;\boldsymbol{\Theta},\boldsymbol{\Xi})$ is even and $\mathrm{ind}(u;\boldsymbol{\Theta},\boldsymbol{\Xi})\neq 1$; If $\mathrm{ind}(u;\boldsymbol{\Theta},\{\Xi_1,\Theta_2\})=1$, then $\chi=2-\frac{n-1}{n-2}$, which is not a integer for $n>3$; If $\mathrm{ind}(u;\boldsymbol{\Theta},\{\Xi_2,\Theta_1\})=1$, then $\chi=-1-\frac{1}{n-2}$, which is also not a integer for $n>3$.

Therefore, for $n=2$ or $n>3$, there is no index 1 curve from $\boldsymbol{\Theta}$, i.e. $\boldsymbol{\Theta}$ is a cocycle in $\widehat{CF}(\widetilde{W},\widetilde{\boldsymbol{a}}',\widetilde{\boldsymbol{a}})$. The case of $\boldsymbol{\Xi}$ is similar. □

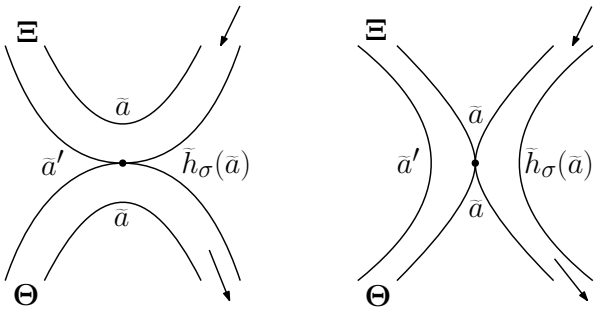

Figure 4.4: Two possible degenerations.

Remark 4.2.3. *Lemma 4.2.2 does not deal with the case of $n = 3$, where the index could be 1 for some χ. Therefore, to show $\boldsymbol{\Theta}$ is a cocycle, we still need to understand the index 1 pseudoholomorphic curves from Θ_2 to Ξ_2, whose projection to $\widetilde{D}$ is the thin strip surrounded by $\widetilde{\gamma}_2'$ and $\widetilde{\gamma}_2$, and also the curves from Θ_1 to Ξ_1, whose projection to $\widetilde{D}$ is the fat strip surrounded by $\widetilde{\gamma}_1'$ and $\widetilde{\gamma}_1$.*

It remains to show that $\Psi \circ \Phi$ induces identity on cohomology (with some nonzero coefficient). The composition of Ψ and Φ is given by the left-hand side of Figure 4.4, which is viewed as a degeneration of a family of curves. The right-hand side of Figure 4.4 shows another degeneration. Observe that the right-hand part of the right degeneration is of index 0. In fact the right degeneration corresponds to the identity map times the count of its left-hand part, which is chain homotopic to $\Psi \circ \Phi$.

Now we count the left-hand part of the right degeneration of Figure 4.4. For convenience, assume $\kappa = 2$, i.e. focus on the arc sliding of $\widetilde{\gamma}_1$ over $\widetilde{\gamma}_2$. The moduli space $\mathcal{M}_J(\boldsymbol{\Xi}, \boldsymbol{\Theta})$ contains curves u with boundary condition which maps $\partial \dot{F}$ to $(\mathbb{R} \times \{1\} \times \widetilde{\boldsymbol{a}}') \cup (\mathbb{R} \times \{0\} \times \widetilde{\boldsymbol{a}})$. There is another restriction on the right degeneration: u passes through $(0, 0, w_1)$ and $(0, 0, w_2)$, where $(0, 0) \in \mathbb{R} \times [0, 1]$ and $w_i \in \widetilde{\boldsymbol{a}}_{\boldsymbol{i}}$. Passing through a generic $\boldsymbol{w} = \{w_1, w_2\}$ is a codimension $2n$ condition. By Lemma 4.1.3, $\mathrm{ind}(\boldsymbol{\Xi}, \boldsymbol{\Theta}) = 2n$ if and only if $n = 2$ or $\chi = 0$ for $n > 3$.

By Theorem 4.2.5 below, the count of $\mathcal{M}_J^{\chi=0}(\boldsymbol{\Xi}, \boldsymbol{\Theta})$ passing a generic $\boldsymbol{w}$ is 1 (mod 2). Thus $\Psi \circ \Phi$ is cochain homotopic to identity with some nonzero coefficient. The case of $\Phi \circ \Psi$ is similar. $\square$

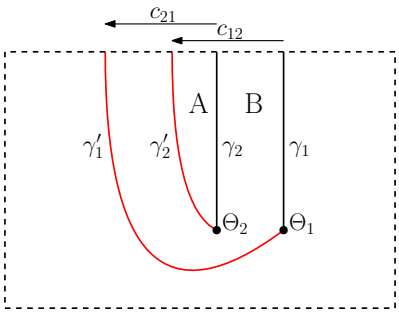

Figure 4.5: Half of the base. We count pseudoholomorphic disks surrounded by $\gamma_1, \gamma_2, \gamma_1', \gamma_2'$.

4.2.1 Half of curve count

There is a half version of the counting problem, where the base is shown as Figure 4.5. The base D can be extended to $\mathbb{C}$ by adding cylindrical ends, denoted by $\bar{D}$. Let $\bar{a}_i$ and $\bar{a}_j'$ be the cylindrical completion of a_i and a_j'. The asymptotic Reeb chords from $\bar{a}_i$ to $\bar{a}_j'$ form a S^{n-1}-family. We then perturb the contact form so that the S^{n-1}-family becomes Morse-Bott and let $\check{c}_{ij}, \hat{c}_{ij}$ be the longer and shorter asymptotic Reeb chords. Let $\boldsymbol{c} = \{\check{c}_{12}, \check{c}_{21}\}$. The problem is to count $\mathcal{M}_{J^\diamond}^{\chi=1,\boldsymbol{w}}(\boldsymbol{c}, \boldsymbol{\Theta})$, which is over the cylindrical extension of the region surrounded by $\gamma_1, \gamma_2, \gamma_1', \gamma_2'$.

Theorem 4.2.4. $\#\mathcal{M}_{J^\diamond}^{\chi=1,\boldsymbol{w}}(\boldsymbol{c}, \boldsymbol{\Theta}) = 1 \ mod\ 2$ *for generic* $\boldsymbol{w}$.

Proof. For $u \in \mathcal{M}_{J^\diamond}^{\chi=1,\boldsymbol{w}}(\boldsymbol{c}, \boldsymbol{\Theta})$, let $v = \pi_{\bar{W}} \circ u : \dot{F} \to \bar{W}$, where $\bar{W}$ is the cylindrical extension of W and F is the unit disk in $\mathbb{C}$.

Recall that $p : \bar{W} \to \bar{D}$ is the projection. $p \circ v : \dot{F} \to \bar{D}$ has degree 2 (resp. 1) over region A (resp. B) of Figure 4.5, which are connected components of $D - \gamma_1 \cup \gamma_1' \cup \gamma_2 \cup \gamma_2'$ with extension. There are two possible branching behaviors: Type *int* has a branch point b that maps to the interior of region A; Type ∂ is more obscure which has two switch points b_1, b_2 on the boundary of region A instead of a branch point. Denote Type ∂_1 for the case b_1, b_2 on γ_2' and Type ∂_2 for b_1, b_2 on γ_2. Choose b_1 as the point closer to the puncture c_{12} (resp. c_{21}) on $\partial\dot{F}$ that maps to γ_2' (resp. γ_2).

There is another codimension-1 constraint. Denote the preimage of $*$ under u as $q(*)$,

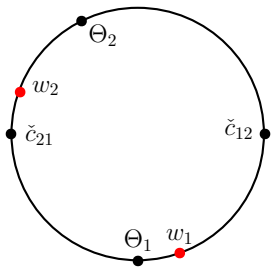

Figure 4.6

and we will often leave this notation out if there is no ambiguity. A possible arrangement of points on $\partial\dot{F}$ is shown as Figure 4.6. Since the projection of u to $\mathbb{R}\times[0,1]$ is a double branched cover and under this projection, $\{q(w_1), q(w_2)\}$, $\{q(\Theta_1), q(\Theta_2)\}$, $\{q(\check{c}_{12}), q(\check{c}_{21})\}$ are mapped to $(0,0), -\infty, +\infty$ respectively, the deck transformation requires the involution:

$$q(\Theta_1)\mapsto q(\Theta_2),\ q(\check{c}_{21})\mapsto q(\check{c}_{12}),\ q(w_2)\mapsto q(w_1). \tag{4.2.6}$$

The counting strategy uses the fact that the mod 2 count $\#\mathcal{M}_{J^\diamond}^{\chi=1,\boldsymbol{w}}(\boldsymbol{c},\boldsymbol{\Theta})$ does not depend on $\boldsymbol{w}$, which allows us to stretch the curve by letting $\boldsymbol{w}$ tend to some limit:

1. Let $|p(w_2)|\gg 0$;
2. Let the width between $\gamma_2,\gamma_2', m\to 0$;
3. Choose w_1 so that $p(w_1)\to z_1$.

Step 1. Denote $\iota=\mathrm{Im}\circ p$. We first observe that as $p(w_1)\to z_1$, either $\iota\circ v(b)\gg\iota(w_2)$ or $\iota\circ v(b_2)\gg\iota(w_2)$. If this is not true, then by Gromov compactness there exists a limiting curve which contradicts the involution condition 4.2.6. Refer to [CHT20] for details.

Step 2. Write $\mathcal{M}_{J^\diamond}^{\chi=1,\boldsymbol{w},\sharp}(\boldsymbol{c},\boldsymbol{\Theta})$ for the curves satisfying $\iota\circ v(b)\gg\iota(w_2)$ or $\iota\circ v(b_1)\geq\iota(w_2)-C$. The case of $\iota\circ v(b)\gg\iota(w_2)$ is shown as the left of Figure 4.7, where the limiting 2-level curve contains $v^{(1)}\cup v^{(2)}\cup v^{(3)}$. The case of $\iota\circ v(b_1)\geq\iota(w_2)-C$ is similar. We push off the bottom singular point a little so that a_1 and a_1' have clean S^{n-1}-intersection, which does not change the moduli space of $v^{(1)}$ by [FOOO09].

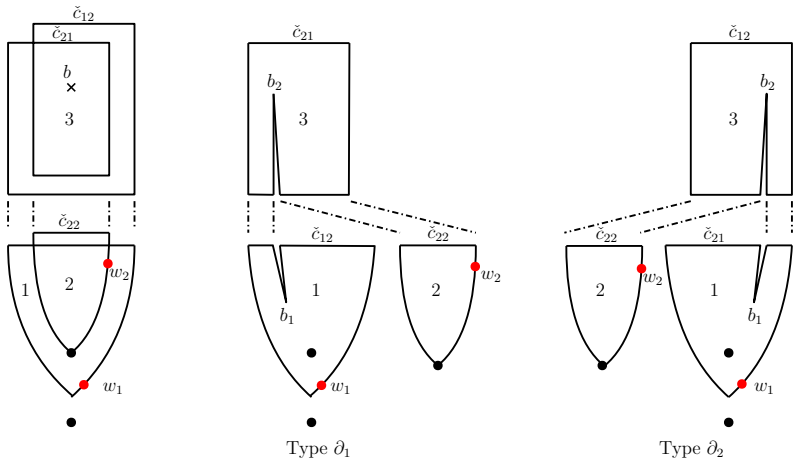

Figure 4.7

The region of $p \circ v^{(1)}$ contains a singular point of a Lefschetz fibration, which can be viewed as the outcome after a Lagrangian surgery from the trivial region without singular points. By Theorem 55.5 of [FOOO09], the moduli space of $v^{(1)}$ is diffeomorphic to S^{n-2}. Therefore the evaluation map of $v^{(1)}$ at $\check{c}_{11}$ sweeps S^{n-2} inside the S^{n-1}-family of Reeb chords, of which the homology class vanishes. The result is $\#\mathcal{M}_{J^\diamond}^{\chi=1,\boldsymbol{w},\sharp}(\boldsymbol{c},\boldsymbol{\Theta}) = 0 \bmod 2$.

Step 3. The remaining case is the curve satisfying $\iota \circ v(b_2) \gg \iota(w_2)$ and $\iota \circ v(b_1) \leq \iota(w_2) - C$. The stretched limiting curves are shown as the middle and the right of Figure 4.7. We expect that such curves exist and contribute 1 (mod 2) to $\mathcal{M}_{J^\diamond}^{\chi=1,\boldsymbol{w}}(\boldsymbol{c},\boldsymbol{\Theta})$.

First we treat Type ∂_1. $v^{(2)}$ is uniquely determined since there is a unique gradient trajectory from $\check{c}_{22}$ to Θ_2 passing through w_2. Denote the bottom-left Reeb chord of $v^{(3)}$ by $\hat{d}_{21}$. We show that the pseudoholomorphic triangle $v^{(3)}$ exists uniquely: The Lefschetz fibration around $v^{(3)}$ is the trivial one $p : \mathbb{C} \times T^*S^{n-1} \to \mathbb{C}$. We can perturb the Lagrangians a_1, a_1', a_2, a_2' in the fiber direction. The case of $n = 2$ is shown as Figure 4.8, where there exists a single pseudoholomorphic triangle.

More generally, the case of $n \geq 2$ is done by the gradient tree argument. Put the perturbed Lagrangians as Figure 4.8 on $T^*S^1 \subset T^*S^{n-1}$ and extend to T^*S^{n-1}. After a further small perturbation, we consider the moduli space of Morse gradient trees with 3

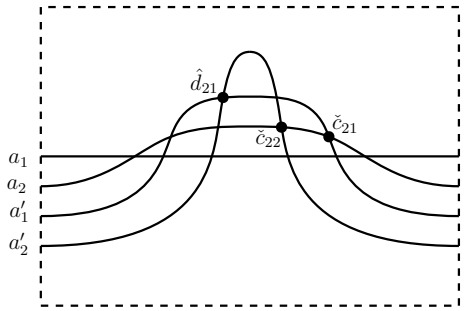

Figure 4.8: The fiber T^*S^1 with perturbed Lagrangians. The sides are identified.

vertices $\check{c}_{22}, \check{c}_{21}, \hat{d}_{21}$. Viewing all vertices as sources of gradient flow, we check that $\mathrm{ind}(\check{c}_{22}) = 0$, $\mathrm{ind}(\check{c}_{21}) = \mathrm{ind}(\hat{d}_{21}) = n - 1$.

By Lemma 4.1.9, the dimension of this moduli space is 0 and it contains a unique gradient tree which corresponds to a single pseudoholomorphic triangle by Theorem 4.1.11. Note that this is almost the same as the example after Theorem 4.1.11.

It remains to count $v^{(1)}$, which is a pseudoholomorphic disk with a slit and a singular point inside. The singular point can be viewed as coming from a Lagrangian surgery [FOOO09], which increases the Fredholm index by $n - 2$. Now the moduli space of $v^{(1)}$ passing through a generic w_1 is of dimension $n - 1$. Consider the evaluation map ev_{21} of $v^{(1)}$ on its top-left end, where the image lies in a S^{n-1}-family of Reeb chords. The gluing condition on both ends says ev_{21} should take the value of $\hat{d}_{21}$. All we need is that ev_{21} intersects $\hat{d}_{21}$ at a unique point. We will show in Type ∂_1, ev_{21} sweeps half of S^{n-1} and the other half is dealt with by Type ∂_2. This is done by a model calculation of explicit pseudoholomorphic curves in Step 3' below.

Step 3'. **A model calculation**. All notations are limited to this step.

We replace the base of $v^{(1)}$ in Type ∂_1 by a standard one, i.e. the unit disk in $\mathbb{C}_z$ with a slit $\{-1 \leq \mathrm{Re}\, z \leq 0\} \cap \{\mathrm{Im}\, z = 0\}$. The Lefschetz fibration over the unit disk is

$$p : (z_1, z_2, \ldots, z_n) \mapsto z_1^2 + z_2^2 + \cdots + z_n^2, \tag{4.2.7}$$

with a critical value at $0 \in \mathbb{C}_z$. It is however more convenient to think of the case $n = 2$ first, and the Lefschetz fibration is

$$p' : (z_1', z_2') \mapsto z_1' z_2', \tag{4.2.8}$$

where $z_1' = z_1 + iz_2$, $z_2' = z_1 - iz_2$. Let T be the Clifford torus $\{|z_1'| = 1\} \times \{|z_2'| = 1\}$ over $|z| = 1$ and let L be the Lagrangian thimble over $\{-1 \leq \operatorname{Re} z \leq 0\} \cap \{\operatorname{Im} z = 0\}$. $T \cap L$ is a clean S^1-intersection over $-1 \in \mathbb{C}_z$.

We consider curves with boundary on $T \cup L$: let $\mathcal{M}_2$ (2 stands for $n = 2$) be the moduli space of holomorphic disks

$$u = (u_1, u_2) : \mathbb{R} \times [0, 1] \to \mathbb{C}^2$$

with standard complex structure J_{std} satisfying

1. $u(\mathbb{R} \times \{0\}) \subset T$ and $u(\mathbb{R} \times \{1\}) \subset L$;
2. $p \circ u$ has degree 1 over $\{|z| < 1\} - \{-1 \leq \operatorname{Re} z \leq 0\} \cap \{\operatorname{Im} z = 0\}$ and degree 0 otherwise;
3. $u(0, 0) = w_1 = (w_{11}, w_{12}) = (1, 1)$.

Condition 3 is essentially the same as that $v^{(1)}$ passes through w_1 in Step 3. It is not hard to see that $\mathcal{M}_2$ is homeomorphic to a line segment where $\partial\mathcal{M}_2$ consists of two curves $z \mapsto (z, 1)$ and $z \mapsto (1, z)$. Figure 4.9 gives a schematic description of $\mathcal{M}_2$, from the top row of $z \mapsto (z, 1)$ to the bottom row of $z \mapsto (1, z)$, where the right-hand column changes the coordinates to (z_1, z_2).

We then consider the evaluation map. The top-left end of $v^{(1)}$ in Type ∂_1 is translated to $e^{i(\pi+\epsilon)} \in \mathbb{C}_z$ for small $\epsilon > 0$. Define $ev_1' : \mathcal{M}_2 \to S^1_{|z_1'|=1}$ as the z_1' projection of the intersection between u and $p'^{-1}(e^{i(\pi+\epsilon)})$, which is shown by red dots in the z_1' column of Figure 4.9. Clearly ev_1' is a homeomorphism between $\mathcal{M}_2$ and $\{e^{i\theta_1} | \pi + \epsilon < \theta_1 < 2\pi\}$.

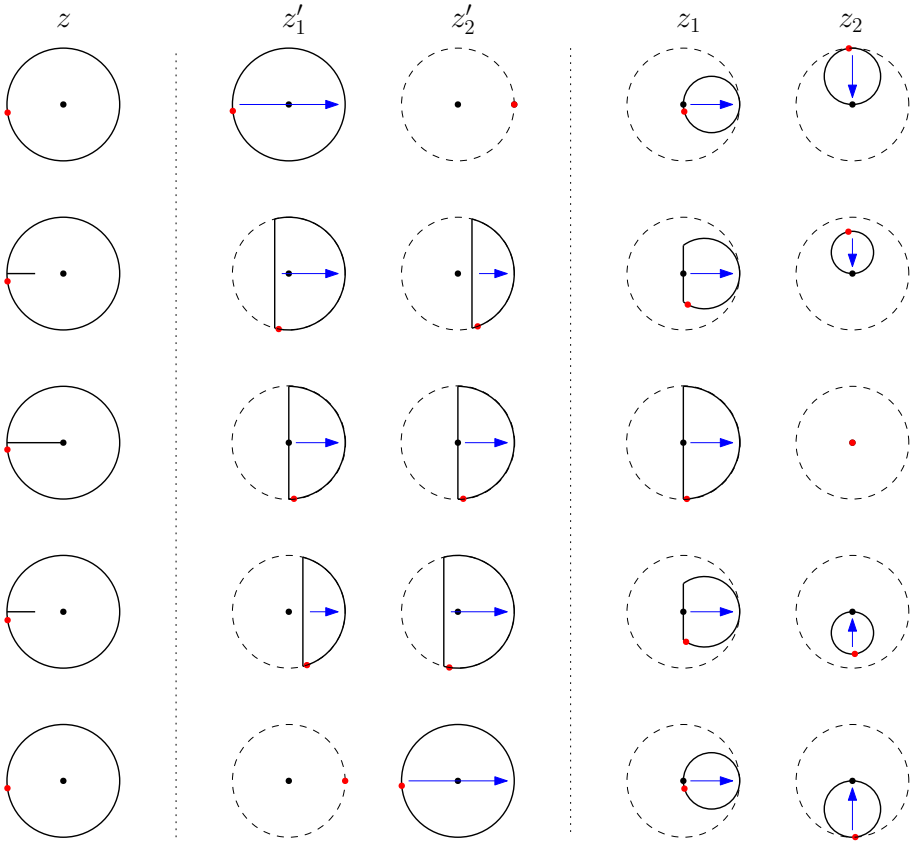

Figure 4.9: The pictorial description of $\mathcal{M}_2$. The left column describes the base $\mathbb{C}_z$. The middle and right column are for two sets of coordinates. Dashed curves denote the unit circle. The red dots indicate $e^{i(\pi+\epsilon)}$ on the left and for their preimages on the middle and right. The arrows indicate images of the arrow from $(0,1)$ to $(0,0)$ on the domain $\mathbb{R}\times[0,1]$. Note that the drawings are not necessarily accurate.

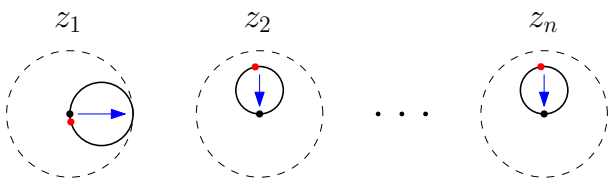

Figure 4.10: $u_{1/\sqrt{n-1},\dots,1/\sqrt{n-1}}$ of the first row in Figure 4.9.

For general $n \geq 2$, define $\mathcal{M}_n$ similar to $\mathcal{M}_2$, where T, L in condition 1 are still the Lagrangian vanishing cycles over the unit circle and $\{-1 \leq \operatorname{Re} z \leq 0\} \cap \{\operatorname{Im} z = 0\}$. Condition 3 is modified to

3'. $u(0,0) = w_1 = (w_{11}, w_{12}, \dots, w_{1n}) = (1, 0, \dots, 0)$.

$\mathcal{M}_2$ in coordinate (z_1, z_2) is viewed as the slice of $\mathcal{M}_n$ that restricts to 0 on $z_3, \dots, z_n$. Observe that for $\mathcal{M}_n$, the coordinates $z_2, z_3, \dots, z_n$ are symmetric. Thus we can recover $\mathcal{M}_n$ from $\mathcal{M}_2$ by a symmetric rotation of z_2-coordinate. Each $u = (z_1, z_2) \in \mathcal{M}_2$ corresponds to a S^{n-2}-family of curves in $\mathcal{M}_n$:

$$u_{\lambda_1,\dots,\lambda_{n-1}} = (z_1, \lambda_1 z_2, \dots, \lambda_{n-1} z_2), \tag{4.2.9}$$

where $\lambda_1^2 + \cdots + \lambda_{n-1}^2 = 1$ and $\lambda_i \in \mathbb{R}$ for $i = 1, \dots, n-1$. Figure 4.10 shows $u_{1/\sqrt{n-1},\dots,1/\sqrt{n-1}}$ recovered from the first row of Figure 4.9.

The new evaluation map ev is defined as the n-tuple of coordinates which projects to $e^{i(\pi+\epsilon)} \in \mathbb{C}_z$. Therefore, $\mathcal{M}_n$ is homeomorphic to D^{n-1}. One can check that $ev : \mathcal{M}_n \to S^{n-1}$ is a homeomorphism to its image, which is half of the vanishing cycle S^{n-1} over $e^{i(\pi+\epsilon)}$.

In case J_{std} is not regular, we apply small perturbation $J^\Diamond$ of J_{std}. One can show that for any $\boldsymbol{z} \in ev_{J_{std}}(\mathcal{M}_n)$, $\#ev_{J^\Diamond}^{-1}(\boldsymbol{z}) = 1 \bmod 2$. Therefore the argument of Step 3 still works. This finishes Step 3'.

Finally we glue $v^{(1)}, v^{(2)}$ and $v^{(3)}$. Still assume we are in Type ∂_1. The involution condition (4.2.6) will fix the neck length: As we take $\iota \circ v(b_2) \to \infty$, $q(\Theta_2)$ approaches $q(\check{c}_{21})$ but

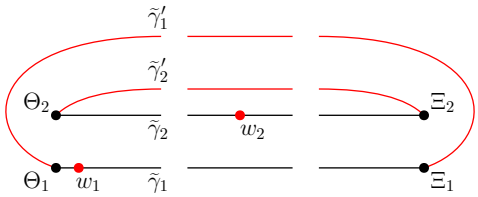

Figure 4.11: The stretched base as $K \gg 0$. $\operatorname{Im} z$ is the horizontal direction.

$|q(w_2) - q(\Theta_2)| \ll |q(w_2) - q(\check{c}_{21})|$. Assume w_1 is close to Θ_1, there is a unique value of $\iota \circ v(b_2)$ for which there exists an involution of F. This completes the proof of Theorem 4.2.4. □

4.2.2 Curve count

The goal of this section is to count the full version of pseudoholomorphic annuli from Ξ_1, Ξ_2 to Θ_1, Θ_2 over the region in Figure 4.3 and prove the following theorem:

Theorem 4.2.5. $\#\mathcal{M}_{J^\diamond}^{\chi=0,\boldsymbol{w}}(\boldsymbol{\Xi}, \boldsymbol{\Theta}) = 1 \mod 2$ *for generic* $\boldsymbol{w}$.

Proof. The strategy is the same as the proof of Theorem 4.2.4: We stretch the curve into several levels by choosing some extreme $\boldsymbol{w}$, then use the restriction of domain involution and gluing conditions to find a unique (mod 2) curve.

We closely follow the proof of Theorem 9.3.7 of [CHT20] and some details are omitted. As before, we write $u : \dot{F} \to \mathbb{R} \times [0,1] \times \widetilde{W}$ for an element in $\mathcal{M}_{J^\diamond}^{\chi=0,\boldsymbol{w}}(\boldsymbol{\Xi}, \boldsymbol{\Theta})$ and let v be its projection to $\widetilde{W}$.

The main idea is to stretch the base $\widetilde{D}$ in $\operatorname{Im} z$ direction as Figure 4.11: Let $\operatorname{Im} z_i = -2K$ and $\operatorname{Im} z_{i+\kappa} = 2K$, $i = 1, \dots, \kappa$ and $K \to +\infty$. The region $\mathcal{R}$ bounded by γ_1, γ_1' is split into 3 parts: $\mathcal{R}_1 = \mathcal{R} \cap \{\operatorname{Im} z \le -K\}$, $\mathcal{R}_2 = \mathcal{R} \cap \{-K \le \operatorname{Im} z \le K\}$ and $\mathcal{R}_3 = \mathcal{R} \cap \{\operatorname{Im} z \ge K\}$. The mod 2 count is independent of $\boldsymbol{w}$. We choose $\widetilde{w}_1$ close to z_1, $\widetilde{w}_2$ close to $\operatorname{Im} z = 0$ and the thin strip $\mathcal{R}'$ between γ_2, γ_2' with width $m \to 0$.

The curve v has degree 2 over $\mathcal{R}'$ and degree 1 over $\mathcal{R} - \mathcal{R}'$. The types of branching behaviors are denoted by 2, $1L$, $1R$, $0LL$, $0LR$, $0RR$. Take $0LR$ for example: 0 means

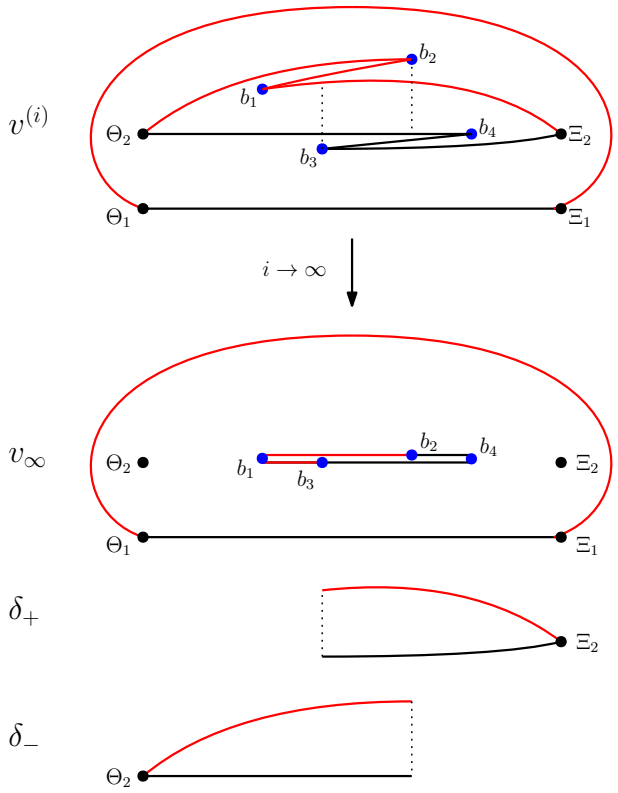

Figure 4.12: The limiting proceduce of Type $0LR$.

the number of interior branch points is 0; L means one pair of switch points is over $\widetilde{\gamma}_2'$; R means one pair of switch points is over $\widetilde{\gamma}_2$. Denote (if exist) interior branch points by $b, b' \in \mathrm{int}(\dot{F})$ and switch points by $b_1, b_2, b_3, b_4 \in \partial\dot{F}$. We assume $\iota(b') > \iota(b)$, $\iota(b_2) > \iota(b_1)$ and $\iota(b_4) > \iota(b_3)$.

Step 1. Suppose $K \gg 0$. Take a sequence of $u^{(i)} \in \mathcal{M}_{J^\Diamond}^{\chi=0,\boldsymbol{w}}(\boldsymbol{\Xi}, \boldsymbol{\Theta})$ so that $v^{(i)} : F^{(i)} \to \widetilde{W}$ with $m^{(i)} \to 0$. In the limit $i \to \infty$, the thin strip tends to a slit, the limiting curve splits into $v_\infty \cup \delta_+ \cup \delta_-$, where δ_+ is a gradient trajectory from Ξ_2 and δ_- is a gradient trajectory to Θ_2, and v_∞ is a pseudoholomorphic annulus. Figure 4.12 describes the limiting procedure in the case of Type $0LR$. In fact we will show that Type $0LR$ is the only nontrivial case.

Step 2. We claim that the limiting slit is long enough, that is, for $K \gg 0$ and $m \to 0$,

$$\max\{\iota(b'), \iota(b_2), \iota(b_4)\} \geq K, \tag{4.2.10}$$

$$\min\{\iota(b), \iota(b_1), \iota(b_3)\} \leq -K. \tag{4.2.11}$$

which are the two endpoints of the slit.

If (4.2.11) is not true, i.e. $\min\{\iota(b), \iota(b_1), \iota(b_3)\} > -K$, then the part of v_∞ in region $\mathcal{R}_1$ has no slit, which can be viewed as the outcome of a Lagrangian surgery on a trivial pseudoholomorphic disk. Similar to Step 2 in the proof of Theorem 4.2.4, the moduli space of pseudoholomorphic disks passing through a generic w_1 is diffeomorphic to S^{n-2}, of which the evaluation map at the cylindrical end has a S^{n-2}-intersection with the S^{n-1}-family of Reeb chords. The evaluation map vanishes at homology level, which contributes 0 (mod 2) to the curve count. The argument for (4.2.10) is similar.

Step 3. We claim that for $K \gg 0$ and m small, if (4.2.10) and (4.2.11) hold, the mod 2 contribution of Type $2, 1L, 0LL, 0RR$ is 0. The reason is that if one considers the involution condition

$$q(\Theta_1) \mapsto q(\Theta_2), \quad q(\Xi_1) \mapsto q(\Xi_2), \quad q(w_1) \mapsto q(w_2) \tag{4.2.12}$$

for a pseudoholomorphic annulus, there is a constraint on the position of Θ_2, Ξ_2, w_2 on the slit in v_∞. One can refer to [CHT20] for detailed discussion that all but Type $0LR$ contradict with (4.2.12)

Step 4. It remains to consider Type $0LR$. Assuming (4.2.10) and (4.2.11) are satisfied, we claim that the contribution of Type $0LR$ is 1 (mod 2).

Although there are other possible arrangements of b_1, b_2, b_3, b_4 on the slit, we just consider the case in Figure 4.12 for illustration. As shown in Figure 4.13, v_∞ is the gluing of two regions: $v_{l,\infty}$ with $\operatorname{Im} z \ll -K$ and $v_{r,\infty}$ with $\operatorname{Im} z \gg -K$, which can be viewed as two pseudoholomorphic disks similar to Step 3' of the previous section. The conditions that w_1

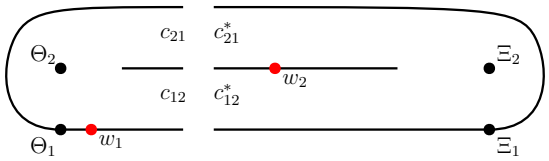

Figure 4.13: v_∞ with a long slit. $\mathcal{R}_1$ on the left and $\mathcal{R}_2 \cup \mathcal{R}_3$ on the right.

is close to Θ_1 and that w_2 sits on the slit will be translated to an explicit model calculation in Step 4' below. For suitable choices of w_1 and w_2, we will show that the space of two disks with $c_{21} = c_{21}^*$, $c_{12} = c_{12}^*$ is homeomorphic to a line segment $\mathcal{I}$. Let $M_{\mathcal{I}}$ be the set of v_∞ glued from the $\mathcal{I}$-family of $(v_{l,\infty}, v_{r,\infty})$.

The involution condition (4.2.12) determines a unique curve inside $M_{\mathcal{I}}$. In conclusion, $\#\mathcal{M}_{J^\diamond}^{\chi=0,\boldsymbol{w}}(\boldsymbol{\Xi}, \boldsymbol{\Theta}) = 1 \bmod 2$. We have proved Theorem 4.2.5 modulo the model calculation below:

Step 4'. **A model calculation**. We use similar notations as in Step 3' of the previous section. Define $\mathcal{M}_l$ for the space of v_l over the left-hand of Figure 4.13 and $\mathcal{M}_r$ for those of v_r over the right-hand side. Both are viewed as maps from $\mathbb{R} \times [0,1]$ to $\mathbb{C}^n$ over the unit circle with one slit $\subset \{-1 \le \operatorname{Re} z \le 0\} \cap \{\operatorname{Im} z = 0\} \subset \mathbb{C}_z$. Consider evaluation maps

$$ev_l, ev_r : \mathcal{M}_l, \mathcal{M}_r \to S^{n-1} \times S^{n-1}, \tag{4.2.13}$$

which are defined below, corresponding to $c_{12}, c_{21}, c_{12}^*, c_{21}^*$ in Figure 4.13. The gluing condition is $ev_l(v_l) = ev_r(v_r)$.

As usual, we first consider the case of $n = 2$ with Lefschetz fibration (4.2.8).

$\mathcal{M}_l$ is defined as holomorphic disks passing through $w_1 = (1,1)$ over $1 \in \mathbb{C}_z$. Note that $\mathcal{M}_l$ is the same as $\mathcal{M}$ in Step 3' of the previous section. Let $w_\pm = e^{i(\pi \pm \epsilon)} \in \mathbb{C}_z$. Define the evaluation map ev_l as

$$\begin{aligned} ev_l : \mathcal{M}_l &\to S^1 \times S^1, \\ v_l &\mapsto (ev_{l+}(v_l), ev_{l-}(v_l)), \end{aligned} \tag{4.2.14}$$

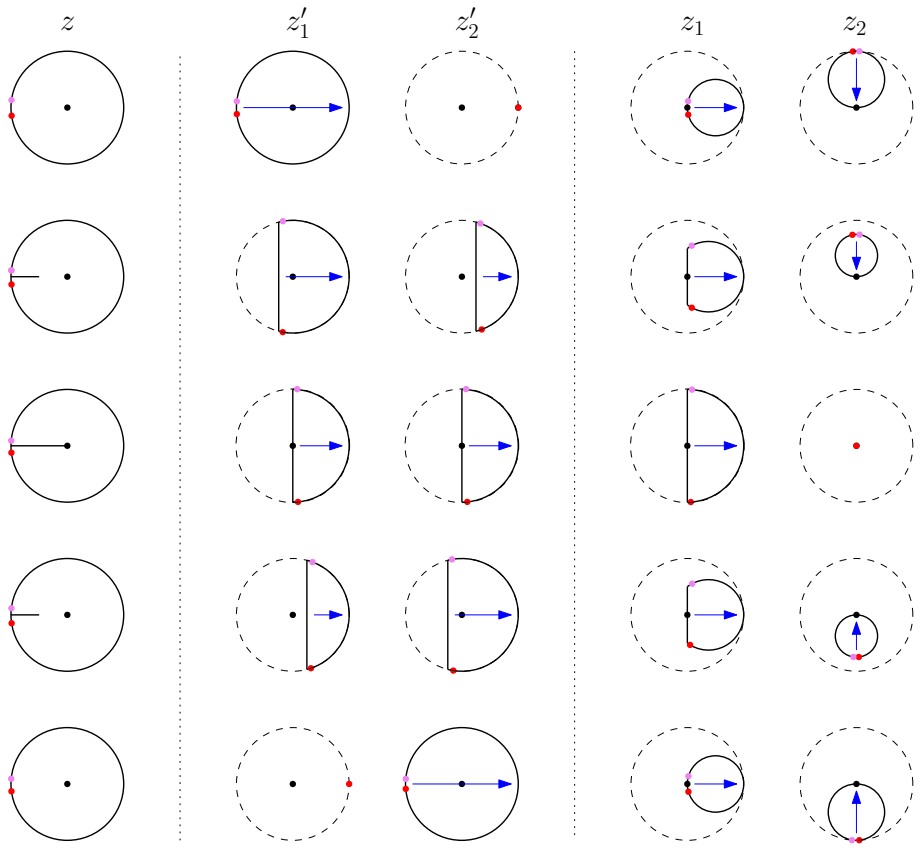

Figure 4.14: The pictorial description of $\mathcal{M}_l$. The left column describes the base $\mathbb{C}_z$. The middle and right columns are for two sets of coordinates. The red and violet dots indicate $e^{i(\pi\pm\epsilon)}$ on the left and their preimages on the middle and right.

where $ev_{l\pm}(v_l)$ is the z_1'-coordinate of the point that projects to $w_\pm$. Figure 4.14 gives a schematic description of $\mathcal{M}_l$, homeomorphic to a line segment, and its evaluation maps $ev_{l\pm}$ denoted by red and violet dots. We also show the maps in coordinates (z_1, z_2) with $z_1' = z_i + iz_2$, $z_2' = z_i - iz_2$.

Since $w_1 = (1, 0)$ in coordinate (z_1, z_2), define $w_1 = (1, 0, 0, \ldots, 0)$ for $n \geq 2$. Then $\mathcal{M}_{l,2}$, the moduli space for $n = 2$, is viewed as the slice of $\mathcal{M}_{l,n}$ that restricts to 0 on $z_3, \ldots, z_n$. Now $\mathcal{M}_{l,n}$ is a symmetric rotation of $\mathcal{M}_{l,2}$ which contains $v' = (z_1, \lambda_1 z_2, \lambda_2 z_3, \ldots, \lambda_{n-1} z_n)$, where $\lambda_1^2 + \cdots + \lambda_{n-1}^2 = 1$, $\lambda_1, \ldots, \lambda_{n-1} \in \mathbb{R}$. Thus $\mathcal{M}_{l,2}$ is homeomorphic to D^{n-1}.

Next we consider $\mathcal{M}_r$ of $v'' : \mathbb{R} \times [0, 1] \to \mathbb{C}^n$. We put the constraint that v'' passes

through $(-r, r) \in L$ for some $r \in [0, 1]$, which corresponds to w_2 sitting on the slit in Figure 4.13. Let $ev_{r\pm}(v'')$ be the z_1'-coordinate of the point that projects to $w_\pm$ and define the map

$$\begin{aligned} ev_r : \mathcal{M}_r &\to S^1 \times S^1, \\ v_r &\mapsto (ev_{r-}(v_r), ev_{r+}(v_r)), \end{aligned} \tag{4.2.15}$$

where $+$ and $-$ are switched because we want to identify $w_\pm$ of v' with $w_\mp$ of v''.

Observe that $\mathcal{M}_{r,2}$ is of dimension 2. Figure 4.15 describes some of the curves inside $\mathcal{M}_{r,2}$. $(-r, r)$ in (z_1', z_2') equals $(0, ir)$ in (z_1, z_2). Thus for $n \geq 2$, if $\mathcal{M}_{r,2}$ is viewed as the slice of $\mathcal{M}_{r,n}$ with $z_3 = \cdots = z_n = 0$, then $\mathcal{M}_{r,n}$ contains curves of $v_r = (\lambda_1 z_1, z_2, \lambda_2 z_1, \ldots, \lambda_{n-1} z_1)$, where $\lambda_1^2 + \cdots + \lambda_{n-1}^2 = 1$, $\lambda_1, \ldots, \lambda_{n-1} \in \mathbb{R}$.

For $n = 2$, we have the following observation:

Claim 4.2.6. *For $n = 2$ and $\epsilon \to 0$, the evaluation map of $\mathcal{M}_l$ and $\mathcal{M}_r$ with images in $S^1 \times S^1$ is described in Figure 4.16. $ev_l(\mathcal{M}_l)$ is the blue line segment and $ev_r(\mathcal{M}_r)$ is the 2-dimensional pink region. Their intersection is a line segment $\mathcal{I}$.*

For general $n \geq 2$, we have the same result:

Lemma 4.2.7. *For $n \geq 2$ and $\epsilon \to 0$, the intersection between $ev_l(\mathcal{M}_l)$ and $ev_r(\mathcal{M}_r)$ is still $\mathcal{I}$.*

Proof of Lemma 4.2.7. Suppose $v_{l,\boldsymbol{\lambda}} = (z_{l1}, \lambda_1 z_{l2}, \ldots, \lambda_{n-1} z_{l2})$ and $v_{r,\boldsymbol{\lambda'}} = (\lambda_1' z_{r1}, z_{r2}, \lambda_2' z_{r1}, \ldots, \lambda_{n-1}' z_{r1})$ satisfy $ev_l(v_{l,\boldsymbol{\lambda}}) = ev_r(v_{r,\boldsymbol{\lambda'}})$ where the 3rd to n-th coordinates are not all zero. Denote

$$\begin{aligned} ev_{l\pm}(v_{l,\boldsymbol{\lambda}}) =& (z_{l1\pm}, \lambda_1 z_{l2\pm}, \ldots, \lambda_{n-1} z_{l2\pm}), \\ ev_{r\mp}(v_{r,\boldsymbol{\lambda'}}) =& (\lambda_1' z_{r1\mp}, z_{r2\mp}, \lambda_2' z_{r1\mp}, \ldots, \lambda_{n-1}' z_{r1\mp}). \end{aligned}$$

Observe that $\operatorname{Im} \lambda_1 z_{l2+} = \operatorname{Im} \lambda_1 z_{l2-}$ and then $z_{r2-} = z_{r2+}$. From c and d in Figure 4.15 we see that $ev_r((z_{r1}, z_{r2}))$ (in coordinate (z_1', z_2')) must lie in $\{\theta_1 + \theta_2 = 2\pi\} \cap \{\pi \leq \theta_1 \leq 3\pi/2\}$ of Figure 4.16. For such curves v (as (a, b, e) in Figure 4.15), $\operatorname{Im} z_{r1-} = -\operatorname{Im} z_{r1+}$ and

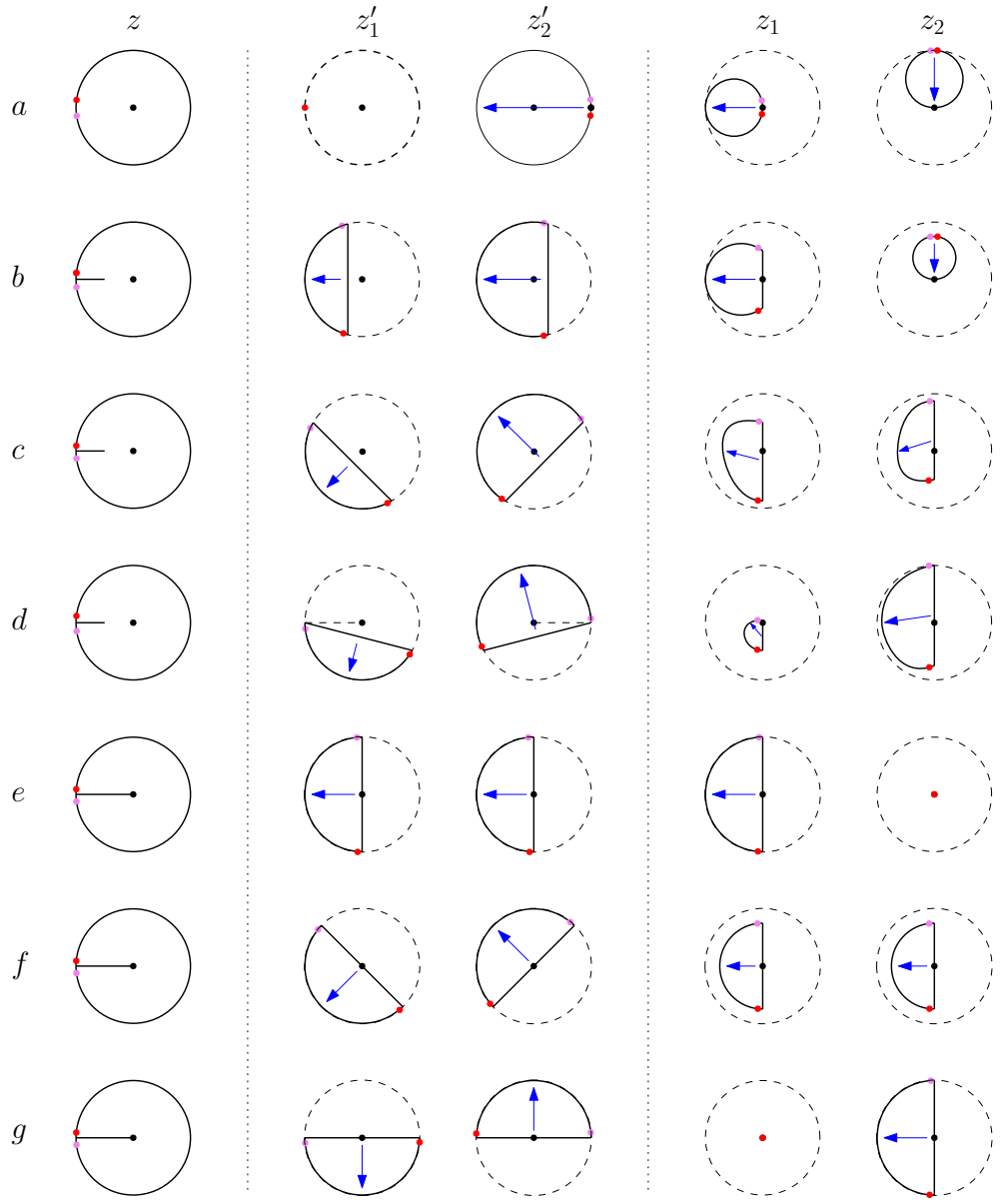

Figure 4.15: The pictorial description of part of $\mathcal{M}_r$. The notations are as before, while the red and violet dots indicate $e^{i(\pi \mp \epsilon)}$ on the left and their preimages on the middle and right.

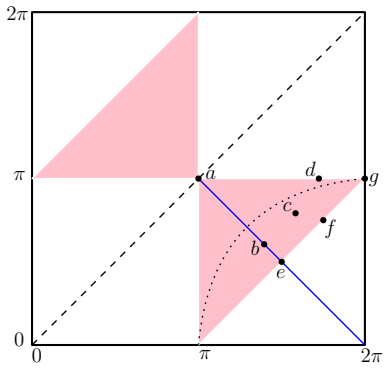

Figure 4.16: The description of ev_l (blue) and ev_r (pink) for $n = 2$. The sides are identified. a-g correspond to curves in Figure 4.15.

$\operatorname{Re} z_{r1-} = \operatorname{Re} z_{r1+}$. Since $\operatorname{Re} z_{l2+} = -\operatorname{Re} z_{l2-}$ and $\operatorname{Im} z_{l2+} = \operatorname{Im} z_{l2-}$, the consequence is that $\lambda_2 z_{l2\pm} = \cdots = \lambda_{n-1} z_{l2\pm} = 0$, which is a contradiction. □

Now we go back to the curve count problem. We want to pick a single curve from the $\mathcal{I}$-family of v_∞ and then glue it to get a unique $v^{(i)}$ for each i.

First we show the position of b_2^∞ determines v_∞ uniquely in $\mathcal{I}$: Consider the slit in v_∞ of Figure 4.12. In the limit $q(w_1) = q(\Theta_1)$, so $q(w_2) = q(\Theta_2) = q(b_2^\infty)$. If we fix b_2^∞, then v''_∞ passes through $(-r, r)$ for some $r \in [0, 1]$, corresponding to fixing a hypersurface in $S^{n-1} \times S^{n-1}$, whose intersection with $S^1 \times S^1$ is the dotted curve in Figure 4.16. The dotted curve intersects the blue line at a single point, which determines v_∞. Moreover, the length of the slit in v'_∞ and v''_∞ are determined and thus b_1^∞ and b_4^∞ are fixed. Finally b_3^∞ is fixed by the involution of F^∞.

Consider then $v^{(i)}$ for large i. From the previous paragraph $\iota(b_2^{(i)})$ will fix a unique v_∞ in $\mathcal{I}$. By Implicit Function Theorem, it will fix a unique $v^{(i)}$ as well, which is close to v_∞. Then observe that the distance between $q(\Theta_2)$ and $q(w_2)$ is a monotone function of $\iota(b_2^{(i)})$: As $\iota(b_2^{(i)})$ increases, the slit gets longer, $b_1^{(i)}$ moves left and $b_4^{(i)}$ moves right. Therefore $q(w_2)$ leaves $q(\Theta_2)$ and approaches $q(\Xi_2)$ on $F^{(i)}$. The involution of $F^{(i)}$ determines a unique $\iota(b_2^{(i)})$ and thus a unique $v^{(i)}$.

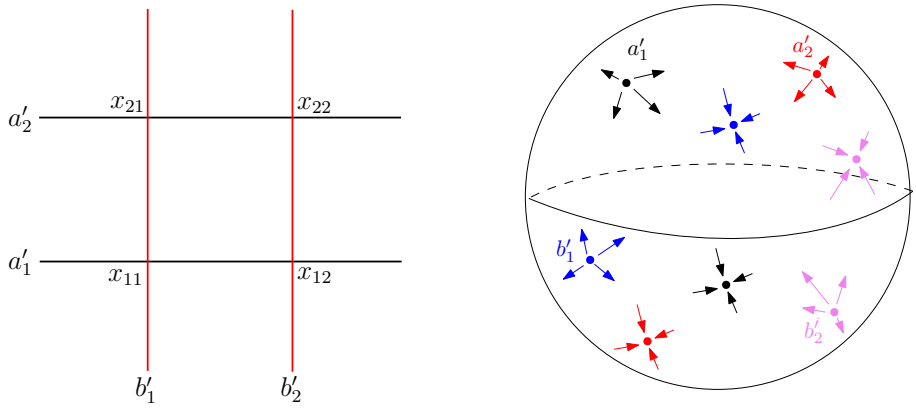

Figure 4.17: The base $\mathbb{C}$ on the left and the fiber T^*S^{n-1} on the right.

This finishes the proof of Theorem 4.2.5. □

4.3 A model calculation of quadrilaterals

We make a model calculation which will be used in Section 4.4 and 4.5. Consider the trivial fibration $\hat{p} : \mathbb{C} \times T^*S^{n-1} \to \mathbb{C}$ and Lagrangian submanifolds $a_i = \{y = i\} \times S^{n-1}$, $i = 1, 2$, $b_j = \{x = j\} \times S^{n-1}$, $j = 1, 2$, where S^{n-1} is the zero section of T^*S^{n-1}. We further modify a_i, b_j to a_i', b_j' by a Hamiltonian perturbation in the fiber direction so that they intersect transversely. Specifically, we choose the restriction of Euclidean metric on S^{n-1} and identify T^*S^{n-1} with TS^{n-1}. Choose Morse functions f_1, f_2, f_3, f_4 on S^{n-1} each with 2 critical points and all of the critical points are disjoint (as the right of Figure 4.17). We can then rescale these Morse functions so that the difference of each pair is still Morse with 2 critical points:

Lemma 4.3.1. *For small enough $\epsilon > 0$, the difference between each pair of functions in $\{\epsilon^3 f_1, \epsilon^2 f_2, \epsilon f_3, f_4\}$ is Morse with 2 critical points.*

Proof. For small enough $\epsilon > 0$, $f_4 - \epsilon f_3$ is a small perturbation of f_4. Since Morse condition is C^∞-stable, $f_4 - \epsilon f_3$ is still Morse with 2 critical points. By a simple induction the proof is finished. □

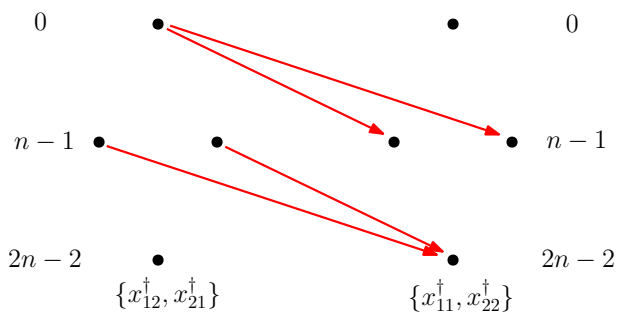

Figure 4.18: The differentials of $\widehat{CF}(\boldsymbol{b}, \boldsymbol{a})$. The generators in the top row have 2 checks, those in the middle row have 1 check and those in the bottom row have no check.

Denote $f_{a_1'} = \epsilon^3 f_1$, $f_{a_2'} = \epsilon^2 f_2$, $f_{b_1'} = \epsilon f_3$, $f_{b_2'} = f_4$, the gradients of which correspond to the fiber projection of a_1', a_2', b_1', b_2'. Let $\check{x}_{ij}, \hat{x}_{ij}$ over x_{ij} be the top and bottom critical points of $f_{b_j'} - f_{a_i'}$, $i, j \in \{1, 2\}$.

Now we compute the differentials of $\widehat{CF}(\boldsymbol{b'}, \boldsymbol{a'})$, which is generated by 8 elements $\{x_{12}^\dagger, x_{21}^\dagger\}$ and $\{x_{11}^\dagger, x_{22}^\dagger\}$, where $\dagger$ denotes a check or hat.

Lemma 4.3.2. *The differential of $\widehat{CF}(\boldsymbol{b'}, \boldsymbol{a'})$ is given by $\hbar$ times the arrows in Figure 4.18. Moreover, a relative grading by Maslov index is denoted in Figure 4.18.*

Proof. Let $u : \dot{F} \to \mathbb{R} \times [0, 1] \times (\mathbb{C} \times T^*S^{n-1})$ be a pseudoholomorphic disk with positive ends $\{x_{12}^\dagger, x_{21}^\dagger\}$ and negative ends $\{x_{11}^\dagger, x_{22}^\dagger\}$. Suppose the complex structure is split, then its projection to $\mathbb{C}$ is a degree 1 map over $[1, 2] \times [1, 2]$, which fixes the cross ratio of the 4 punctures on $\partial \dot{F}$.

Then we consider the projection of u to the fiber direction T^*S^{n-1}, denoted by $w : \dot{F} \to T^*S^{n-1}$. By the construction above a_1', a_2', b_1', b_2' are graphical near $S^{n-1} \subset T^*S^{n-1}$, with respect to Morse functions $f_{a_i'}, f_{b_j'}$, $i, j = 1, 2$. The domain of the Morse moduli space is shown in Figure 4.19, where inner edges are ignored and arrows denote the direction of $-\nabla(f_{\text{right}} - f_{\text{left}})$.

Viewing all boundary vertices as sources of gradient flow, observe that $\check{x}_{ij}$ is of Morse index $n - 1$ if $i \neq j$ and 0 if $i = j$; $\hat{x}_{ij}$ is of Morse index 0 if $i \neq j$ and $n - 1$ if $i = j$. By

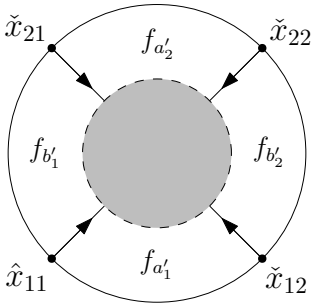

Figure 4.19

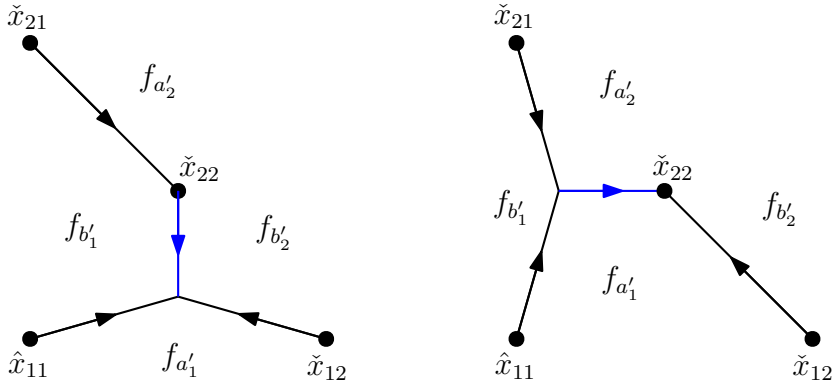

Figure 4.20: Two possible gradient trees on S^{n-1}. The moduli space is parametrized by the length of the inner (blue) edge.

Lemma 4.1.9,

$$\mathrm{ind}(w) = \Big(\#\text{checks in } \{x_{12}^\dagger, x_{21}^\dagger\} + \#\text{hats in } \{x_{11}^\dagger, x_{22}^\dagger\} - 3\Big)\,(n-1) + 1. \tag{4.3.1}$$

Therefore, the Morse moduli space with respect to the arrows in Figure 4.18 is of $\mathrm{ind}(w) = 1$ and the case of gradient tree on S^{n-1} from $\{\check{x}_{12}, \check{x}_{21}\}$ to $\{\hat{x}_{11}, \check{x}_{22}\}$ is shown in Figure 4.20.

By Theorem 4.1.11, the Fukaya moduli space is diffeomorphic to the Morse moduli space, so we can think of gradient trees instead of pseudoholomorphic disks. Taking the base direction into consideration, we check that

$$\mathrm{ind}(u) = \mathrm{ind}(w). \tag{4.3.2}$$

For example, still consider the case of Figure 4.20: The two gradient trees are parametrized by the length of their inner edges. As the inner length tends to zero, the left and right

gradient trees tend to the same one. As the inner edge of the left one tends to the bottom generator of $f_{b'_2} - f_{b'_1}$, its length tends to infinity and $q(\check{x}_{21})$ approaches $q(\check{x}_{22})$. Similarly, as the inner edge of the right one tends to the top generator of $f_{a'_2} - f_{a'_1}$, its length tends to infinity and $q(\check{x}_{12})$ approaches $q(\hat{x}_{22})$. Since the cross ratio on the domain is fixed by the base direction, the result is that the algebraic count of w is one. This verifies $\mathrm{ind}(u) = 1$ and the arrows in Figure 4.18.

If we set $\{\check{x}_{12}, \check{x}_{21}\}$ to be of grading 0, we can verify the relative grading of generators in Figure 4.18 by Lemma 4.1.3, (4.3.1), (4.3.2) and the convention that $|\hbar| = 2 - n$, where the difference of grading is given by Maslov index.

□

4.4 Invariance under Markov stabilization

A Markov stabilization is given as Figure 4.21: σ is a κ-strand braid which intersects D along $\boldsymbol{z} = \{z_1, \ldots, z_k\}$. On the base D, σ is viewed as an element of $\mathrm{Diff}^+(D, \partial D, z)$, which restricts to identity near γ_0. Without loss of generality, we construct a positive Markov stabilization between γ_0 and γ_1: Let c be an arc from z_0 to z_1 which is disjoint from other γ_j, perform a positive half twist along c, then we get a $(\kappa+1)$-strand braid given by $\sigma \circ \sigma_c$.

Now we consider the fiber and Lagrangians. Let $p' : W' \to D$ be the standard Lefschetz fibration with regular fiber T^*S^{n-1} and critical values $\boldsymbol{z'} = \{z_0, \ldots, z_\kappa\}$ and $p : W \to D - N(\gamma_0)$ be its restriction to $D - N(\gamma_0)$. Let a_j denote the Lagrangian thimble over γ_j. Let h_σ be an element of $\mathrm{Symp}(W, \partial W)$ which descends to σ and $h'_\sigma \in \mathrm{Symp}(W', \partial W')$ be its extension to W' by identity. Finally, let $\tau_c \in \mathrm{Symp}(W', \partial W')$ be the Dehn twist along the Lagrangian sphere over c.

The proof of invariance under Markov stabilization is the same as Theorem 9.4.2 of [CHT20], and we briefly restate its proof here:

Theorem 4.4.1. *$\widehat{CF}(W, h_\sigma(\boldsymbol{a}), \boldsymbol{a})$ and $\widehat{CF}(W', h'_\sigma \circ \tau_c(\boldsymbol{a}'), \boldsymbol{a}')$ are isomorphic cochain com-*

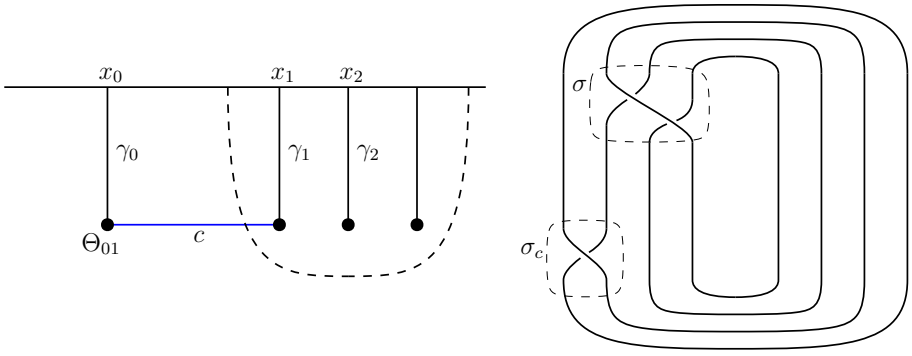

Figure 4.21: Markov stabilization along c.

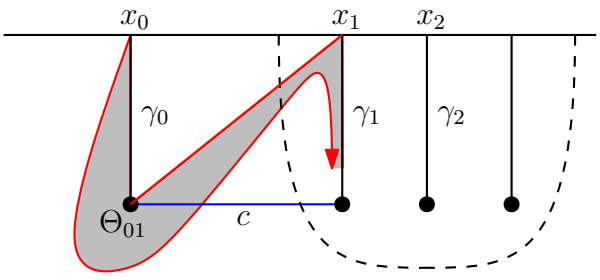

Figure 4.22: The red half-arcs are $\sigma \circ \sigma_c(\gamma_0)$ and $\sigma \circ \sigma_c(\gamma_1)$. The shaded region denotes the curve we are gluing.

plexes for specific choices of almost complex structure and $h_\sigma(\boldsymbol{a})$ and $h'_\sigma \circ \tau_c(\boldsymbol{a}')$ after a Hamiltonian isotopy.

Proof. We directly construct a homomorphism $\Phi_s : \widehat{CF}(W, h_\sigma(\boldsymbol{a}), \boldsymbol{a}) \to \widehat{CF}(W', h'_\sigma \circ \tau_c(\boldsymbol{a}'), \boldsymbol{a}')$ and show it is a cochain isomorphism. The notations are as in Figure 4.22.

Consider the κ-tuples in $\widehat{CF}(W, h_\sigma(\boldsymbol{a}), \boldsymbol{a})$: it may or may not contain $\{x_1\}$. Similarly, the κ-tuples in $\widehat{CF}(W', h'_\sigma \circ \tau_c(\boldsymbol{a}'), \boldsymbol{a}')$ may contain either $\{x_0, x_1\}$ or $\{\Theta_{01}\}$. In fact there is a linear isomorphism:

$$\Phi_s : \widehat{CF}(W, h_\sigma(\boldsymbol{a}), \boldsymbol{a}) \to \widehat{CF}(W', h'_\sigma \circ \tau_c(\boldsymbol{a}'), \boldsymbol{a}'), \tag{4.4.1}$$

$$\{x_1\} \cup \boldsymbol{y}' \mapsto \{x_0, x_1\} \cup \boldsymbol{y}', \boldsymbol{y} \mapsto \{\Theta_{01}\} \cup \boldsymbol{y},$$

For convenience of gluing below, we put $h_\sigma(a_1)$ and $h'_\sigma \circ \tau_c(a_0)$ in a position so that they go over the same arc near γ_1. Rigorously, let $\gamma_1 = \{\operatorname{Re} z_1\} \times [-1, 0] \subset D$ and $\epsilon > 0$ be small. The projections $\sigma(\gamma_1)$ and $\sigma \circ \sigma_c(\gamma_0)$ are written as $\zeta_1 \cup \zeta_2 \cup \zeta_3$ and $\zeta'_1 \cup \zeta_2 \cup \zeta_3$. The main requirement is that ζ_2 be a common neck, for example, set $\zeta_2 = \{\operatorname{Re} z_1 - \epsilon\} \times [-2/3, -1/3]$. Refer to Figure 4.22.

We compare the differential of $\widehat{CF}(W', h'_\sigma \circ \tau_c(\boldsymbol{a}'), \boldsymbol{a}')$ and $\widehat{CF}(W, h_\sigma(\boldsymbol{a}), \boldsymbol{a})$. If u' goes from $\{x_0, x_1\} \cup y'_1$ to $\{x_0, x_1\} \cup y'_2$, then u' is in bijection with u that goes from $\{x_1\} \cup y'_1$ to $\{x_1\} \cup y'_2$ since the strip from x_0 to x_0 is trivial. Similarly, u' that goes from $\{\Theta_{01}\} \cup y_1$ to $\{\Theta_{01}\} \cup y_2$ is in bijection with u that goes from y_1 to y_2. There are no curves from $\{x_0, x_1\} \cup y'_1$ to $\{\Theta_{01}\} \cup y_2$ and no curves from $\{x_1\} \cup y'_1$ to y_2. The nontrivial case is that, if u' goes from $\{\Theta_{01}\} \cup y_1$ to $\{x_0, x_1\} \cup y'_2$, then it is in bijection with u that goes from y_1 to $\{x_0\} \cup y'_2$, where u' comes from u by replacing the end containing x_1 by the shaded region in Figure 4.22. The bijection comes from Lemma 4.3.2 which says the curve over the shaded region has algebraic count 1. The gluing details are omitted. □

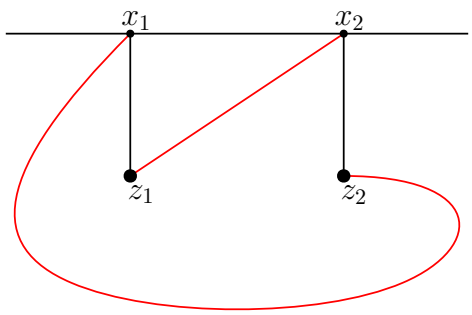

Figure 4.23: The braid representation of an unknot on D.

4.5 Examples

In this section we consider some simple links and compute their cohomology groups $Kh^\sharp(\widehat{\sigma})$ in the sense of Theorem 4.1.4, with coefficient ring $\mathbb{F}[\mathcal{A}][\![\hbar,\hbar^{-1}]$ when $n=2$ and $\mathbb{F}[\![\hbar,\hbar^{-1}]$ when $n>3$, where $\hbar$ is of grading $2-n$. We assume that $\mathbb{F}$ is of characteristic 2 for simplicity.

4.5.1 Unknots

Figure 4.23 shows the 2-strand braid representation of an unknot. In the Morse-Bott family of Reeb chords, x_1, x_2 are viewed as longer Reeb chords (top generators) and z_1, z_2 are viewed as shorter Reeb chords (bottom generators). The only possible differential in $\widehat{CF}(\widetilde{W}, \widetilde{h}_{\sigma_{\text{unknot}}}(\widetilde{\boldsymbol{a}}), \widetilde{\boldsymbol{a}})$ counts quadrilaterals u with $\{x_1, x_2\}$ at positive ends and $\{z_1, z_2\}$ at negative ends. The projection of u to D has degree 1 over the region bounded by the loop $x_1 \to z_2 \to x_2 \to z_1 \to x_1$ and degree 0 over its complement.

Proposition 4.5.1. *$Kh^\sharp(\widehat{\sigma}_{\text{unknot}})$ is freely generated by $\{x_1, x_2\}$ and $\{z_1, z_2\}$, where the difference of grading between these two generators is 2 (mod $n-2$):*

generators	*grading*
$\{x_1, x_2\}$	0
$\{z_1, z_2\}$	2

Proof. Similar to the proof of Lemma 4.3.2, we check that the pseudoholomorphic disk u with $\{x_1, x_2\}$ at positive ends and $\{z_1, z_2\}$ at negative ends is of Fredholm index n and

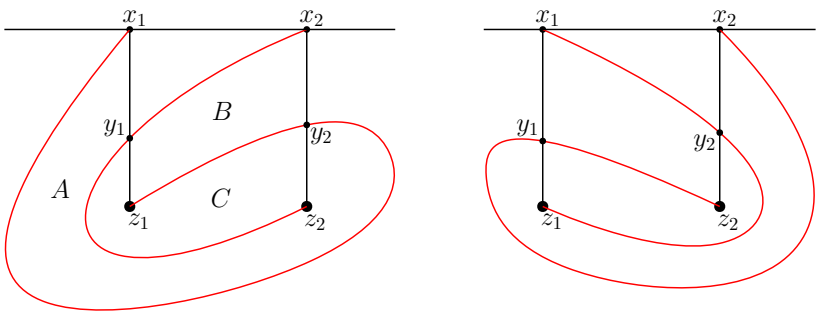

Figure 4.24: The braid representation of the left-handed Hopf link (left) and the right-handed Hopf link (right).

Maslov index $2n-2$. Therefore, $\{x_1, x_2\}$ and $\{z_1, z_2\}$ are both cocycles and thus generators of $Kh^\sharp(\widehat{\sigma}_{\text{unknot}})$. □

4.5.2 Hopf links

We then consider the 2-strand braid representation of a left-handed Hopf link as the left-hand side of Figure 4.24. 'A' to 'C' denote the corresponding regions on the base D. For example, we use 'A' + 'B' to represent the union of region 'A' and 'B'.

Lemma 4.5.2. *$\widehat{CF}(\widetilde{W}, \widetilde{h}_{\sigma_{\text{left Hopf}}}(\widetilde{\boldsymbol{a}}), \widetilde{\boldsymbol{a}})$ contains the following (mod 2) differential relations:*

$$d\{x_1, z_2\} = \hbar\{\hat{y}_1, \check{y}_2\} + \hbar\{\check{y}_1, \hat{y}_2\}, \tag{4.5.1}$$

$$d\{x_2, z_1\} = \hbar\{\hat{y}_1, \check{y}_2\} + \hbar\{\check{y}_1, \hat{y}_2\}, \tag{4.5.2}$$

$$d\{\check{y}_1, \hat{y}_2\} = \hbar\{z_1, z_2\}, \tag{4.5.3}$$

$$d\{\hat{y}_1, \check{y}_2\} = \hbar\{z_1, z_2\}. \tag{4.5.4}$$

Proof. All nontrivial index 1 pseudoholomorphic curves with count 1 (mod 2) are listed as follows, where we label the regions with positive weights after projection to base D:

regions	ends of generators
A	$\{x_1, z_2\} \to \{\check{y}_1, \hat{y}_2\}/\{\hat{y}_1, \check{y}_2\}$
B	$\{x_2, z_1\} \to \{\check{y}_1, \hat{y}_2\}/\{\hat{y}_1, \check{y}_2\}$
C	$\{\check{y}_1, \hat{y}_1\}/\{\hat{y}_1, \check{y}_1\} \to \{z_1, z_2\}$

To see this, after projection to D, the domain with positive weights is bounded by one of the following loops:

1. $y_1 \to x_1 \to y_2 \to z_2 \to y_1$,
2. $y_1 \to z_1 \to y_2 \to x_2 \to y_1$,
3. $y_1 \to z_2 \to y_2 \to z_1 \to y_1$,
4. $y_1 \to x_1 \to y_2 \to x_2 \to y_1$,

Note that x_1, x_2, z_1, z_2 should be viewed as top generators at positive ends or as bottom generators at negative ends. Specifically they give no constraints.

Case 1. This corresponds to region A. u is a quadrilateral with $\{x_1, z_2\}$ at positive ends and $\{\check{y}_1, \hat{y}_2\}$ or $\{\hat{y}_1, \check{y}_2\}$ at negative ends. By Lemma 4.3.2, $\mathrm{ind}(u) = 1$ and $\langle\{x_1, z_2\}, \{\check{y}_1, \hat{y}_2\}\rangle = \langle\{x_2, z_1\}, \{\hat{y}_1, \check{y}_2\}\rangle = \hbar \bmod 2$.

Case 2. This corresponds to region B. u is a quadrilateral with $\{x_2, z_1\}$ at positive ends and $\{\check{y}_1, \hat{y}_2\}$ or $\{\hat{y}_1, \check{y}_2\}$ at negative ends. This is similar to Case 1. Therefore, $\mathrm{ind}(u) = 1$ and $\langle\{x_2, z_1\}, \{\check{y}_1, \hat{y}_2\}\rangle = \langle\{x_2, z_1\}, \{\hat{y}_1, \check{y}_2\}\rangle = \hbar \bmod 2$.

Case 3. This corresponds to region C. u is a quadrilateral with $\{z_1, z_2\}$ at negative ends. Since z_1, z_2 are bottom generators, we need one check and one hat at positive ends due to Lemma 4.3.2 so that there is a nontrivial count of u. Therefore we get (4.5.3) and (4.5.4).

Case 4. This corresponds to region $A + B + C$. u is a quadrilateral with $\{x_1, x_2\}$ at positive ends and $\{y_1, y_2\}$ at negative ends. x_1, x_2 are viewed as top generators and there are two critical points inside the domain. We check that $\mathrm{ind}(u) = n$ for $\{\check{y}_1, \check{y}_2\}$ at negative ends; $\mathrm{ind}(u) = 2n - 1$ for $\{\hat{y}_1, \check{y}_2\}$ and $\{\check{y}_1, \hat{y}_2\}$ at negative ends; $\mathrm{ind}(u) = 3n - 2$ for $\{\hat{y}_1, \hat{y}_2\}$ at negative ends. Therefore there is no such u with index 1. $\square$

Corollary 4.5.3. *If we set* $|\{x_1, x_2\}| = 0$*, then* $Kh^\sharp(\widehat{\sigma}_{\text{left Hopf}})$ *is freely generated by the following generators with the corresponding relative grading (mod* $n-2$*):*

generators	*grading*
$\{x_1, x_2\}$	0
$\{x_2, z_1\} + \{x_1, z_2\}$	2
$\{\check{y}_1, \check{y}_2\}$	2
$\{\hat{y}_1, \hat{y}_2\}$	4

The computation for the right-handed Hopf link is similar. As shown in Figure 4.24, the braid representation of the right-handed Hopf link is the mirror of the left-handed one. Note that there is a bijection of pseudoholomorphic curves between these two Hopf links: Each curve in the left-handed moduli space corresponds to a curve in the right-handed one, where the positive and negative ends are exchanged, as well as the checks and hats. As a consequence, the grading by Maslov index is also reversed. Specifically, the right-handed Hopf link satisfies:

Lemma 4.5.4. $\widehat{CF}(\widetilde{W}, \widetilde{h}_{\sigma_{\text{right Hopf}}}(\widetilde{\boldsymbol{a}}), \widetilde{\boldsymbol{a}})$ *contains the following (mod 2) differential relations:*

$$d\{\check{y}_1, \hat{y}_2\} = \hbar\{x_1, z_2\} + \hbar\{x_2, z_1\}, \tag{4.5.5}$$

$$d\{\hat{y}_1, \check{y}_2\} = \hbar\{x_1, z_2\} + \hbar\{x_2, z_1\}, \tag{4.5.6}$$

$$d\{z_1, z_2\} = \hbar\{\check{y}_1, \hat{y}_2\} + \hbar\{\hat{y}_1, \check{y}_2\}. \tag{4.5.7}$$

Corollary 4.5.5. *If we set* $|\{x_1, x_2\}| = 0$*, then* $Kh^\sharp(\widehat{\sigma}_{\text{right Hopf}})$ *is freely generated by the following generators with the corresponding relative grading (mod* $n-2$*):*

generators	*grading*
$\{x_1, x_2\}$	0
$\{x_1, z_2\}$	-2
$\{\hat{y}_1, \hat{y}_2\}$	-2
$\{\check{y}_1, \check{y}_2\}$	-4

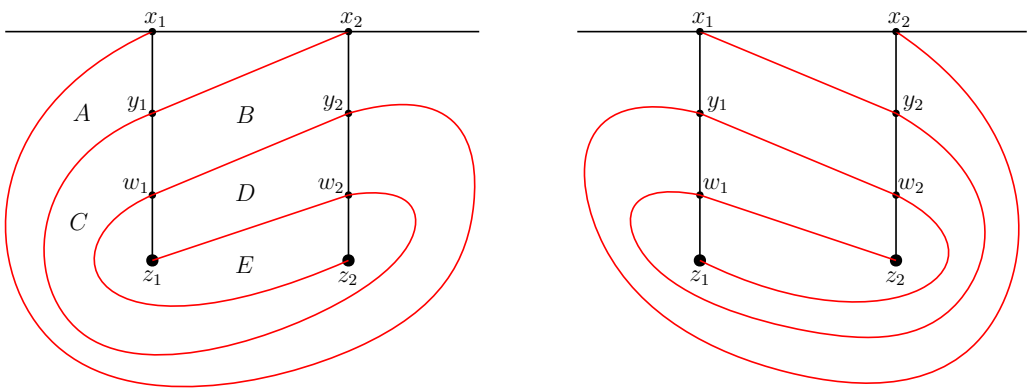

Figure 4.25: The braid representation of the left-handed trefoil (left) and the right-handed trefoil (right).

4.5.3 Trefoils

The left-hand side of Figure 4.25 shows the 2-strand braid representation of a left-handed trefoil, where 'A' to 'E' denote the corresponding regions on the base D.

Lemma 4.5.6. *$\widehat{CF}(\widetilde{W}, \widetilde{h}_{\sigma_{\text{left trefoil}}}(\widetilde{\boldsymbol{a}}), \widetilde{\boldsymbol{a}})$ contains the following (mod 2) differential relations:*

$$
\begin{aligned}
d\{x_1, \check{w}_2\} &= \hbar\{\check{y}_1, \hat{y}_2\} + \hbar\{\hat{y}_1, \check{y}_2\},\\
d\{x_1, \hat{w}_2\} &= \hbar\{\hat{y}_1, \hat{y}_2\} + \hbar\{\check{y}_2, z_1\} + \hbar\{\check{y}_1, z_2\}\\
d\{x_2, \check{w}_1\} &= \hbar\{\check{y}_1, \hat{y}_2\} + \hbar\{\hat{y}_1, \check{y}_2\},\\
d\{x_2, \hat{w}_1\} &= \hbar\{\hat{y}_1, \hat{y}_2\} + \hbar\{\check{y}_1, z_2\} + \hbar\{\check{y}_2, z_1\},\\
d\{\check{y}_1, z_2\} &= \hbar\{\check{w}_1, \hat{w}_2\} + \hbar\{\hat{w}_1, \check{w}_2\},\\
d\{\hat{y}_1, z_2\} &= \hbar\{\hat{w}_1, \hat{w}_2\},\\
d\{\check{y}_2, z_1\} &= \hbar\{\check{w}_1, \hat{w}_2\} + \hbar\{\hat{w}_1, \check{w}_2\},\\
d\{\hat{y}_2, z_1\} &= \hbar\{\hat{w}_1, \hat{w}_2\},\\
d\{\check{w}_1, \hat{w}_2\} &= \hbar\{z_1, z_2\},\\
d\{\hat{w}_1, \check{w}_2\} &= \hbar\{z_1, z_2\},\\
d\{\check{y}_1, \hat{y}_2\} &= \hbar\{\check{w}_1, \check{w}_2\},\\
d\{\hat{y}_1, \check{y}_2\} &= \hbar\{\check{w}_1, \check{w}_2\},\\
d\{\hat{y}_1, \hat{y}_2\} &= \hbar\{\check{w}_1, \hat{w}_2\} + \hbar\{\hat{w}_1, \check{w}_2\}.
\end{aligned}
$$

Proof. All nontrivial index 1 pseudoholomorphic curves with count 1 (mod 2) are listed as follows:

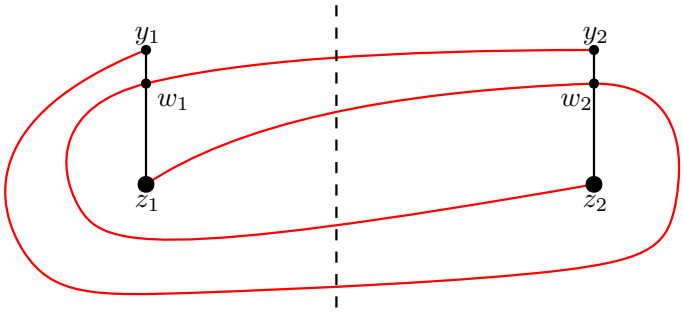

Figure 4.26: Horizontal stretch of region $C + D + E$.

regions	ends of generators
A	$\{x_1, \check{w}_2\} \to \{\check{y}_1, \hat{y}_2\}/\{\hat{y}_1, \check{y}_2\}$, $\{x_1, \hat{w}_2\} \to \{\hat{y}_1, \hat{y}_2\}$
B	$\{x_2, \check{w}_1\} \to \{\check{y}_1, \hat{y}_2\}/\{\hat{y}_1, \check{y}_2\}$, $\{x_2, \hat{w}_1\} \to \{\hat{y}_1, \hat{y}_2\}$
C	$\{\check{y}_1, z_2\} \to \{\check{w}_1, \hat{w}_2\}/\{\hat{w}_1, \check{w}_2\}$, $\{\hat{y}_1, z_2\} \to \{\hat{w}_1, \hat{w}_2\}$
D	$\{\check{y}_2, z_1\} \to \{\check{w}_1, \hat{w}_2\}/\{\hat{w}_1, \check{w}_2\}$, $\{\hat{y}_2, z_1\} \to \{\hat{w}_1, \hat{w}_2\}$
E	$\{\check{w}_1, \hat{w}_2\} \to \{z_1, z_2\}$, $\{\hat{w}_1, \check{w}_2\} \to \{z_1, z_2\}$
$A + C + E$	$\{x_1, \hat{w}_2\} \to \{\check{y}_2, z_1\}$
$B + C + E$	$\{x_2, \hat{w}_1\} \to \{\check{y}_2, z_1\}$
$A + D + E$	$\{x_1, \hat{w}_2\} \to \{\check{y}_1, z_2\}$
$B + D + E$	$\{x_2, \hat{w}_1\} \to \{\check{y}_1, z_2\}$
$C + D + E$	$\{\check{y}_1, \hat{y}_2\}/\{\hat{y}_1, \check{y}_2\} \to \{\check{w}_1, \check{w}_2\}$, $\{\hat{y}_1, \hat{y}_2\} \to \{\check{w}_1, \hat{w}_2\}/\{\hat{w}_1, \check{w}_2\}$

The proof is similar to Lemma 4.5.2. While the regions $B + D + E$ and $C + D + E$ are more interesting for the critical points inside.

Consider the region $C + D + E$ first. We stretch the region $C + D + E$ as Figure 4.26 which is similar to Figure 28 of [CHT20]. The dashed line is viewed as a gluing condition of a point constraint of both sides. Each side is equivalent to a disk with a slit. The slits must lie over the vertical black lines. Now both sides are disk models similar to Figure 4.9, that is, 2 point constraints on the boundary will fix a unique pseudoholomorphic disk. Take $\{\check{y}_1, \hat{y}_2\} \to \{\check{w}_1, \check{w}_2\}$ for example: On the right-hand side of Figure 4.26, $\hat{y}_2$ and $\check{w}_2$ are point constraints, so there is a unique disk over the right-hand side which also fixes the gluing

condition along the dashed line. On the left-hand side, $\check{y}_1$ imposes no constraint but $\check{w}_1$ and the dashed line are 2 point constraints, which fixes a unique disk. Therefore, there is a unique disk from $\{\check{y}_1, \hat{y}_2\}$ to $\{\check{w}_1, \check{w}_2\}$.

Similarly, the region $B + D + E$ is viewed as a disk with slits. $\hat{w}_1, \check{y}_1$ are viewed as point constraints and x_2, z_2 impose no constraints. There is a unique disk from $\{x_2, \hat{w}_1\}$ to $\{\check{y}_1, z_2\}$ for the same reason as above. □

Corollary 4.5.7. *If we set* $|\{x_1, x_2\}| = 0$*, then* $Kh^\sharp(\widehat{\sigma}_{\text{left trefoil}})$ *is freely generated by the following generators with the corresponding relative grading (mod* $n - 2$*):*

generators	*grading*
$\{x_1, x_2\}$	0
$\{x_1, \check{w}_2\} + \{x_2, \check{w}_1\}$	2
$\{\check{y}_1, \check{y}_2\}$	2
$\{x_1, \hat{w}_2\} + \{x_2, \hat{w}_1\}$	3
$\{\check{y}_1, z_2\} + \{\check{y}_2, z_1\}$	4
$\{\hat{y}_1, z_2\} + \{\hat{y}_2, z_1\}$	5

The computation for the right-handed trefoil is similar and the proof is omitted:

Lemma 4.5.8. *$\widehat{CF}(\widetilde{W}, \widetilde{h}_{\sigma_{\text{right trefoil}}}(\widetilde{\boldsymbol{a}}), \widetilde{\boldsymbol{a}})$ contains the following (mod 2) differential relations:*

$$
\begin{aligned}
d\{\check{y}_1, \hat{y}_2\} &= \hbar\{x_1, \hat{w}_2\} + \hbar\{x_2, \hat{w}_1\},\\
d\{\hat{y}_1, \check{y}_2\} &= \hbar\{x_1, \hat{w}_2\} + \hbar\{x_2, \hat{w}_1\},\\
d\{\check{y}_1, \check{y}_2\} &= \hbar\{x_1, \check{w}_2\} + \hbar\{x_2, \check{w}_1\},\\
d\{\check{w}_1, \hat{w}_2\} &= \hbar\{\hat{y}_1, z_2\} + \hbar\{\hat{y}_2, z_1\} + \hbar\{\check{y}_1, \check{y}_2\},\\
d\{\hat{w}_1, \check{w}_2\} &= \hbar\{\hat{y}_1, z_2\} + \hbar\{\hat{y}_2, z_1\} + \hbar\{\check{y}_1, \check{y}_2\},\\
d\{\check{w}_1, \check{w}_2\} &= \hbar\{\check{y}_1, z_2\} + \hbar\{\check{y}_2, z_1\},\\
d\{z_1, z_2\} &= \hbar\{\check{w}_1, \hat{w}_2\} + \hbar\{\hat{w}_1, \check{w}_2\},\\
d\{\hat{y}_1, z_2\} &= \hbar\{x_1, \check{w}_2\} + \hbar\{x_2, \check{w}_1\},\\
d\{\hat{y}_2, z_1\} &= \hbar\{x_1, \check{w}_2\} + \hbar\{x_2, \check{w}_1\},\\
d\{\hat{w}_1, \hat{w}_2\} &= \hbar\{\check{y}_1, \hat{y}_2\} + \hbar\{\hat{y}_1, \check{y}_2\}
\end{aligned}
$$

Corollary 4.5.9. *If we set $|\{x_1, x_2\}| = 0$, then $Kh^\sharp(\widehat{\sigma}_{\text{right trefoil}})$ is freely generated by the following generators with the corresponding relative grading (mod $n-2$):*

generators	*grading*
$\{x_1, x_2\}$	0
$\{x_1, \hat{w}_2\}$	-2
$\{\hat{y}_1, \hat{y}_2\}$	-2
$\{x_1, \check{w}_2\}$	-3
$\{\hat{y}_1, z_2\} + \{\hat{y}_2, z_1\}$	-4
$\{\check{y}_1, z_2\}$	-5

Bibliography

[Abo10] Mohammed Abouzaid, *A geometric criterion for generating the Fukaya category*, Publ. Math. Inst. Hautes Études Sci. (2010), 191–240.

[Abo12] Mohammed Abouzaid, *On the wrapped Fukaya category and based loops*, J. Symplectic Geom. **10** (2012), 27–79.

[AS06] Alberto Abbondandolo and Matthias Schwarz, *On the Floer homology of cotangent bundles*, Comm. Pure Appl. Math. **59** (2006), 254–316.

[AS10a] Alberto Abbondandolo and Matthias Schwarz, *Floer homology of cotangent bundles and the loop product*, Geom. Topol. **14** (2010), 1569–1722.

[AS10b] Mohammed Abouzaid and Paul Seidel, *An open string analogue of Viterbo functoriality*, Geom. Topol. **14** (2010), 627–718.

[Aur14] Denis Auroux, *A beginner's introduction to Fukaya categories*, *Contact and symplectic topology*. **26**. Bolyai Soc. Math. Stud. János Bolyai Math. Soc., Budapest, 2014, 85–136.

[BZCHN20] David Ben-Zvi, Harrison Chen, David Helm, and David Nadler, *Coherent Springer theory and the categorical Deligne-Langlands correspondence*, preprint 2020. arXiv: 2010.02321.

[CG10] Neil Chriss and Victor Ginzburg, *Representation theory and complex geometry*, Modern Birkhäuser Classics. Reprint of the 1997 edition. Birkhäuser Boston, Ltd., 2010.

[CGH12] Vincent Colin, Paolo Ghiggini, and Ko Honda, *The equivalence of Heegaard Floer homology and embedded contact homology via open book decompositions I*, preprint 2012. arXiv: 1208.1074.

[CGHH11] Vincent Colin, Paolo Ghiggini, Ko Honda, and Michael Hutchings, *Sutures and contact homology I*, Geom. Topol. **15** (2011), 1749–1842.

[CHT] Vincent Colin, Ko Honda, and Yin Tian, *Towards a definition of Khovanov homology for links in fibered* 3*-manifolds*, in preparation.

[CHT20] Vincent Colin, Ko Honda, and Yin Tian, *Applications of higher-dimensional Heegaard Floer homology to contact topology*, preprint 2020. arXiv: 2006.05701.

[CR08] Joseph Chuang and Raphaël Rouquier, *Derived equivalences for symmetric groups and $\mathfrak{sl}_2$-categorification*, Ann. of Math. (2) **167** (2008), 245–298.

[Dui76] Hans Duistermaat, *On the Morse index in variational calculus*, Advances in Math. **21** (1976), 173–195.

[EENS13] Tobias Ekholm, John B Etnyre, Lenhard Ng, and Michael G Sullivan, *Knot contact homology*, Geometry & Topology **17** (2013), 975–1112.

[ES19] Tobias Ekholm and Vivek Shende, *Skeins on branes*, preprint 2019. arXiv: 1901.08027.

[Flo88] Andreas Floer, *Morse theory for Lagrangian intersections*, J. Differential Geom. **28** (1988), 513–547.

[FO97] Kenji Fukaya and Yong-Geun Oh, *Zero-loop open strings in the cotangent bundle and Morse homotopy*, Asian J. Math. **1** (1997), 96–180.

[FOOO09] Kenji Fukaya, Yong-Geun Oh, Hiroshi Ohta, and Kaoru Ono, *Lagrangian intersection Floer theory: anomaly and obstruction. Part II*, **46**. AMS/IP Studies in Advanced Mathematics. American Mathematical Society, Providence, RI, 2009.

[GPS18] Sheel Ganatra, John Pardon, and Vivek Shende, *Sectorial descent for wrapped Fukaya categories*, preprint 2018. arXiv: 1809.03427.

[GPS20] Sheel Ganatra, John Pardon, and Vivek Shende, *Covariantly functorial wrapped Floer theory on Liouville sectors*, Publ. Math. Inst. Hautes Études Sci. **131** (2020), 73–200.

[GS05] Iain Gordon and J Toby Stafford, *Rational Cherednik algebras and Hilbert schemes*, Advances in Math. **198** (2005), 222–274.

[HTY] Ko Honda, Yin Tian, and Tianyu Yuan, *Higher-dimensional Heegaard Floer homology and Hecke algebras*, in preparation.

[Iac08] Vito Iacovino, *A simple proof of a theorem of Fukaya and Oh*, preprint 2008. arXiv: 0812.0129.

[Kho00] Mikhail Khovanov, *A categorification of the Jones polynomial*, Duke Math. J. **101** (2000), 359–426.

[KL09] Mikhail Khovanov and Aaron D. Lauda, *A diagrammatic approach to categorification of quantum groups. I*, Represent. Theory **13** (2009), 309–347.

[KL87] David Kazhdan and George Lusztig, *Proof of the Deligne-Langlands conjecture for Hecke algebras*, Invent. Math. **87** (1987), 153–215.

[KR08] Masaki Kashiwara and Raphaël Rouquier, *Microlocalization of rational Cherednik algebras*, Duke Math. J. **144** (2008), 525–573.

[Lip06] Robert Lipshitz, *A cylindrical reformulation of Heegaard Floer homology*, Geom. Topol. **10** (2006), 955–1096.

[Lus98] George Lusztig, *Bases in equivariant K-theory*, Represent. Theory **2** (1998), 298–369.

[Man06] Ciprian Manolescu, *Nilpotent slices, Hilbert schemes, and the Jones polynomial*, Duke Math. J. **132** (2006), 311–369.

[Man07] Ciprian Manolescu, *Link homology theories from symplectic geometry*, Adv. Math. **211** (2007), 363–416.

[Mil63] John Milnor, *Morse theory*, Annals of Mathematics Studies, No. 51. Based on lecture notes by M. Spivak and R. Wells. Princeton University Press, Princeton, N.J., 1963.

[MS19] Cheuk Yu Mak and Ivan Smith, *Fukaya-Seidel categories of Hilbert schemes and parabolic category $\mathcal{O}$*, preprint 2019. arXiv: `1907.07624`.

[MS21] Hugh Morton and Peter Samuelson, *DAHAs and skein theory*, Comm. Math. Phys. **385** (2021), 1655–1693.

[Nak99] Hiraku Nakajima, *Lectures on Hilbert schemes of points on surfaces*, American Mathematical Society, 1999.

[OS04] Peter Ozsváth and Zoltán Szabó, *Holomorphic disks and topological invariants for closed three-manifolds*, Ann. of Math. (2) **159** (2004), 1027–1158.

[Per08] Timothy Perutz, *Hamiltonian handleslides for Heegaard Floer homology*, preprint 2008. arXiv: `0801.0564`.

[Rou08] Raphael Rouquier, *2-Kac-Moody algebras*, preprint 2008. arXiv: 0812.5023.

[SS06] Paul Seidel and Ivan Smith, *A link invariant from the symplectic geometry of nilpotent slices*, Duke Math. J. **134** (2006), 453–514.

[Syl19] Zachary Sylvan, *On partially wrapped Fukaya categories*, J. Topol. **12** (2019), 372–441.

[Vas05] Eric Vasserot, *Induced and simple modules of double affine Hecke algebras*, Duke Math. J. **126** (2005), 251–323.

[Wil08] Brandon Williams, *Computations in Khovanov Homology*, University of Illinois at Chicago, Chicago, Illinois (2008).

[Yua] Tianyu Yuan, *The finite Hecke algebra from higher-dimensional Heegaard Floer homology*, in preparation.